RAL INTERACTING PROTEIN (Ralbp1): LINKING GLUTATHIONE CONJUGATE TRANSPORT TO OXIDATIVE STRESS DEFENSES AND SIGNALING PATHWAYS

by

DILKI C. WICKRAMARACHCHI

Presented to the Faculty of the Graduate School of

The University of Texas at Arlington in Partial Fulfillment

of the Requirements

for the Degree of

DOCTOR OF PHILOSOPHY

THE UNIVERSITY OF TEXAS AT ARLINGTON

December 2007

ACKNOWLEDGEMENTS

Upon reflection, it is truly hard to comprehend how much I learnt as a graduate student and the impact it had on changing my life and just how grateful I am to have had the experience. Although my knowledge of biochemistry and molecular biology is much richer than it was before, it is the people who taught me, worked with me, and befriend me, I will remember the most.

I am deeply indebted to my supervisor, Dr. Sanjay Awasthi, for his guidance, constructive and stimulating suggestions and encouragement during the time of research as well as in preparation of this thesis.

I would also like to offer my sincere gratitude to all my laboratory colleagues for making this dissertation a possibility. Dr. Sushma Yadav, thank you so much for your inspiring advice and guidance. You are a teacher, a colleague, a friend and family all combined together to me. Thank you so much Dr. Singhal and Mrs. Singhal, for introducing me to proteomics and cell culture. The countless hours of teaching by all three of you molded me into the person I am today.

I was fortunate to work under the guidance of Dr. Dwight Kono during the research internship. You opened my eyes to novel things in research as well as showed me the path to become an independent scientist. Dr. Kono, thank you so much.

I would also like to thank my present and former committee members, Drs E. Bellion, S. Mandal, D. Rudkevich and Z. Shelly for their valuable advice on the project.

Also I want to thank Dr. Ewa Zajac and Mr. Aalok Nadkar, for help, support and valuable hints as well as being there to share ups and downs of research. Special thanks go to Kenneth and Megan Drake, who are like family to me. Both of you helped me in various ways from settling down in the USA during my initial days to date in accomplishing the Ph.D.

Also I am deeply grateful to Dr. Thamara Janaratne who is like a sister to me. Thank you so much for standing by me in my ups and downs and motivating me. Life would not have being the same without your inspiration.

Thank you so much University of Texas at Arlington (UTA), for opening me the doors to explore the world of research.

I am also grateful to all my friends who helped me in numerous ways. Though I could not include all the names, all the support and the company all of you provided during last few years, gave me the strength to accomplish this challenge.

Last but not the least I would like to thank all my family members for the encouragement and support. Little Tommy (my brother Isuru), a pain most of the time but always helped me out when I most needed it. Thank you Tommy for all your help and more than anything for keeping me from getting stressed out. My sister Rajitha and her husband Mathisha, thank you for standing by me and encouraging me to go on with life, when I felt it's the end of the world. Words of thanks go to my brother Indrajith and his wife Kalyani, for their encouragement.

Lastly I owe so much to my parents who stood by me in my ups and downs. It's the loving encouragement you shed on me and the faith you had in me that made me go

this far. Thank you so much amma and thaththa, (my mom and dad), none of this would have been possible with out you.

December 12, 2007

ABSTRACT

RAL INTERACTING PROTEIN (Ralbp1): LINKING GLUTATHIONE CONJUGATE TRANSPORT TO OXIDATIVE STRESS DEFENSES AND SIGNALING PATHWAYS

Publication No. _____

Dilki C. Wickramarachchi, Ph.D.

The University of Texas at Arlington, 2007

Supervising Professor: Sanjay Awasthi, M.D.

The glutathione-conjugate transporter protein DNP-SG ATPase was demonstrated to be identical to the independently cloned Ral-effector, Ralbp1. Glutathione-conjugate transport is linked to substrate-stimulated ATPase activity, while GTPase stimulating activity (GAP-activity), and clathrin-coated pit-binding activity was demonstrated for this protein by different groups of investigators. The relationship between these activities and physiological functions of Ralbp1 were not clear. The present studies were designed to address the hypothesis that the ability of Ralbp1 to couple the hydrolysis of ATP with the movement of substances, i.e. its transport activity, is the crucial element that allows Ralbp1 to function as a stress-defense protein.

Results of these studies, demonstrating 1) the requirement of Ralbp1 for PKCα mediated resistance-signaling, 2) the identification of transmembrane spanning domains of Ralbp1 and requirement of membrane anchorage for transport function, and 3) the requirement of transport function for clathrin-dependent ligand-receptor endocytosis to occur, offer strong evidence in support of this proposal.

TABLE OF CONTENTS

ACKNOWLEDGEMENTS ii

ABSTRACT v

LIST OF ILLUSTRATIONS xii

LIST OF TABLES xvi

Chapter

1. INTRODUCTION…….. 1

1.1 Oxidative Stress……. 1

1.1.1 Generation of reactive oxygen species 1

1.1.2 Effects on biological macromolecules 3

1.2 Cellular defense mechanisms 8

1.2.1 ATP binding cassette of transporter proteins 9

1.2.2 Non-ABC family of transporter proteins 18

1.3 The scope of the dissertation 27

2. METHODS AND MATERIALS USED IN STRUCTURE FUNCTION ANALYSES 29

2.1 Abstract……..... 29

2.2 Introduction and background 30

2.3 Materials…… 32

2.3.1 Reagents…. 32

2.3.2 Supplies used for molecular biological procedures..... 37

2.3.3 Kits……..... 38

2.3.4 Others……..... 38

2.3.5 Buffers..... 39

2.3.6 Cell lines…..... 41

2.4 Methods……..... 42

2.4.1 Preparation of affinity resin for the purification of glutathione *S*-transferases (GSTs) 42

2.4.2 Determination of GST activity..... 43

2.4.3 Purification of GSTs from mouse liver 44

2.4.4 Synthesis of 2,4-dinitrophenyl *S*-glutathione (DNP-SG) 48

2.4.5 Molecular cloning..... 50

2.4.6 Preparation of cyanogen bromide (BrCN)-activated Sepharose 4B resin..... 55

2.4.7 Purification of recombinat Ralbp1 from *E. coli* BL21(DE3) 55

2.4.8 Purification of rec-Ralbp1 by Ni-NTA affinity chromatography..... 59

2.4.9 Transformation..... 61

2.4.10 Plasmid DNA purification (Mini prep)..... 62

2.4.11 Restriction endonuclease digestion 64

2.4.12 Agarose gel electrophoresis 65

2.4.13 Gel purification of DNA from agarose gels using QIAquick gel extraction kit..... 66

2.4.14 Determination of the DNA concentration 67

2.4.15 Preparation of competent *E. coli* DH5α 68

2.4.16 Preparation of competent *E. coli* BL21 (DE3) 68

2.4.17 Determination of protein concentration – Bradford assay 69

2.4.18 Sodium dodecyl sulfate-polyacrylamide gel electrophoresis (SDS-PAGE) 71

2.4.19 Western blotting 73

2.4.20 Reconstitution of rec-Ralbp1 into proteoliposomes 75

2.4.21 Transport studies using proteoliposomes of rec-Ralbp1 75

2.4.22 Transient transfection 77

2.4.23 Determination of antibiotic concentration lethal to cells 78

2.4.24 Stable transfection 78

2.4.25 Purification of RNA 79

2.4.26 Reverse transcriptase polymerase chain reaction (RT-PCR) 81

2.4.27 Drug sensitivity assay 81

2.4.28 siRNA transfection 83

2.4.29 *In vitro* site directed mutagenesis – substitution mutations 84

2.4.30 Ralbp1 mediated uptake studies 87

2.4.31 Ralbp1 mediated endocytosis 87

2.4.32 Immunohistochemical localization of Ralbp1 88

2.4.33 *In vitro* site directed mutagenesis – deletion mutations 90

3. Ralbp1 AS AN ARBITRATOR OF
PKCα MEDIATED DRUG RESISTANCE SIGNALING 92

3.1 Abstract..... 92

3.2 Introduction and background..... 93

3.3 Results and Discussion..... 94

3.3.1 Phosphorylation of Ralbp1 by PKCα 94

3.3.2 Effects of PKCα mediated phosphorylation
on transport function of rec-Ralbp1 95

3.3.3 Differential expression of PKCα in SCLC
and NSCLC cell lines and suppression by siRNA 97

3.3.4 PKCα depletion, effects on doxorubicin transport
activity of Ralbp1 in SCLC and NSCLC 99

3.3.5 The effect of PKCα depletion on
cell survival of SCLC and NSCLC..... 101

3.3.6 Effect of depletion of PKCα on resistance
against doxorubicin mediated cytotoxicity 103

3.3.7 Requirement of Ralbp1 for PKCα attributed
resistance against doxorubicin mediated cytotoxicity 104

3.4 Conclusions……..... 106

4. IDENTIFICATION OF MEMBRANE ANCHORING
DOMAINS OF Ralbp1 AND CELLULAR LOCALIZATION 108

4.1 Abstract……..... 108

4.2 Introduction and background..... 109

4.3 Results and Discussion..... 113

4.3.1 Membrane localization of Ralbp1 113

4.3.2 Co-localization of Ralbp1 with a
membrane associated protein 114

4.3.3 Identification of membrane associated domains of Ralbp1 115

4.3.4 Effects of deletions on transport properties of Ralbp1 116

4.3.5 Identification of cell surface epitopes of Ralbp1 118

4.4 Conclusions..... 120

5. Ralbp1 AS A NOVEL LINK IN STRESS DEFENSE AND SIGNALING PATHWAYS 121

5.1 Abstract..... 121

5.2 Introduction and background..... 122

5.3 Results and Discussion..... 130

5.3.1 Construction of substitution mutants of potential glutathione conjugate site 130

5.3.2 Expression of substitution mutants of potential glutathione conjugate binding site in *E. coli* 135

5.3.3 Effects of potential glutathione conjugate site mutations on *in vitro* Melphalan transport 138

5.3.4 Effects of potential glutathione conjugate site mutations on cellular Melphalan uptake 141

5.3.5 Cellular localization of full length wild type and the transport deficient mutants Ralbp1 145

5.3.6 Endocytosis studies 147

5.4 Conclusions..... 153

REFERENCES 155

BIOGRAPHICAL INFORMATION 176

LIST OF ILLUSTRATIONS

Figure		Page
1.1	Reactive oxygen species (ROS) and proteins, oxidation of proline	5
1.2	Oxidative damage to nucleic acids	5
1.3	Lipid peroxidation pathway	7
1.4	Topology, P-glycoprotein (Pgp)	11
1.5	Topology of structural type I and II MRPs	14
1.6	Topology of breast cancer resistant protein (BCRP/ ABCG2/ MXR)	16
1.7	Potential structural motifs in primary structure of Ralbp1	21
1.8	Pathway: receptor mediated endocytosis	23
2.1	Synthesis of DNP-SG	43
2.2	Coomassie–Stained SDS-PAGE of purified GST from mouse liver	48
2.3	Absorbance spectrum of DNP-SG – first fraction	49
2.4	Absorbance spectrum of DNP-SG – second fraction	50
2.5	Plasmid map of prokaryotic expression vector pET30a(+)	51
2.6	*E. coli* DH5α competent cells transformed with pET30a(+)-Ralbp1 cultured on LB agar containing kanamycin (50 µg/ml)	53
2.7	pET30a(+) cloned with Ralbp1 undigested samples 1-5	54
2.8	pET30a(+) cloned with Ralbp1 digested with BamH I and Xho I	54
2.9	*E. coli* BL21(DE3) transformed with pET30a(+)/Ralbp1 cultured on LB agar containing kanamycin (50 µg/ml)	56

2.10 SDS-PAGE of samples at different purification steps 58

2.11 SDS-PAGE of purified recombinant Ralbp1 58

2.12 Western blot of purified recombinant Ralbp1 using polyclonal antibodies 59

2.13 Western blot: Ni-NTA affinity purified rec-Ralbp1 60

2.14 Standard curve for Bradford assay 71

2.15 Reduction of MTT into purple formazan 82

2.16 Overview: site directed mutagenesis 85

3.1 PKCα mediated phosphorylation of rec-Ralbp1 94

3.2 Effect of PKCα phosphorylation on uptake of [^{3}H]-DNP-SG 96

3.3 Effect of PKCα phosphorylation on uptake of [^{3}H]-LTC_4 97

3.4 Western blot with anti-PKCα IgG 99

3.5 PKCα depletion, effects on transport function of Ralbp1 (*in vitro*) 100

3.6 Depletion of PKCα mediated phosphorylation, effects on cell survival of SCLC and NSCLC 102

3.7 Depletion of PKCα on resistance against doxorubicin mediated cytotoxicity in SCLC and NSCLC 103

3.8 Effect of PKCα depletion on IC_{50} value of doxorubicin in Ralbp1$^{+/+}$ and Ralbp1$^{-/-}$ MEF cells 105

4.1 Membrane proteins 110

4.2 Sequence homology of Ralbp1 with vector peptides and membrane associated proteins 112

4.3 Cell surface localization of Ralbp1 113

4.4 Co-localization of Ralbp1 with protein her2/neu 114

4.5 Effects of deletion mutations on cellular expression of Ralbp1 115

4.6 ATP dependent transport of DOX 117

4.7 ATP dependent transport of DNP-SG 117

4.8 Identification of cell surface epitopes of Ralbp1 119

5.1 Evolution of glutathione *S*-transferases 124

5.2 Catalytic activity of GST 126

5.3 Sequence alignment of Ralbp1 with other glutathione conjugate binding proteins 129

5.4 pcDNA3.1 cloned with substitution mutants of Ralbp1 131

5.5 pcDNA3.1 cloned with substitution mutants of Ralbp1, digested with restriction endonucleases, BamH I and Xho I 132

5.6 pET30a(+) cloned with substitution mutants of Ralbp1 (undigested) 133

5.7 pET30a(+) cloned with substitution mutants of Ralbp1, digested with restriction endonucleases, BamH I and Xho I 134

5.8 Expression of Ralbp1 and the substitution mutants in *E. coli* crude cell lysate 136

5.9 Expression of Ralbp1 and the substitution mutants in *E. coli* crude cell lysate 137

5.10 Melphalan IC_{50} values of Ralbp1$^{-/-}$ MEFs transfected with full length and transport deficient mutants of Ralbp1 140

5.11 Melphalan uptake of Ralbp1$^{-/-}$ MEFs transfected with full length Ralbp1 and transport deficient mutants of Ralbp1 143

5.12 Fold retention of Melphalan in Ralbp1$^{-/-}$ MEFs transfected with full length Ralbp1 and transport deficient mutants of Ralbp1 144

5.13 Immunohistochemical localization of full length wild type and transport deficient mutants Ralbp1 146

5.14 Endocytosis of epidermal growth factor (EGF) by wild type full length and transport deficient mutants of Ralbp1 149

5.15 Fluorescence intensity from endocytosis of EGF by Ralbp1$^{-/-}$ MEFs transfected with Ralbp1 and its transport deficient mutants.....150

5.16 The relative effect of Ralbp1 mutants on melphalan uptake, IC_{50} and endocytosis of EGF 152

5.17 Interactions of Ralbp1 with glutathione conjugates.....153

LIST OF TABLES

Table Page

1.1 Pathways of cellular oxidant generation 3

2.1 Schematic protocol for GST assay in a 1.5 ml cuvette 44

2.2 Purification table for GSTs from mouse liver 46

2.3 pET30a(+) sequence landmarks..... 52

2.4 Concentration and absorbance values of BSA standard solutions..... 70

2.5 Composition of stacking gel and resolving gel during SDS-PAGE 72

5.1 Electrostatic interactions between 1-(*S*-glutathionyl)-2,4-dinitrobenzene (GSDNB) and GSTs 125

5.2 Melphalan IC_{50} values of Ralbp1$^{-/-}$ MEFs transfected with full length or transport deficient mutants of Ralbp1 139

5.3 Melphalan uptake of Ralbp1$^{-/-}$ MEFs transfected with full length or transport deficient mutants of Ralbp1 142

5.4 Fluorescent intensity from endocytosis of EGF by Ralbp1$^{-/-}$ MEFs transfected with Ralbp1 and its transport deficient mutants.....150

5.5 Correlation of Melphalan IC_{50}, uptake and endocytosis activities of different Ralbp1 mutants 151

CHAPTER 1

INTRODUCTION

1.1 Oxidative Stress

Biological systems are sustained by energy transfer processes based on sequential, linked, oxidation-reduction reactions. Inherent inefficiencies in these pathways of electron flow results in "leakages" which, take the form of free radicals (Echtay 2007). Dissolved molecular oxygen is the most frequent electron acceptor, giving rise to superoxide anion (Echtay 2007). Through the activity of enzymes such as superoxide dismutase (SOD) and catalase as well as heavy metals, superoxide anion is converted to a plethora of more reactive free radicals (Echtay 2007). Oxidative stress is a situation when the balance between the generation and consumption of reactive oxygen species (ROS) is tilted towards generation.

1.1.1 Generation of reactive oxygen species

Induction of cytochrome P450 (CYP450) enzymes is another pathway by which cellular reactive oxygen species are generated, particularly superoxide anion and hydrogen peroxide. CYP450 2E1, which catalyzes the oxygenation of substrates such as ethanol, is capable of generating a burst of reactive ROS near the substrate oxidation

site (Kwon et al. 2005). Also it is known that CYP450 4A induces the formation of peroxisomes, resulting in an increase in the H_2O_2 production.

Reactive oxygen species are generated in immune defense during an inflammation. Activated phagocytes, neutrophils, eosinophils and macrophages produce superoxide anion, hydrogen peroxide and reactive nitrogen species such as nitric oxide as a mechanism of killing pathogens. Due to their non-specificity, ROS can exert damaging effects against pathogens present within the vicinity without relying on more precise mechanisms such as those mediated by opsonizing antibodies. Due to the nonspecificity of ROS-mediated injury, the 'innocent-bystander' surrounding normal tissues are also subjected to injury. Genotoxic injury exerted by ROS formed at a site of inflammation or infection has been cited as a potential explanation for the observed increase in malignancy in organs subjected to chronic infection or inflammation. The pathogenesis of hepatocellular carcinoma, bladder carcinoma and mesothelioma among others have being linked specifically with conditions associated with increased ROS generation in tissue due to inflammation.

Inflammation or infection are not the only significant sources of ROS in biological tissues. Though endogenous oxidative metabolism is a significant chronic source of ROS that may be responsible for aging, cellular levels of ROS can also increase dramatically when exposed acutely or chronically to exogenous sources such as high-energy radiation, drugs and/or their metabolites and environmental pollutants including heavy metals and polycyclic aromatic hydrocarbons and/or their metabolites. Transition metals such as iron, copper, chromium, vanadium and cobalt can undergo

single electron transfers to produce hydroxyl radicals through Fenton and Harber-Weiss reaction. Non-metal catalysts such as quinones also trigger the generation of ROS through redox cyling by the formation of semi-quinones and hydroquinones.

Table 1.1 Pathways of cellular oxidant generation (Klaunig et al. 2004)

Type	Reaction
1. Reduction of molecular oxygen	$O_2 + e^- \longrightarrow O_2^{-\bullet}$ (superoxide anion) $O_2^{-\bullet} + H_2O \longrightarrow HO_2^{\bullet}$ (hydroperoxyl radical) $HO_2^{\bullet} + e^- + H \longrightarrow H_2O_2$ (hydrogen peroxide) $H_2O_2 + e^- \longrightarrow OH^- + {}^{\bullet}OH$ (hydroxyl radical)
2. Production of reactive nitrogen species	L-arginine + $O_2 \longrightarrow$ NO (nitric oxide) + L-citrulline $O_2^{-\bullet} + {}^{\bullet}NO \longrightarrow ONOO^-$ (peroxynitrite) $ONOO^- + CO_2 \longrightarrow ONOOCO_2^-$ (nitrosoperoxy carbonate) $ONOOCO_2^- \longrightarrow {}^{\bullet}NO_2$ (nitrogen dioxide) + CO_3^- (carbonate anion radical)
3. Fenton reaction	$H_2O_2 + Fe^{2+} \longrightarrow OH^- + {}^{\bullet}OH + Fe^{3+}$

1.1.2 Effects on biological macromolecules

Effects of ROS vary according to their electron reduction potential. Superoxide anions are less reactive, but can react with transition metals to become more reactive hydroxyl radicals. Among the reactive nitrogen species, nitric oxide (NO), generated by immune system are biological signals in diverse physiological processes including smooth muscle relaxation (Moncada et al. 1991; Ignarro et al. 1987; Rapoport et al. 1983; Furchgott et al. 1980), neurotransmission and immune regulation (Moncada et al.

1991; Furchgott et al. 1980). Peroxynitrite which is formed by the reaction between nitric oxide and superoxide anion, is much more reactive. Severe level of oxidative stress causes ATP depletion, blockage of controlled apoptotic cell death and necrosis. Many diseases such as atherosclerosis, Parkinson's disease, Alzheimer's disease, systemic lupus erythematosus as well as aging indicated a close link with cellular oxidative stress (Kovacic et al. 2003).

Reactive oxygen species and proteins

Oxidative damage to proteins is specifically targeted towards aromatic amino acids and sulfur-containing amino acids. Amino acids such as proline and histidine undergo fragmentation giving rise to irreversible modifications that target peptides for degradation by cellular proteases. On the other hand, sulfur-containing amino acids undergo reversible modifications such as disulfide bond formation (cysteine) and S-nitrosothiol formation (cysteine and methionine) (Stadtman et al. 2003; Wink et al 1994). These modifications may play a role in regulating metabolic events during oxidative stress.

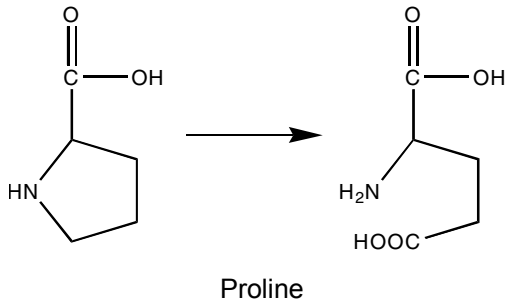

Proline

Figure 1.1 Reactive oxygen species (ROS) and proteins, oxidation of proline (http://www.bb.iastate.edu/~jat/glutchp.html) (with permission)

Oxidative damage on nucleic acids

Nucleic acids are pentose-phosphate polymers that are susceptible to be attacked by hydroxyl radicals. Hydrogen could be abstracted from as well as added to either sugar or base moiety of a nucleotide. Due to the low reduction potential, a single electron is transferred from guanine to the hydroxyl radical resulting in the formation of a guaninyl radical (Giese 2002; Imlay 2003). 8-Oxoguanine is the most prevalent product of oxidative damage of purines. Thymine glycol is the foremost product of free radical damage of pyrimidines.

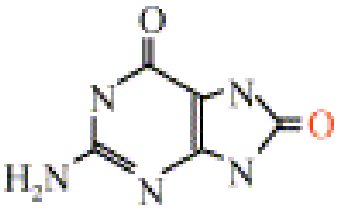

8-oxoguanine

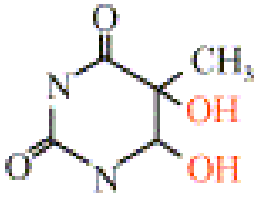

Thymine glycol

Figure 1.2 Oxidative damage on nucleic acids (Slupphaug et al. 2003)

Effects of ROS on lipids

Reactive oxygen species cause membrane lipid peroxidation, a radical initiated chain reaction that self propagates. The initiation of lipid peroxidation occurs through abstraction of a hydrogen atom from methylene groups of polyunsaturated fatty acids that are highly susceptible for oxidation (Echtay 2007). The removal of $H^{\bullet}$ by $OH^{\bullet}$ yields lipid alkyl radicals ($R^{\bullet}$), which rapidly combines with O_2 to yield $ROO^{\bullet}$ (lipid peroxyl radical), which can again abstract a $H^{\bullet}$ from lipids to yield ROOH (lipid hydroperoxide) and another $R^{\bullet}$. The presence of heavy metals such as Fe^{+2} accelerate this process even further (Echtay, 2007). Diagrammatic representation of the lipid peroxidation pathway is given bellow (figure 1.3).

These processes leading to oxidative degradation and further fragmentation of polyunsaturated fatty acids such as arachidonic acid give rise to products such as leukotrienes and alkenals (ex: 4-hydroxynonenal, 4HNE). Leukotrienes are potent inducers of inflammation; prior to their chemical identification as glutathione-conjugates formed from oxidative metabolism of arachidonic acid, these compounds were collectively referred to as SRS-A (slow-reacting substance of anaphylaxis) because of their potent ability to induce anaphylaxis. 4HNE, in contrast, has pleiotropic concentration dependent effects ranging from inhibition of cell growth and induction of differentiation, to apoptosis and necrosis (Esterbauer et al. 1980).

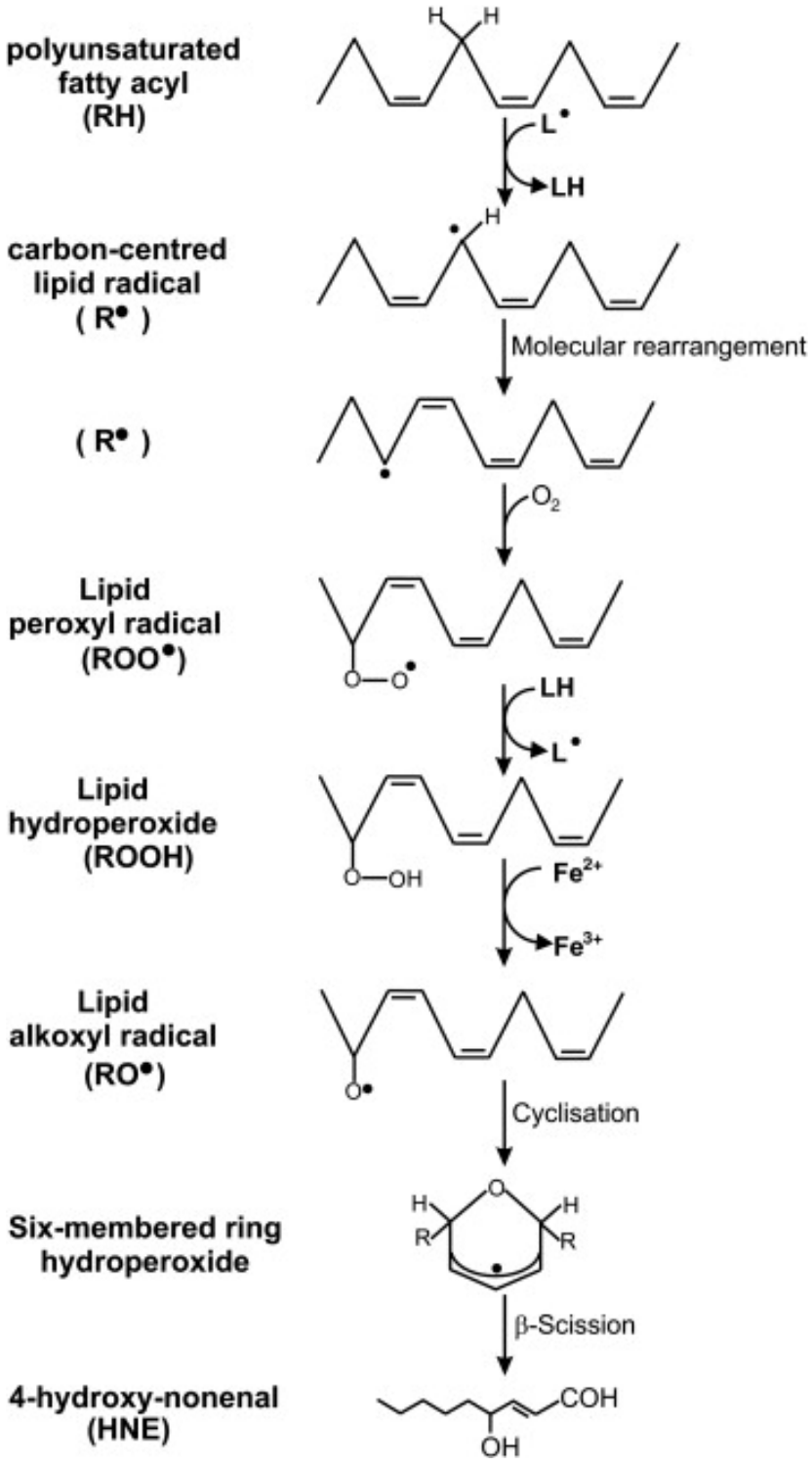

Figure 1.3 Lipid peroxidation pathway (Echtay 2007)

1.2 Cellular defense mechanisms

The cellular defenses against oxidative stress include enzymatic pathways and non-enzymatic chemical antioxidant defenses. The enzymes with antioxidant properties include SOD, catalase, GSH peroxidase and GST, while non-enzymatic antioxidant defenses include carotenoids, vitamin C and E as well as GSH.

Superoxide dismutase, a copper-zinc enzyme present in lymph, plasma and synovial fluid, converts the superoxide anion into hydrogen peroxide. Detoxification of hydrogen peroxide is carried out by catalase, a heme protein present in peroxisomes. Hydrogen peroxide is also detoxified through glutathione peroxidase, a seleno-protein found in cytoplasm and mitochondria. GST catalyzes the formation of glutathione-electrophile conjugates (GS-E) from endogenous electrophiles such as lipid-alkenals and exogenous toxins (xenobiotics). These GS-E are subsequently transported out of the cell by various transporter proteins. Gamma-glutamyl cysteine synthetase and glutathione synthetase are the key enzymes in the de-novo synthesis of GSH. GSH is maintained in a reduced state through the action of GSH reductase, which catalyzes the oxidation of NADPH to $NADP^+$ linked to the reduction of GSH-disulfide (GSSG) to GSH. These enzymes play an important antioxidant function by virtue of their ability to regulate GSH levels.

Studies described in this dissertation are focused on xenobiotic and endobiotic detoxification through efflux by transporter proteins. Xeno/endobiotics undergo detoxification through a three step process, phase I, phase II and phase III. During phase I, functional groups (OH, NH_2, SH, COOH) are either introduced or exposed through

the activity of enzymes such as CYP450, epoxide hydrolases, esterases and amidases. During phase II, hydrophilicity of the xeno/ endobiotics are greatly increased by biotransformation reactions such as glucuronidation, sulfonation, acetylation, methylation as well as conjugation with glutathione. These reactions are catalyzed by GSTs, UDP-glucuronosyl transferases, sulfotransferases, epoxide hydrolases or quinine reductase. The next step, efflux of the conjugates formed during phase II biotransformation by various transporter proteins, is referred to collectively as phase III. Phase III transporter proteins fall in to two broad categories, ATP binding cassette of transporters (ABC transporters) and non-ABC transporters based on the sequence homology.

1.2.1 ATP binding cassette of transporter proteins

These consist of one of the largest super family of proteins comprising members from prokaryotes to humans (Jones et al. 2004). As the name implies, these proteins transport substrates across intracellular as well as plasma membranes by utilizing ATP. The structure of a typical ABC transporter include two trans-membrane domains consisting several (6-11) α-helices spanning across the phospholipid bi-layer, one or two ATP-binding domains known as Walker motifs A (GXXGXGKT/S) and B (R/KX(7-8)hhhhD) where h stands for any hydrophobic residue, separated by 90-120 amino acids, and a signature sequence (LSGGQ). The trans-membrane domains bring about the substrate specificity, while nucleotide binding domains bind and hydrolyze ATP, providing energy for the active transport. The arrangement of the trans-membrane

(TM) and nucleotide binding domains (NBD) generally followed the pattern NH_3^+-TM-NBD-TM-NBD-COO^-. ABC transporters with one TM domain and NBD are known as half transporters and these form homo/ hetero dimers during the transport.

Although the mechanism of transport is incompletely understood, it is known that the conformational changes caused by binding of ATP decreases the affinity of the protein for the substrate, resulting in efflux of the substrate. Fifty ABC transporters have being classified in to 7 families; ABC(A-G) by the Human Genome Organization. Due to their efflux properties, ABC transporters bring about drug accumulation defect causing multi drug resistance (MDR). Some of the most studied proteins causing MDR include P-glycoprotein (Pgp) belonging to ABCB1 sub family, multi drug resistance protein (MRP) that belongs to ABCC sub family, and breast cancer resistance protein (BCRP) a member of ABCG. P-glycoprotein transports cationic and neutral organic compounds, while MRP carries out the transport of organic anionic compounds such as GSH conjugates.

P-glycoprotein (Pgp)

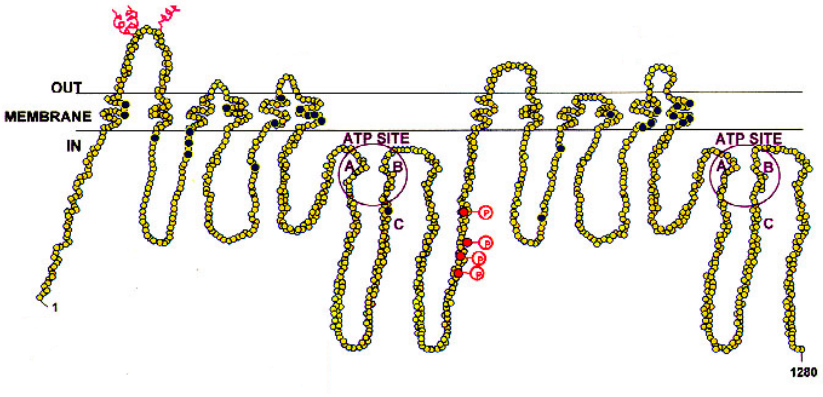

Figure 1.4 Topology, P-glycoprotein (Pgp) (Ambudkar et al. 1999)

Pgp which belongs to ATP binding cassette subfamily B1, is also known as ABCB1 and MDR1. Pgp was initially discovered by Juliano et al. in 1976 as a surface phosphoglycoprotein over expressed in Chinese hamster ovary cell line with MDR phenotype (Juliano et al. 1976). Subsequently, it was cloned from mouse and human cells by PCR amplification of the MDR locus (Ambudkar et al. 1999; Chen et al. 1986; Gros et al. 1986). The human *MDR1* gene is positioned on chromosome 7, region q21.1 (Ambudkar et al. 1999; Bellamy 1996; Callen et al. 1987; Chin et al. 1989). *MDR1* gene consists of 28 exons, encoding a 1280 amino acid transporter (~170 kDa) (Schwab et al. 2003). The structure of Pgp is composed of two homologous halves, each containing six trans-membrane domains and an ATP-binding/ hydrolyzing domain. These domains are connected to each other by flexible linker peptides (Ambudkar et al. 1999; Horio et al. 1988). From the 28 exons, 14 exons code for each half of the protein (Roninson 1991).

The expression of the Pgp in human tissues has being assessed by monoclonal antibodies against Pgp on frozen tissue sections. Pgp is expressed on apical surfaces of the cells. High level of Pgp is present in kidney and liver as well as on proximal tubule cells and hepatocytes (Ambudkar et al. 1999; Bellamy 1996). This pattern of expression is consistent with the activity of Pgp in secretion of xeno/ endobiotics into urine and bile. The expression of Pgp on mucosal surfaces of the lower gastrointestinal tract (jejunum, ileum, colon) epithelial cells suggest a role in preventing the uptake of substrates from the gastro intestinal tract (Thiebaut et al. 1987). Significant but lower level of expression of Pgp in the capillary endothelial cells in brain and testes are thought to play an important role in preventing the accumulation of drugs in brain and testis (Ambudkar et al. 1999; Bellamy 1996; Cordon-Cardo et al. 1989; Thiebaut et al. 1989). The expression of Pgp in placenta suggests its role in protecting the fetus from toxic xenobiotics (Ambudkar et al. 1999; Sugawara et al. 1988; Willingham et al. 1987).

Pgp bears a wide spectrum of substrate specificity with diverse chemical structures. Some of the substrates include drugs such as colchicine and tacrolimus, chemotherapeutic agents, etoposide, adriamycin and vinblastine, lipids, steroids, xenobiotics, peptides, bilirubin, cardiac glycosides such as digoxin, immunosuppressive agents (cyclosporine), glucocorticoids such as dexamethasone as well as HIV-type 1 antiretroviral therapy agents like protease inhibitors and non-nucleoside reverse transcriptase inhibitors.

Multi drug resistance protein (MRP)

Multi drug resistance (associated) protein1 (MRP1) was initially discovered by Cole et al. in H69 small cell lung cancer cells that showed multi drug resistance phenotype (Cole et al. 1992). Subsequently, MRP2 (gene *cMOAT*) was cloned in 1996 by Paulusma et al., and Konig et al. (Borst 2002; Konig et al. 1996; Paulusma et al. 1996). Genomic sequence analyses indicated the presence of number of potential ABC transporters, and as a result MRP3, 4 and 5 have been demonstrated to be functional transporters (Allikmets et al. 1996; Borst & Elferink 2002; Kool et al. 1997). With the addition of few more members MRP6, MRP7 (Borst & Elferink 2002; Hopper et al. 2001), MRP8 and MRP9 (Borst & Elferink 2002; Tammur et al. 2001) to the MRP family is expected to be completed.

Although all MRP1-5 are organic anion pumps, they differ in substrate specificity, tissue distribution and intracellular location. MRPs are broadly categorized into two structural groups; one with 17 trans-membrane segments (MRP1, 2, 3, 6) and another with 12 trans-membrane segments (MRP4, 5, 7, 8). It appears that TMD_0 does not play any role in catalytic function or in intracellular routing of MRP (Bakos et al. 1998; Borst & Elferink 2002). Structural studies on MRP by many individual groups are in process.

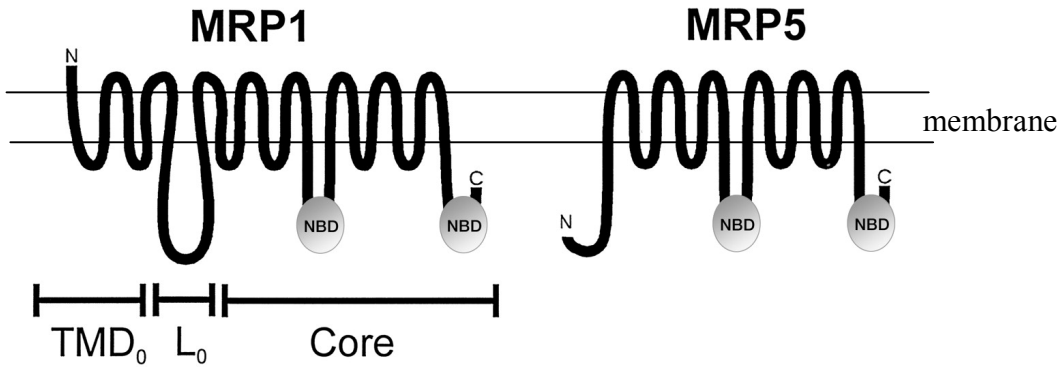

Figure 1.5 Topology of structural type I and II MRPs (Borst & Elferink 2002)

MRP1 is a versatile GSH conjugate pump which carries out the transport of variety of drugs conjugated to GSH, sulfate and glucuronate as well as unconjugated anionic drugs and dyes. It is seen that neutral/ basic amphipathic drugs are co-transported with GSH as well. Studies by Evers et al. have indicated that GSH acts stoichometrically during the co-transport (Borst & Elferink 2002; Evers et al. 2000). The substrate specificity of MRP2 is also similar to MRP1 (Borst & Elferink 2002; Konig et al. 1999; Renes et al. 2000) while, MRP3 differs by being unable to transport GSH. Although MRP4 and 5 both are organic anion pumps, they differ from other MRPs by their ability to transport cyclic nucleotides and nucleotide analogs. The substrate specificity of MRP6, still remains to be elucidated.

Studies conducted on evaluation of physiological functions of MRP1 indicate it to be a high affinity transporter of LTC_4. During normal physiological conditions MRPs play a protective role towards bone marrow precursor cells, testicles, inner ear and brain. Being an integral part of the epithelial cells of these sensitive organs, MRPs prevent the harm caused by accumulation of xeno/ endobiotics by active efflux of xeno/

endobiotics. Several independent studies have revealed that MRPs contribute significantly toward the transport of endogenous steroid conjugates (Borst & Elferink 2002; Hirohashi et al. 1999; Hirohashi et al. 2000; Zeng et al. 2000). The physiological functions of MRP4 and 5 are yet to be defined. Due to their ability to transport cyclic nucleotides, MRP4/ 5 may play a role in signal transduction by removal of cGMP.

The studies on tissue distribution of MRP1 show that it is expressed in virtually all human tissues, and in most human tumor cell lines. However tissue distribution of MRP2 and MRP3 are much more restricted than that of MRP1 (Borst & Elferink 2002; Dietrich et al. 2001a; Dietrich et al. 2001b; Fromm et al. 2000; Gotoh et al. 2000; Mottino et al. 2000; Schaub et al. 1997). Both are prominently present in liver, gut and kidney (Borst & Elferink 2002; Kool et al. 1997; Scheffer et al. 2002). Tissue specific expression of MRP4 and MRP5 has not been elucidated. Analyses of RNA from various tissues suggest a ubiquitous expression for MRP5 with high levels in skeletal muscle and brain (Belinsky et al. 1998; Borst & Elferink 2002; Kool et al. 1997; McAleer et al. 1999; Zhang et al. 2000). Human MRP6 is mostly expressed in kidney and liver (Belinsky et al. 1999; Borst & Elferink 2002; Kool et al. 1997; Kool et al. 1999).

Breast cancer resistance protein (BCRP/ ABCG2/ MXR)

Breast cancer resistance protein (BCRP) which belongs to ABCG2 subfamily of transporters was first discovered by Doyle et al. from a breast cancer cell line with MDR phenotype (Doyle et al. 1998; Krishnamurthy et al. 2006). The protein was thus named after the breast cancer cell line from which it was isolated, though its expression in breast cancer is generally low. Subsequently Allikmets and Miyake et al. independently isolated a cDNA identical to BCRP from human placenta (Allikmets et al. 1998; Krishnamurthy & Schuetz 2006) and from highly mitoxantrone resistant human colon carcinoma cell line (MXR) (Krishnamurthy & Schuetz 2006; Miyake et al. 1999), respectively.

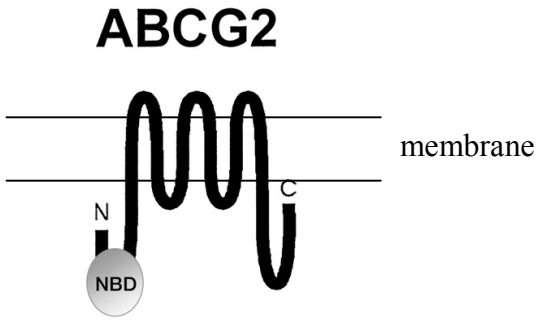

Figure 1.6 Topology of breast cancer resistant protein (BCRP/ ABCG2/ MXR) (Borst & Elferink 2002)

ABCG2 gene is localized at 4q22 between the markers D4S2462 and D4S1557 (Knutsen et al. 2000; Krishnamurthy & Schuetz 2006). The ABCG2 gene spans more than 66 kb and is compromised of 16 exons (ranging from 60 to 532 bp) and 15 introns (Bailey-Dell et al. 2001; Krishnamurthy & Schuetz 2006). ABCG2 differs from MRP and Pgp family of transporters by being a half transporter bearing a single nucleotide

binding domain (NBD) and six putative trans-membrane domains. The 3 N-linked glycosylation sites indicate that BCRP is a glycoprotein (Krishnamurthy & Schuetz 2006; Mohrmann et al. 2005). The transport function of the BCRP is acquired by homo dimerization of the protein. Homo dimerization was confirmed by the dissociation of 140 kDa ABCG2 complex into 70 kDa monomeric units under reducing conditions (Mohrmann et al. 2005).

The substrate specificity of BCRP includes a broad range of anti cancer drugs such as doxorubicin (DOX), etoposide, methotrexate and its polyglutamates, mitoxantrone, nucleoside drugs such as lamivudine (3TC), zidovudine (AZT), natural compounds such as flavonoids, sulfated estrogens, as well as protease inhibitors used for the treatment of HIV (Allen et al. 1999; Doyle et al. 1998; Krishnamurthy & Schuetz 2006; Litman et al. 2000; Miyake et al. 1999; Rabindran et al. 1998).

The results of a study where the expression of ABCG2 mRNA in 50 different human tissues analyzed revealed, that ABCG2 was not expressed in heart, lung, kidney, spleen, pancreas, skeletal muscle, thymus or peripheral blood leukocytes (Doyle et al. 2003; Krishnamurthy & Schuetz 2006). Placenta showed the highest expression of ABCG2, indicating the possibility of regulation of its expression by sex hormones. Liver and small intestine also display a high expression, while the expression in the blood brain barrier was comparable to that of Pgp (Cisternino et al. 2004; Cooray et al. 2002; Eisenblatter et al. 2003; Krishnamurthy & Schuetz 2006). During normal physiological conditions ABCG2 may play a role in protection of these tissues and organs from toxic accumulation of drugs and cytotoxins.

1.2.2 Non-ABC family of transporter proteins

In addition to the ATP binding cassette (ABC family) of proteins, there are other non-ABC family of proteins that mediate multi-drug resistance. These include the proteins that do not bear the typical structural motifs of the ABC proteins, trans-membrane helices, Walker motifs and the ABC-signature motif. Ral interacting protein (Ralbp1) and major vault protein (MVP) are two such examples.

Ral interacting protein 1 (Ralbp1)

In search of glutathione conjugate transporters, LaBelle et al. discovered DNP-SG ATPase from human erythrocytes. It was designated as DNP-SG ATPase after its ability to hydrolyze ATP in the presence of glutathione conjugates (LaBelle et al. 1986). Eventually its expression in other tissues was revealed (Sharma et al. 1990; Yadav et al. 2007). Crude membrane vesicles from human erythrocytes as well as the proteoliposomes reconstituted with purified DNP-SG ATPase from erythrocytes, catalyzed the transport of not only anionic glutathione conjugates but also cationic amphiphilic drugs such as doxorubicin and daunomycin (Awasthi et al. 1994; Awasthi et al. 2007; Singhal et al. 1991; Yadav et al. 2007).

The molecular identity of DNP-SG ATPase initially remained elusive due to the poor yield during purification as well as rapid proteolytic degradation. SDS-PAGE of the protein purified to homogeneity from erythrocytes as well as other tissues indicated a dominant peptide band with molecular weight of 38 kDa consistently along with several other peptides of higher molecular weight (Awasthi et al. 1998a; Awasthi et al.

1998b; Awasthi et al. 1994; Awasthi et al. 1991; Saxena et al. 1992; Sharma et al. 1990). In the beginning substrate stimulated activity of 38 kDa peptide lead to the erroneous conclusion of the molecular weight of the protein (Awasthi et al. 1991; Saxena et al. 1992; Singhal et al. 1991) which later proved to consist of the N and C terminal domains of the protein.

More direct evidence for the transport function of the DNP-SG ATPase was achieved by transport studies using artificial proteoliposomes to reconstitute transport activity. These studies established the characteristics of transport function, ATP dependence, temperature dependence, osmotic sensitivity, voltage insensitivity and saturable behavior with respect to ATP as well as the transported substrate (allocrite) (Awasthi et al. 2001; Awasthi et al. 2002; Awasthi et al. 1999; Drake et al. 2007; Sharma et al. 2004; Singhal et al. 2006a; Singhal et al. 2003; Singhal et al. 2006b; Singhal et al. 2005a; Singhal et al. 2005b; Stuckler et al. 2005; Yadav et al. 2004). Furthermore, the distinct nature of DNP-SG ATPase was confirmed by immunological studies (Awasthi et al. 1998a; Awasthi et al. 1998b; Awasthi et al. 1994).

Molecular identity of DNP-SG ATPase was obtained by screening human bone marrow expression library with antibodies against DNP-SG ATPase purified from erythrocytes (Awasthi et al. 2000). Anti DNP-SG ATPase antibodies were used to screen Ralbp1, which had been identified as a Ral effector protein with GTPase activity by other investigators (Jullien-Flores et al. 1995). Being able to purify the recombinant Ralbp1 with DNP-SG affinity chromatography, the same aberrant behavior in SDS-PAGE (Awasthi et al. 2003a; Awasthi 2006) and similar kinetics as to DNP-SG ATPase

(Awasthi et al. 2000; Singhal et al. 2001) all confirmed that DNP-SG ATPase and Ralbp1 to be identical.

Ralbp1 is ubiquitously expressed from Drosophila to humans (Cantor et al. 1995; Jullien-Flores et al. 1995; Park et al. 1995; Quaroni et al. 1999). The gene encoding Ralbp1 which consist of 11 exons and 9 introns is localized on chromosome 18p11.22. Ralbp1 is a 76 kDa protein with splice variants at 67 kDa, 80 kDa and 102 kDa (cytocentrin) (Hu et al. 2003; Quaroni & Paul 1999). Primarily it is expressed in the plasma membrane or nuclear membrane and also in cytoplasm, allied with the cytoskeleton.

Structural motifs of Ralbp1

Primary structure of Ralbp1 can be divided into four regions. N terminal domain (aa 1-209), is rich in antennapedia homeodomain homologous peptides. These peptides are known to be capable of transporting of wide range of substrates across membranes. Two central domains include, one carrying a Rac/CDC42 GAP (through aa 210-357) activity, while the other binds to activated Ral (aa 391- 499). A C-terminal coiled-coil domain (aa 500-647) has subsequently been shown to interact with Reps1/ POB1, cdc2(CDK1) and Hsf-1. These structural features link Ralbp1 to a confounding array of physiological functions including clathrin-coated-pit mediated receptor ligand endocytosis of epidermal growth factor receptor (EGFR), insulin receptor (IR) and transforming growth factor β (TGFβ) as well as mitosis signaling (Awasthi et al. 2003a; Matsuzaki et al. 2002; Oosterhoff et al. 2003; Quaroni & Paul 1999; Rosse et al. 2003).

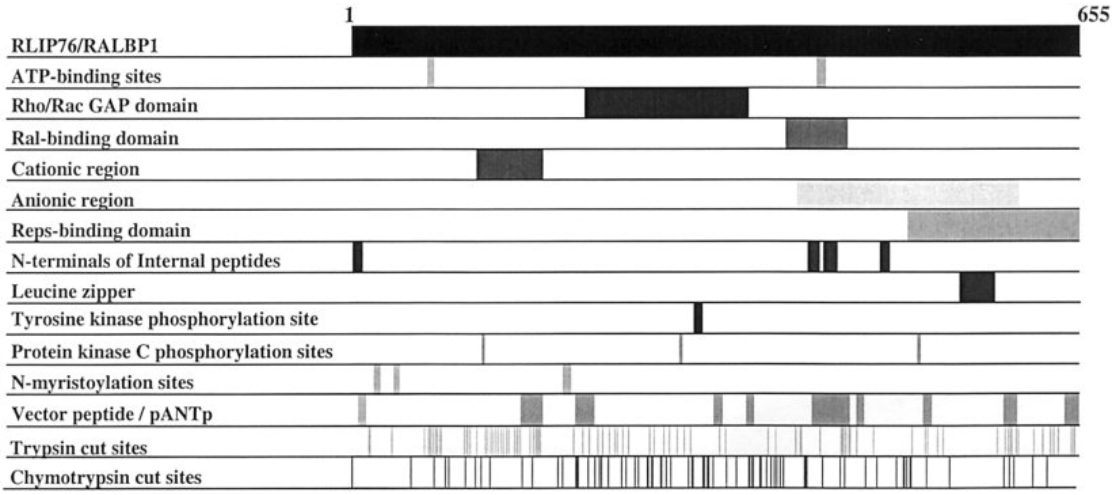

Figure 1.7 Potential structural motifs in primary structure of Ralbp1 (Awasthi et al. 2003a)

From the sequence alignment studies of Ralbp1 using Blast search engine the following sites were identified as potential candidate motifs in the primary structure of Ralbp1. N terminal and C terminal ATP binding domains at amino acids 69-74 and 418-425 respectively; several N-myristoylation sites were located at amino acids 21-26, 40-45 and 191-196; N-glycosylation site at amino acid 341-344; cyclic adenosine monophosphate (cAMP) binding site at amino acid 113-116; cAMP dependent protein kinase phosphorylation sites at amino acids 308-315; leucine zipper pattern at amino acids 547-578; several protein kinase C and casein kinase II phosphorylation sites and trypsin and chymotrypsin cut sites. Two ATP binding sites on N and C terminal domains (Awasthi et al. 2001), PKCα phosphorylation sites (Awasthi et al. 2002; Singhal et al. 2006b; Singhal et al. 2005a), several regions that have high sequence homology with the vector peptides and membrane associated proteins, that play an

important role in transport and membrane anchorage (Yadav et al. 2004) and a cell surface domain (Yadav et al. 2004) have being experimentally confirmed through site directed mutagenesis studies using substitution and deletion mutant analyses.

Role of Ralbp1 in endocytosis

Ralbp1 is a novel link between glutathione (GSH) linked oxidant defense, phase I and II biotransformation, stress signaling, receptor-ligand pair endocytosis and Ral and Rac-1 signaling pathways (Awasthi et al. 2000; Awasthi et al. 2003b; Awasthi et al. 1994; Cheng et al. 2001; Jullien-Flores et al. 1995; Morinaka et al. 1999; Yang et al. 2003). The role of Ralbp1 in G-protein signaling includes mainly its functions as an effector protein bridging Ras-Ral pathways. It is regulated by Ral and displays GTPase (GAP) activity (inhibitory) toward Rho proteins most importantly cdc42, a pro-apoptotic G-protein that exerts an inhibitory effect on Ras. Ralbp1 is also an integral component of complexes containing Ral, calthrin-adaptor protein AP2, POB1 (partner of Ralbp1) and Epsin which are involved in the clathrin-coated-pit mediated receptor ligand endocytosis, a mechanism for internalizing receptor-ligand pairs that terminate signaling.

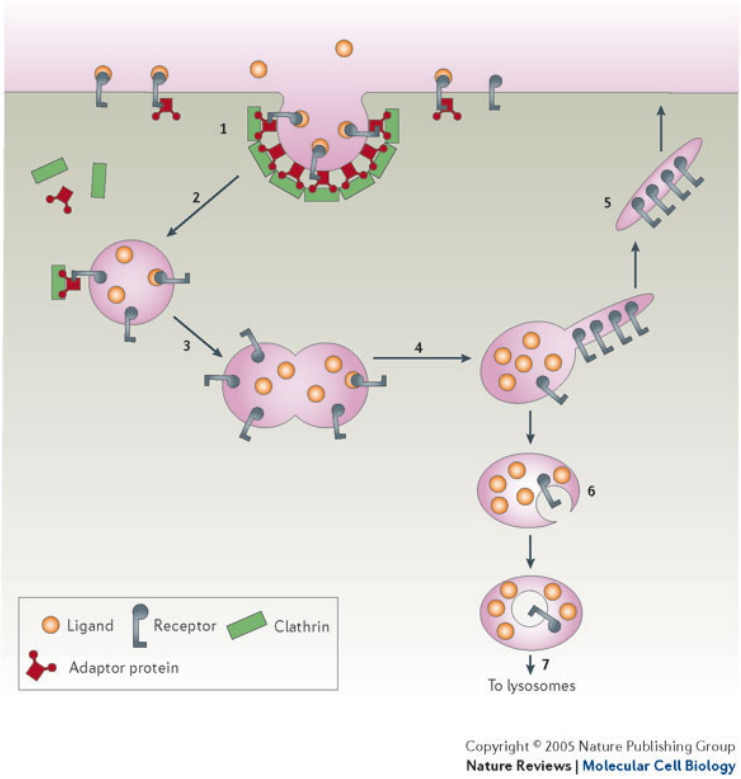

Figure 1.8 Pathway : receptor mediated endocytosis (Roth 2006)

As the pits are coated with receptor – ligand –clathrin – AP2 (adaptor protein)-Ralbp1-Epsin complexes, they deepen until they are pinched off from the membrane (1). Following internalization, the clathrin coat disassembles (2). The vesicle fuses with other newly uncoated vesicles or internalized membranes to form endosomes (3). The ligands are released (4), the receptors are recycled back to the membrane (5), and the ligands are degraded by fusing with the lysosomes (6)

Ralbp1 and POB1 are downstream molecules of small GTP binding protein Ral. The presence of EH domain in both Ralbp1 as well as POB1 suggest them to play a role in clathrin-dependent endocytosis (Morinaka et al. 1999). Upon investigation it has been seen this hypothesis to be true by both proteins being involved in receptor mediated endocytosis together with Epsin and EPS15. In the course of endocytosis Ralbp1, POB1, Epsin, EPS15 form a complex with alpha-adaptin of AP2. During the mitotic phase of the cell, complex formation is reduced by phosphorylation of Epsin by p34cdc2. Phosphorylation inhibits the complex formation by inhibiting the binding of POB1 to EH domain (Kariya et al. 2000; Paul et al. 1993; Quaroni & Paul 1999).

In the event of endocytosis, Ras activation activates RalGEFs which in turn activates Ral. Activated Ral associates with Ral effector Ralbp1 and recruited it to the membrane (Jullien-Flores et al. 2000). Ralbp1 sorts out the plasma membrane clathrin adaptor AP2 complex from the trans-golgi net work clathrin adaptor AP1 complex. AP2 works exclusively at plasma membrane while AP1 works at golgi network. Ralbp1 binds specifically with mu2 subunit of the AP2. C terminal domain of Ralbp1 is involved in EGF receptor endocytosis via an interaction with POB1 (Nakashima et al. 1999).

Requirement of GTPases at various stages of a coated pit cycle has been demonstrated in endocytosis assays in semi-intact cells (Carter et al. 1993; Jullien-Flores et al. 2000). Role of dynamin clearly established the requirement of GTP binding proteins at the stage of membrane docking of AP2 and the role during formation of coated pits remains to be elucidated. Membrane targeting and docking of AP2 rely on

the interaction of AP2 with phospholipids and integral membrane proteins. The mu 2 subunit is responsible for interactions with various cargo proteins with tyrosine based signal Y-X-X-O. Therefore mu 2/ Y-X-X-O serve as part of docking mechanism for the membrane requirement of AP2. Hence it is hypothesized that mu 2/ Ralbp1 interactions modulate the ability of mu 2 to bind Y-X-X-O signal containing proteins, thus regulating membrane association of AP2 and formation of coated pits.

Equilibrium between GTP and GDP-bound Ral could regulate the association of AP2 with the membrane. Trapping Ral in its GTP bound form stabilizes the mu/ Ralbp1 binding with membranes and thus disrupts the dynamic cycles of AP membranes interactions, i.e. association and dissociation that are required for coated pits assembly and disassembly (Jullien-Flores et al. 2000). Therefore Ral in its GTP bound from inhibits the endocytosis.

During mitotic phase POB1, Ralbp1 and Epsin are phosphorylated by p34cdc2. Phosphorylation of Ralbp1 does not effect binding with POB1 or vice versa. Receptor-mediated endocytosis is completely arrested during mitosis by disassembly of its complex with POB1 and alpha adaptin. Phosphorylated Ralbp1 may associate with centrosome. It is being hypothesized that during mitotic phase Ralbp1/ POB1 may interact with different proteins and function in assembly of mitotic apparatus as they are involved in assembly of receptor and endocytotic proteins during the interphase.

Ralbp1 in stress resistance

The stress inducible nature of Ralbp1 has being demonstrated in several different malignant cell lines, with various types of stresses, such as chemical (e.g. doxorubicin, naphthalene), oxidative (ROS), radiation (UV, x-ray) or heat (Awasthi et al. 2003a; Awasthi et al. 2005; Awasthi et al. 2004; Cheng et al. 2001; Yang et al. 2003). It has being experimentally established that Ralbp1 is required for PKCα mediated cell proliferation pathways (Singhal et al. 2006b; Singhal et al. 2006c) as well as for protection through heat shock proteins (HSPs) (Hu & Mivechi 2003; Kamal et al. 2003; Kampinga 2006; Sharma et al. 2001).

Depletion of PKCα causes a 30 % decrease in rate of proliferation of mouse embryonic fibroblast cells (MEFs). This decrease is absent in Ralbp1 gene knockout ($Ralbp1^{-/-}$) MEFs. PKCα stimulate doxorubicin resistance by increased efflux, in $Ralbp1^{+/+}$ MEFs while $Ralbp1^{-/-}$ MEFs lack this phenotype completely. These results lead to the definitive conclusion that Ralbp1 is downstream of PKCα and is required for PKCα mediated signal proliferation (Singhal et al. 2006b; Singhal et al. 2006c).

During normal physiological conditions, expression of HSPs are regulated by sequestering the transcription factor Hsf-1 by an interaction with Ralbp1 (Hu & Mivechi 2003). During heat shock, under the activation of Ral, Hsf-1:Ralbp1 complex dissociates and hence the expression of heat shock proteins are transcriptionally activated by Hsf-1 (Sharma et al. 2001). However despite the induction of HSPs, $Ralbp1^{-/-}$ mice are markedly sensitive to radiation, which could be overcome by intra-peritoneal administration of Ralbp1 in proteoliposomes (Awasthi et al. 2005). That is,

HSPs (known to be radiation protective proteins) also cannot function in the absence of Ralbp1.

1.3 The scope of the dissertation

Ralbp1 is linked with certain cellular functions including membrane plasticity and movement (as a primary 'effector' in the Ral pathway, perhaps functioning as a GTP-ase activating protein, or GAP), and as a component of clathrin coated pit mediated receptor ligand endocytosis – a process that mediates movement of membrane vesicles. In addition, the association of Ralbp1 to movement also occurs in context of the mitotic spindle, to which Ralbp1 migrates, from the endocytotic vesicle, during mitosis. It was unclear how these other functions were related to the fundamental biochemical observations that; 1) Ralbp1 is a very active ATPase, 2) that is stimulated further by certain compounds, 3) and it can couple the nucleotide hydrolysis to transport these compounds across membranes. It became clear that answers to these questions would only be elucidated through structure-function analyses that directly and specifically address the contribution of individual structural motifs in Ralbp1 towards its ATP-ase activity and transport-activity. Stated another way, construction of a mutant which lacked transport activity but not endocytosis, mitosis or GAP activity would be sufficient to affirm the null hypothesis that transport activity is not required for the other functions of Ralbp1 to occur. A long and complex series of experiments were undertaken to achieve the goals of these structure-function analyses. These studies ranged from the purification of glutathione *S*-transferases for the synthesis of the

glutathione-conjugate needed for affinity purification of Ralbp1 to site directed mutagenesis of Ralbp1 followed by *in vitro* analyses of functional effects.

CHAPTER 2

METHODS AND MATERIALS USED IN STRUCTURE FUNCTION ANALYSES

2.1 Abstract

In order to perform structure/ function analyses, there must be well defined measures of function, and well defined protocols for altering structure. The model system thus created should be able to effectively test the function of any given mutant. Using genetic techniques for silencing gene expression in cultured cells, and using mouse embryonic fibroblasts that completely lack Ralbp1, a reliable model system was designed to test the hypotheses that 1) Ralbp1 can associate with membrane, and 2) Ralbp1 glutathione-conjugate (GS-E) affinity and transport activity will directly determine various functional measurements.

2.2 Introduction and background

The overall goal of structure-function analyses is the identification of important elements of structure that impart a particular function. The precise definition of functions including accuracy and precision, and the use of a number of functions as endpoints for testing the hypothesis was considered a priority. In Dr. Awasthi's laboratory, methods had been established to measure certain characteristics of Ralbp1 including ATPase activity, substrate-stimulated ATPase activity, *in-situ* transport activity in artificial liposome and cell membrane liposomes, and cytotoxic protection in cultured cells. Additional methods established during the course of present studies included genetic methods for depletion and over-expression of Ralbp1, delivery of Ralbp1 purified protein encapsulated in liposomes, as well as a focused major effort on identification and generation of deletion and substitution mutants of Ralbp1, followed by their functional analysis.

The present study is divided into three phases. The first phase addressed the question of role of Ralbp1 as an arbitrator of PKCα mediated signaling pathways as a cause for differential drug resistance associated with diverse cell lines. Identification of membrane anchoring domains and the requirement of membrane anchorage for transport function of Ralbp1 was analyzed in phase two. The third phase addressed the question of whether GS-E transport activity is an integral requirement for manifestation of functional consequences such as drug-resistance, drug-accumulation defects, or endocytosis rates. During the analyses of first two questions, a novel combination of antibodies and siRNA were used for the suppression of wild-type protein present in

lung cancer cells. For the latter, we used Ralbp1 homozygous knockout mouse (Ralbp1$^{-/-}$ mouse) embryonic fibroblasts (MEFs) to measure the relative effects on restoration of functional activities including drug-resistance, drug-accumulation defects, and rate of endocytosis of fluorescence-tagged epidermal growth factor (EGF).

Though the ultimate experimental designs for these experiments were quite straightforward, a large number of methods needed to be established and standardized in order to assess the function of the mutants. These assays were first standardized using recombinant protein that is available in Dr. Awasthi's laboratory, expressed without any alterations. It is purified by dinitrophenyl *S*-glutathione (DNP-SG) affinity chromatography that was used to purify DNP-SG ATPase/ Ralbp1 from human tissues. This is a ligand affinity method in which the affinity matrix consist of BrCN-activated Sepharose 4B-DNP-SG. Optimal preparation of DNP-SG, however requires a large quantity of enzymatically active GST. For this, GSTs purified from mouse liver were used.

This chapter describes all the biological and biochemical methods and the materials (with their sources), used throughout the present study.

2.3 Materials

2.3.1 Reagents

Supplier

a. Sigma Aldrich, St. Louis, MO

I. Adenosine triphosphate (ATP), M.W. 507.1 ($C_{10}H_{16}N_5O_{13}P_3$)

II. Ammonium acetate, M.W. 77.1 ($NH_4C_2H_3O_2$)

III. β-mercaptoethanol (BME), M.W. 78.13 (C_2H_6OS)

IV. BrCN-activated Sepharose 4B resin

V. 1-Chloro 2,4-dinitrobenzene (CDNB), M.W. 202.5 ($C_6H_3ClN_2O_4$)

VI. Dimethylsulfoxide (DMSO), M.W. 78.1 (C_2H_6OS)

VII. Epoxy activated Sepharose 6B resin

VIII. Ethylene glycol tetraacetic acid (EGTA), M.W. 380.35 ($C_{14}H_{24}N_2O_{10}$)

IX. Ethylene diamine tetraacetic acid (EDTA), M.W. 292.2 ($C_{10}H_{16}N_2O_8$)

X. Ethanolamine (MEA), M.W. 61.1 (C_2H_7NO)

XI. Glutathione (GSH), M.W. 307.1 ($C_{10}H_{17}N_3O_6$)

XII. Geneticin (G418 disulfate salt), M.W. 692.7 ($C_{20}H_{40}N_4O_{10}.2H_2SO_4$)

XIII. Isopropyl β-D-1-thiogalactopyranoside (IPTG), M.W. 238.3 ($C_9H_{18}O_5S$)

XIV. Kanamycin, M.W. 484.5 ($C_{18}H_{36}N_4O_{11}$)

XV. Magnesium chloride, M.W. 95.0 ($MgCl_2$)

XVI. Melphalan (MEL), M.W. 305.1 ($C_{13}H_{18}C_{12}N_2O_2$)

XVII. Polidocanol ($C_{12}E_9$)

XVIII. 3-(4,5-dimethylthiazol-2-yl)-2,5-diphenyltetrazolium bromide (MTT), M.W. 414.3 ($C_{18}H_{16}BrN_5S$)

XIX. Phenylmethylsulfonyl fluoride (PMSF), M.W. 174.1 ($C_7H_7FO_2S$)

XX. Perchloric acid, M.W. 100.4 ($HClO_4$)

XXI. Sodium hydrogen carbonate, M.W. 84 ($CHNaO_3$)

XXII. Tris(hydroxymethyl)aminomethane (Tris-HCl), M.W. 121.1 ($C_4H_{11}NO_3$)

XXIII. 60% Acrylamide bis-acrylamide

XXIV. Ammonium persulfate (APS), M.W. 228.2 ($(NH_4)_2S_2O_8$)

XXV. SDS-PAGE sample buffer, pH 6.8

XXVI. N,N,N',N',-tetramethylethylenediamine (TEMED), M. W. 116.2

XXVII. Glycine, M. W. 75 ($C_2H_5NO_2$)

XXVIII. Ethidium bromide (EtBr), M.W. 394 ($C_{21}H_{20}BrN_3$)

XXIX. Ficol

XXX. Calcium chloride, M.W. 111 ($CaCl_2$)

XXXI. Dithiothritol (DTT), M.W. 154 ($C_4H_{10}O_2S_2$)

XXXII. Potassium acetate (KAc), M.W. 98 (CH_3COOK)

XXXIII. Bradford reagent

XXXIV. Hydrogen peroxide, M.W. 34 (H_2O_2)

XXXV. Soybean asolectin

XXXVI. Cholesterol

XXXVII. Scintillation fluid

XXXVIII. Agarose

XXXIX. Formaldehyde, M.W. 30 (CH_2O)

XL. 3-[N-morpholino]propane sulfonic acid (MOPs), M.W. 209.2 ($C_7H_{15}NO_4S$)

b. Gibco life sciences, CA

I. RPMI-1640 medium

II. Sodium pyruvate (100 mM)

III. Heat inactivated fetal bovine serum certified

IV. Penicillin-streptomycin (100X)

V. Tryphan blue stain 0.4 %

VI. Phosphate-buffered saline (PBS)

VII. Trypsin-EDTA

VIII. HEPES (10 mM)

IX. Hank's balanced salt solution (HBSS) without calcium chloride, magnesium chloride or magnesium sulfate

X. Glucose (4.4 g/L)

XI. Sodium bicarbonate (1.5 g/L)

c. Adria laboratories, Columbus, OH

I. Doxorubicin (Adriamycin), M.W. 543.5 ($C_{27}H_{29}NO_{11}$)

d. Whatman International Ltd., Madison, England

I. Diethylaminoethyl cellulose (DE-52) anion exchanger

e. Bio-Rad laboratories, Hercules, CA

I. Bio-Beads (SM-2 adsorbant)

II. Butylhydroxytoluene (BHT), M.W. 220.3 ($C_{15}H_{24}O$)

III. Broad range protein molecular weight marker

IV. Sodium dodecyl sulfate (SDS), M.W.288.4 ($C_{12}H_{25}NaO_4S$)

V. 3-(N-morpholino) propanesulfonic acid (MOPS), M.W. 209.2 ($C_7H_{15}NO_4S$)

VI. Sucrose, M.W. 342.3 ($C_{12}H_{22}O_{11}$)

f. Amersham Corp., Arlington Heights, IL

I. [^{14}C]Doxorubicin (specific activity, 57 mCi/mmol)

g. Em science, Gibbstown, NJ

I. Boric acid, M.W. 61.8 ($H_2B_4O_7$)

II. Chloroform, M.W. 119.4 ($CHCl_3$)

III. Potassium phosphate (dibasic), M.W. 174.1 (HK_2PO_4)

IV. Potassium phosphate (monobasic), M.W.136 (H_2KPO_4)

V. Hydrochloric acid, M.W.63.4 (HCl)

VI. Sodium acetate, M.W. 82.0 (CH_3COONa)

VII. Sodium chloride, M.W. 58.4 (NaCl)

VIII. Sodium borate, M.W. 127.7 (BNa_3O_3)

IX. Potassium chloride, M.W. 74.5 (KCl)

h. Mallinckrodt, Phillipsburg, PA

I. Phosphoric acid, M.W.98 (H_3PO_4)

II. Methanol (MeOH), M.W.32 (CH_4O)

III. Acetonitrile, M.W. 41 (C_2H_3N)

IV. Ethyl alchol (EtOH), M.W. 46 (C_2H_5OH)

i. Moravek Biochemicals Inc., CA

I. [^{14}C]-Melphalan

j. Fisher Scientific, PA

I. Paraformaldehyde

2.3.2 Supplies used for molecular biological procedures

A. Thermophilic DNA polymerase (vent DNA polymerase) (2 000 U/mL) (New England Biolabs, Beverly, MA)

B. Restriction endonuclease BamH I (20 000 U/mL) (New England Biolabs, Beverly, MA)

C. Restriction endonuclease Xho I (20 000 U/mL) (New England Biolabs, Beverly, MA)

D. NE buffer 2 (10X) (New England Biolabs, Beverly, MA)

E. Bovine serum albumin (BSA) (100X) (New England Biolabs, Beverly, MA)

F. Magnesium chloride ($MgCl_2$) (100 mM) (New England Biolabs, Beverly, MA)

G. T4 DNA ligase (400 000 cohesive end units/ mL) (New England Biolabs, Beverly, MA)

H. Deoxynucleotides (dNTPs) (Applied Biosystems, CA)

I. HPLC grade oligo nucleotide primers (Biosynthesis Inc., TX),

J. Prokaryotic expression vector pET30a(+) (Novagen Inc., WI)

K. Competent *E. coli* DH5α (Invitrogen, CA)

L. Competent *E. coli* BL21(DE3) (Invitrogen, CA)

M. NZY^+ broth (Invitrogen, CA)

N. Trypton (for culture media) (Difco laboratories, Detroit, MI)

O. Yeast (for culture media) (Difco laboratories, Detroit, MI)

P. 1 kB DNA ladder (Invitrogen, CA)

Q. Reverse transcriptase (Invitrogen, CA)

R. Reverse transcriptase buffer (5X) (Invitrogen, CA)

2.3.3 Kits

A. TransMessenger transfection reagent (Qiagen, CA)

B. QuickChange II site directed mutagenesis kit (Stratagene, CA)

C. Mini prep plasmid purification kit (Qiagen, CA)

D. QIAquick gel extraction kit (Qiagen, CA)

E. RNeasy mini kit (Qiagen, CA)

2.3.4 Others

A. Gene specific siRNA (experimental) and scrambled siRNA (negative control) (Dharmacon research laboratories, CO)

B. Polyclonal rabbit anti-human rec-Ralbp1 IgG and pre immune IgG were prepared and purified as described previously (Awasthi et al. 2000; Awasthi et al. 2001)

C. Custom made polyclonal antibodies against various regions of Ralbp1 (Alpha Diagnostics, San Antonio, TX)

D. Human herceptin (her2/neu) antibodies (Genentech Inc., CA)

E. Human IgG (Baxter Healthcare Corp, CA)

F. FITC-conjugated goat anti-rabbit and FITC-conjugated goat anti-human antibodies (Vector laboratories Inc., Burlingame, CA)

G. Rhodamine red x-conjugated goat anti-rabbit antibodies (Jackson Immuno Research laboratories (West Grove, PA)

H. Tetramethyl rhodamine conjugated Epidermal growth factor (rhodamine EGF) (Molecular probes, OR)

I. Mounting media (Vector laboratories, CA)

J. Nucleic acid stain DAPI (Molecular Probes, OR)

K. Horseradish peroxidase-conjugated goat anti-rabbit secondary antibodies (Sigma Aldrich, MO)

L. Lipofectamine 2000 reagent (Invitrogen, CA)

2.3.5 Buffers

1. Potassium phosphate buffer (1 M monobasic and 1 M dibasic potassium phosphate buffer pH 7.2)
2. GST assay buffer (100 mM potassium phosphate buffer pH 6.5)
3. GST elution buffer (50 mM Tris-HCl pH 9.6 containing 1.4 mM BME, 10 mM GSH final pH 7.2)
4. Linking buffer (44 mM sodium hydrogen phosphate and potassium phosphate buffer pH 7.0)

5. Affinity buffer (22 mM phosphate buffer containing 1.4 mM BME pH 7.0)
6. Coupling buffer (0.1 M sodium hydrogen carbonate containing 0.5 M sodium chloride pH 7.9)
7. Buffer A (10 mM potassium phosphate buffer pH 7.0)
8. Buffer B (22 mM potassium phosphate buffer pH 7.0)
9. Ralbp1 Washing buffer (Ralbp1 lysis buffer containing 150 mM NaCl, 9.9 mM EDTA and 0.01 % SDS, pH 7.4)
10. Ralbp1 Lysis buffer (10 mM Tris-HCl pH 7.4 containing 50 µM BHT, 0.1 mM EDTA, 100 µM PMSF, and 1.4 mM BME)
11. Ralbp1 Elution buffer (Ralbp1 lysis buffer containing 10 mM $MgCl_2$, 10 mM ATP, 0.025 % Polidocanol, 0.2 mM DNP-SG)
12. Reconstitution buffer (10 mM Tris-HCl pH 7.4 containing 4 mM $MgCl_2$, 1 mM EGTA, 10 mM KCl, 40 mM sucrose, 2.8 mM BME, 0.05 mM BHT, 0.025 % Polidocanol)
13. Transport buffer (10 mM Tris-HCl pH 7.4, containing 4 mM $MgCl_2$, 1 mM EGTA, 100 mM KCl, 40 mM sucrose)
14. 0.5 M potassium chloride in 0.1 M sodium acetate, pH 4.0
15. 0.5 M potassium chloride in 0.1 M sodium borate, pH 8.0
16. TAE buffer (40 mM Tris-HCl pH 8.3 containing 2 mM EDTA, 10 mM sodium acetate)

17. RNA running buffer (40 mM MOPS containing 2 mM EDTA and 10 mM sodium acetate, pH 7.0)
18. Sigma DNA loading buffer (20 % ficol 400, 0.1 M EDTA, 1 % SDS and 0.25 % bromophenol blue, pH 8.0)
19. Sigma protein loading buffer (6 % glycerol, 0.2 M BME, 2 % SDS, 0.002 % bromophenol blue in 0.0625 M Tris-HCl, pH 6.8)
20. Sigma Bradford reagent (85 % phosphoric acid, Coomassie brilliant blue G-250, 95 % methanol, water)

2.3.6 Cell lines

A. Wild type mouse embryonic fibroblast cells ($MEFs^{+/+}$)
B. Ralbp1 gene knockout embryonic fibroblast cells ($MEFs^{-/-}$)
C. Human small cell lung cancer (SCLC) cell lines, H182, H1417, H1618 (American Type Culture Collection (ATCC), Manassas, VA)
D. Human non small lung cancer (NSCLC) cell lines. H226 (squamous cell carcinoma), H1395, H2347 (adenocarcinoma), H358 (bronchio alveolar) (American Type Culture Collection (ATCC), Manassas, VA)

2.4 Methods

2.4.1 Preparation of affinity resin for the purification of glutathione S-transferases (GST)

Isoenzymes of GSTs from mice liver were purified by affinity chromatography using epoxy activated sepharose 6B resin with covalently attached GSH groups, utilizing the high affinity of GSTs towards GSH.

Sepharose 6B resin which was purchased from Sigma-Aldrich as a lyophilized powder was soaked in de-ionized water for several hours at 4 ^{o}C to obtain a 3.5 fold increase in the volume. The resin was then washed twice with linking buffer. Since GSH tend to undergo oxidation to form GS-SG, the derivatization was carried out under nitrogen. In order to couple the GSH molecules, the resin was incubated with 0.1 % GSH solution at 37 ^{o}C for 12 h with gentle shaking. Afterwards the un-reacted GSH was removed by washing with de-ionized water. Then the unreacted epoxy groups were blocked by incubating with 1 M ethanolamine, pH 8.0 for 3 h at room temperature with gentle shaking. Upon completion the excess ethanolamine molecules were removed with de-ionized water. Then the resin was further equilibrated with buffers, KCl/ CH_3COONa followed by KCl/ Na_3BO_3 and affinity buffer in the particular order to facilitate the ionic strength and the pH of the resin optimum for the binding with the GSTs.

2.4.2 Determination of GST activity

The purification was monitored using GST-activity towards CDNB. One unit (1 U) enzyme activity was defined as 1 µmol/min product (DNP-SG) formation at 25 ^{o}C. This assay is based on the following substitution reaction:

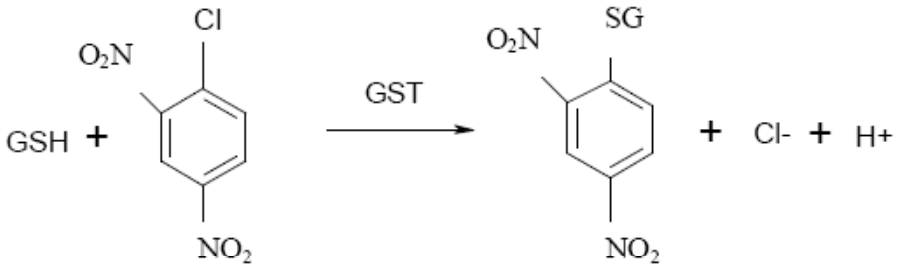

Figure 2.1 Synthesis of DNP-SG

CDNB is a high-affinity substrate of GST. The reaction product, 2,4-dinitrophenyl-*S*-glutathione (DNP-SG) formation at room temperature, was assessed by measuring the absorbance at 340 nm since the molar extinction coefficient of DNP-SG (9.6 $mM^{-1}cm^{-1}$) was significantly greater than that of CDNB (0.6 $mM^{-1}cm^{-1}$) (Awasthi et.al 2007). During the GST activity measurement the concentration of the two substrates, CDNB and GSH were maintained such that the enzymes (GSTs) were saturated. Hence the rate of the reaction or the activity of the enzyme is directly proportional to the amount of enzyme present in the reaction. The amount of each reactant component used is indicated in the table below.

Table 2.1 Schematic protocol for GST assay in a 1.5 mL cuvette

Component	Blank	Experimental
GST Assay Buffer (µL)	850	830
10 mM GSH (µL)	100	100
20 mM CDNB (µL)	50	50
Enzyme (GSTs) (µL)	-	20

The reaction components were added to the cuvette in the order: 1) GST assay buffer, 2) GSH, 3) CDNB followed by 4) enzyme (GSTs). The components were mixed together by inverting the cuvette and the absorbance at 340 nm was measured immediately. A reaction mixture consisting of the two substrates GSH and CDNB in GST assay buffer excluding the enzyme (GSTs) was used as the blank. Each reaction was carried out in triplicate.

2.4.3 Purification of GSTs from mouse liver

The glutathione *S*-transferase (GSTs) family of enzymes consist of several cytosolic, mitochondrial and microsomal proteins, which play a key role in detoxification of wide range of xeno and endobiotics. These enzymes contribute to the phase II biotransformation of a wide variety of electrophilic substrates by conjugation of reduced glutathione (GSH) and thereby increasing the solubility and excretion. Although GSTs are distributed throughout the body, animal liver, the organ in which the detoxification occurs extensively comprises more GSTs than the other organs.

Therefore mouse liver was used for the purification of GSTs using GSH-affinity chromatography.

GSTs from the mouse liver were purified according to the procedure published by Singhal et al. (Singhal et al. 1992a; Singhal et al. 1992b). Wild type male mouse liver (1 g) was chopped and transferred to a corex tube and washed with PBS. A 10 % homogenate was prepared by addition of 10 mL of buffer A and homogenizing for 15 s, twice with the aid of a tissuemizer (Tekmar Company). The supernatant was collected after centrifugation for 45 min at 28,000 x g at 4 ^{o}C. From the supernatant, 200 µL was separated to determine the GST activity in the crude fraction. The rest of the protein was dialyzed in buffer A, overnight. After dialysis the crude protein extract was transferred to a corex tube and centrifuged at 28,000 x g for 30 min at 4 ^{o}C. A 50 µL aliquot was separated for GST activity measurements and the rest of the supernatant fluid was applied on GSH-Sepharose affinity resin (1 mL of resin binds up to 2 mg GST protein in the homogenate). The homogenate was incubated with the resin at 4 ^{o}C with gentle shaking, over night. The supernatant fluid containing the unbound protein was discarded after centrifugation at 1,000 x g for 4 min at 4 ^{o}C. The resin was washed with buffer B several times until the O.D. at 280 nm became zero. Once the non-specifically bound proteins were washed off from the column, GSTs were eluted with elution buffer (2.5 mL each time twice). Each time the resin was incubated with elution buffer for 10 min at 4 ^{o}C with gentle shaking, followed by centrifugation at 2,000 x g for 4 min at 4 ^{o}C. The supernatant fraction (purified GST) was dialyzed against buffer A over night at

4 ^{o}C. A sample (~ 50 µL) from the supernatant fraction, before dialysis was separated for GST activity measurements. Purified GST was stored at 4 ^{o}C.

Three separate purifications were carried out from male mouse liver. Fold purification at each step was determined by preparation of purification table by determining the concentration of protein and GST activity against CDNB, at each step. Bradford assay was used to determine the protein concentration.

Table 2.2 Purification table for GSTs from mouse liver[1]

Fraction	Volume	Activity (U/mL)	Protein (mg/mL)	Activity (U)	Sp. Act. U/mg	Yield (%)
28,000 x g supernatant fraction before dialysis	10 mL	8.9	5.7	89	1.56	100
after dialysis	10 mL	8.4	5.2	84	1.62	81.1
GST activity unabsorbed fraction	10 mL	0.7	4.4	7	0.16	4.1
GSH affinity chromatography before dialysis	5 mL	13.8	0.38	69	36.3	78
after dialysis	5 mL	13.2	0.36	66	36.7	74

[1]Spectrophotometric method was used to assay GST, with CDNB as the model substrate. Each measurement was performed in triplicate. Activity was calculated using the equation (slope x factor x dilution x homogenate percentage) U/mL. Specific activity was determined by dividing the total activity by the amount of total protein. Percent yield of purification was defined as the ratio of activity of the purified fraction and activity of the crude fraction.

The amount of total protein in the initial tissue homogenate (28,000 x g supernatant fraction) was 57 mg/g tissue. With a steady decrease in the amount of total protein with each subsequent purification step, the concentration of the protein in the purified fraction was 1.8 mg/g. Concurrently the total GST activity 89 units, of the initial fraction decreased to 66 units upon completing the purification. The specific activity on the other hand increased with each purification fold, being 1.56 U/mg in the initial homogenate and increasing up to 36.7 U/mg in the purified GST.

GST consists of several isozymes and the level of expression of isozymes varies from one species to another as well as the tissue. Human liver has a higher expression of GSTα while mouse liver has a higher expression of GST pi (Singhal et al. 1990, Singhal et al. 1992). The SDS-PAGE, of purified GST from mouse liver consisted of three distinct molecular weight bands seen at 23 kDa, 25 kDa and 26.5 kDa. These are known to correspond to pi, alpha and mu isozymes of GST, with GST pi as the predominating isozyme. Importantly, no other significant protein contaminants were seen. The activity assays confirmed that the enzyme was active. This purified fraction was used for the enzymatic synthesis of DNP-SG.

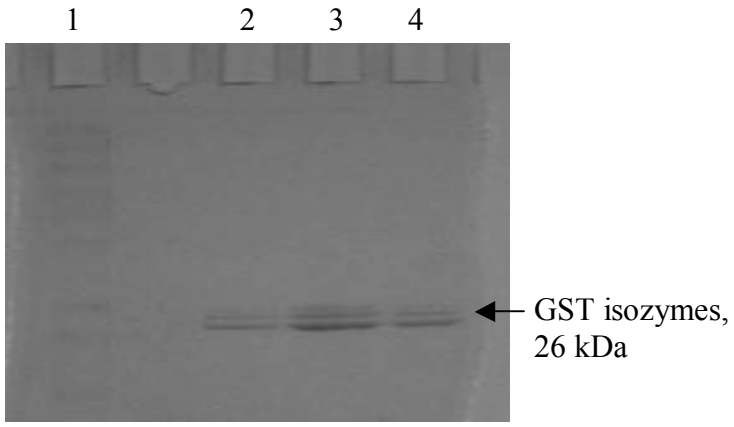

Figure 2.2 Coomassie-Stained SDS-PAGE of purified GST from mouse liver

Samples in the gel were as follows; broad range protein Ladder (lane 1), purified GST isozymes (sample 1-3) (lanes 2-3)

2.4.4 Synthesis of 2,4-dinitrophenyl S-glutathione (DNP-SG)

Ralbp1, previously referred to as DNP-SG ATPase, can be purified by DNP-SG affinity chromatography due to its high affinity towards DNP-SG. Indeed, the recombinant Ralbp1 protein expressed in bacteria is still purified using essentially the same DNP-SG-affinity chromatography method used for purification of DNP-SG ATPase from eukaryotic tissues (Sharma et al. 1991). Thus, it was necessary to prepare DNP-SG affinity resin for purification and studies of recombinant Ralbp1. DNP-SG was synthesized by an enzymatic pathway utilizing GST to catalyze the reaction between two substrates, GSH and CDNB utilizing a procedure described by Awasthi (Awasthi et al. 1981).

Two substrates, GSH (15 mM) and CDNB (400 mM) were reacted in the presence of the catalyzing enzyme, GST (5 U) under anaerobic conditions protected

from light. The reaction was carried overnight. Un-reacted CDNB was removed from the product by washing with ethanol. The products were further purified by carrying out thin layer chromatography (TLC) with acetonitrile and de-ionized water with a ratio of 7:2 as the mobile phase. The bright yellow spot corresponding to DNP-SG was scraped off and extracted with de-ionized water to obtain pure DNP-SG. The purity and concentration of the product DNP-SG was determined by scanning the absorbance spectra in the wavelength range 200 – 500 nm and measuring the absorbance at 340 nm. Concentration was calculated using the Beer-Lambert law, using the molar extinction coefficient of DNP-SG at 340 nm as 9.6.

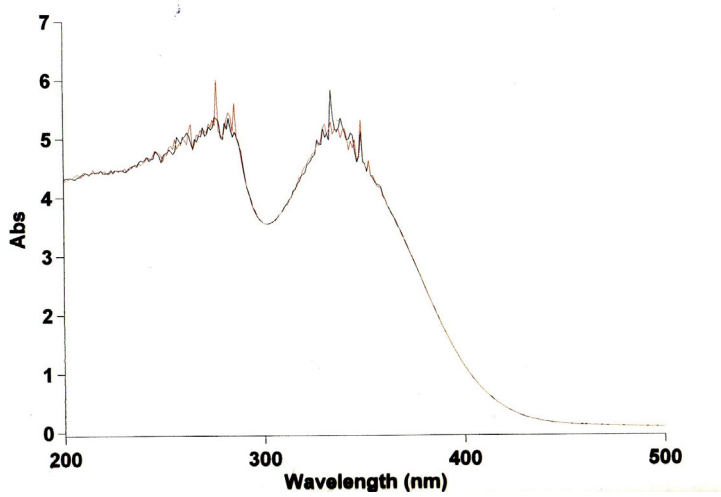

Figure 2.3 Absorbance spectrum of DNP-SG – first fraction

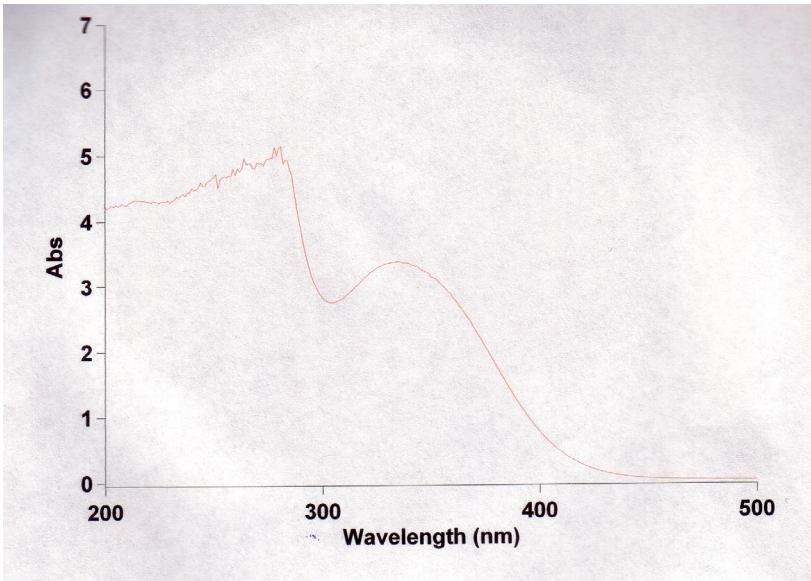

Figure 2.4 Absorbance spectrum of DNP-SG – second fraction

2.4.5 Molecular cloning

cDNA encoding human Ralbp1 gene was amplified by polymerase chain reaction (PCR), using prokaryotic plasmid vector, pET30a(+) cloned with Ralbp1 as the template. The PCR reaction conditions consisted of an initial denaturing step of 5 min at 95.0 ^{o}C followed by 30 cycles of 30 s at 95.0 ^{o}C, 30 seconds at 60.0 ^{o}C and 1 min at 72.0 ^{o}C. The final extension step consisted of 7.0 minutes at 72.0 ^{o}C. The sequence of the forward and the reverse primers used during the PCR were as follows.

Forward primer 5'-GGCGGATCCATGACTGAGTGCTTCCT-3'

Reverse primer 5'-CCGCTCGAGTAGATGGACGTCTCCTTCCTATCCC-3'

Two restriction endonuclease sites BamH I (forward primer) and Xho I (reverse primer) are underlined.

The composition of the PCR reaction mixture consisted of 500 ng of DNA template, forward and reverse primers (30 pmol each), 2.5 µM dNTPs, 1X thermopol buffer, 1X BSA and 2.5 units of vent DNA polymerase. Amplified PCR product of Ralbp1 (1968 bp) was separated from un-reacted primers and template DNA by carrying out 1 % agarose gel electrophoresis and gel-purified with the aid of QIAquick gel extraction kit from Qiagen as described in the methods. Gel-purified PCR product was then digested with restriction endonucleases BamH I and Xho I, over night.

In order to create a recombinant Ralbp1 vector construct that could be expressed in *E. coli*, the gene encoding human Ralbp1 which was amplified by PCR was cloned into the prokaryotic expression vector pET30a(+) from Novagen, CA. The plasmid vector map and the sequence landmarks of pET30a(+) are as given bellow.

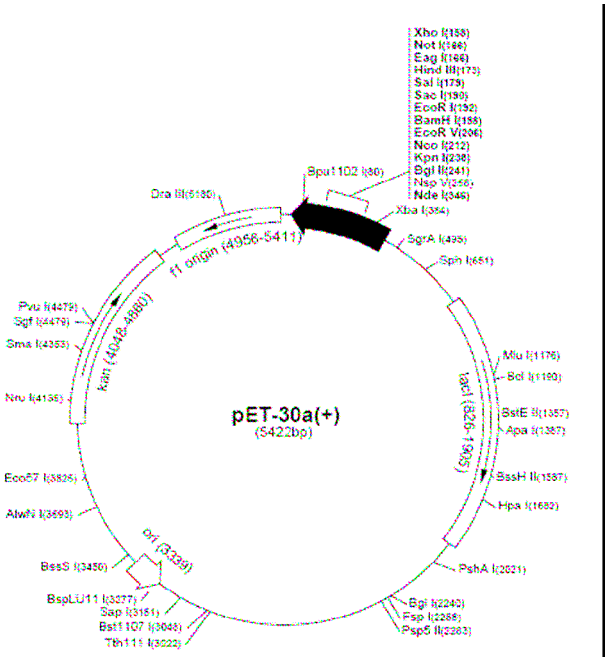

Figure 2.5 Plasmid map of prokaryotic expression vector pET30a(+) (Novagen, CA)

Table 2.3 pET30a(+) sequence landmarks (Novagen, CA)

Feature	Nucleotide position
T7 Promoter	419 -435
T7 Transcription start	418
His Tag coding sequence	327 -344
S Tag coding sequence	249 - 293
Multiple cloning sites (Nco I – Xho I)	158 - 217
His Tag coding sequence	140 -157
T7 Terminator	26 -72
lacI coding sequence	826 - 1905
pBR322 origin	3339
Kanamycin coding sequence	4048 - 4860
f1 origin	4956 - 5411

To facilitate the ends compatible with the gene to be cloned (Ralbp1 flanked by restriction endonucleases BamH I and Xho I) prokaryotic plasmid vector pET30a(+) was also digested with restriction endonucleases BamH I and Xho I. Both linearized pET30a(+) plasmid vector and the amplified Ralbp1 gene was separated from undigested DNA by carrying out 1 % agarose gel electrophoresis and gel purified as mentioned before.

Concentration of the linearized vector and the insert DNA (Ralbp1) was determined by measuring the absorbance at 260 nm. Ligation reactions were carried out using T4 DNA ligase from New England Biolabs with a vector DNA to insert DNA in a ratio of 1:3. The composition of the ligation reaction mixture included T4 DNA ligase buffer (1X), vector DNA, insert DNA, T4 DNA ligase (400,000 U/ml) and de-ionized water to get a final volume of 20 µl. Reactions were carried out at room temperature (~ 25 ^{o}C) for 2 h. Upon completion, chemically competent *E. coli* DH5α (Invitrogen, CA) were transformed with 10 µL of the ligation mixture.

Prokaryotic plasmid vector pET30a(+) consists of gene encoding kanamycin resistance. Hence competent *E. coli* cells transformed with successfully ligated plasmid construct were screened by kanamycin resistance.

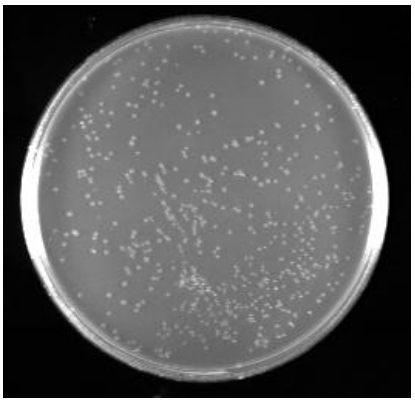

Figure 2.6 *E. coli* DH5α competent cells transformed with pET30a(+)-Ralbp1 cultured on LB agar containing kanamycin (50 µg/mL)

Several colonies were screened for the success of the ligation by purifying plasmid DNA from several over night cultures formed by inoculating a single colony in 10 mL of LB media containing kanamycin (50 µg/mL). Plasmid DNA was purified using QIAprep Spin Miniprep Kit from Qiagen according to the manufacture's protocol. An aliquot of each DNA sample was digested with restriction endonuclease BamH I and Xho I and analyzed by 1 % agarose gel electrophoresis.

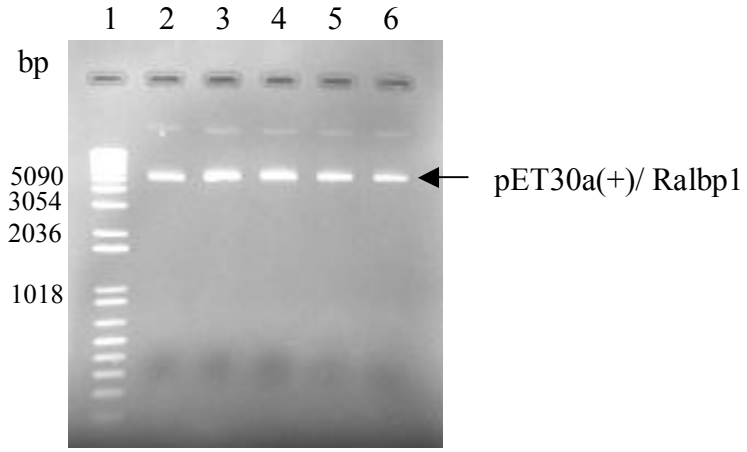

Figure 2.7 pET30a(+) cloned with Ralbp1 undigested samples 1-5

Samples in the gel were as follows; 1 kB plus DNA ladder (lane 1), pET30a(+)/ Ralbp1 samples 1-5 (undigested) (lanes 2-6)

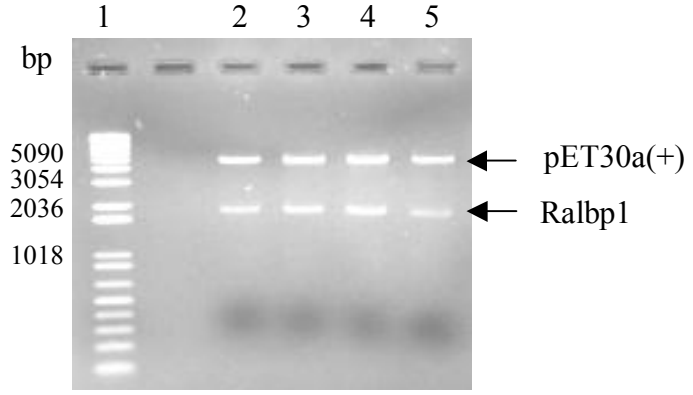

Figure 2.8 pET30a(+) cloned with Ralbp1 digested with BamH I and Xho I

Samples in the gel were as follows; 1 kB plus DNA ladder (lane 1), pET30a(+)/ Ralbp1 samples 1-4 (digested with BamH I and Xho I) (lanes 2-5)

2.4.6 Preparation of cyanogen bromide (BrCN)-activated Sepharose 4B resin

Recombinant Ralbp1 was purified from a bacterial culture using BrCN-activated Sepharose 4B resin derivatized with DNP-SG, utilizing the high affinity of Ralbp1 towards DNP-SG.

BrCN-activated Sepharose 4B resin which was purchased from Sigma-Aldrich as a lyophilized powder was equilibrated with 1 mM HCl twice, protected from light, at 4 ^{o}C for 30 min each time. Afterwards the resin was equilibrated with coupling buffer twice. In order to covalently attach the DNP-SG groups, the resin was equilibrated with 3 mM DNP-SG in coupling buffer at 4 ^{o}C for 12 h protected from light. Upon completion, excess, unbound DNP-SG was removed by washing the resin with coupling buffer. Un-reacted active sites were then blocked by equilibrating the resin with 1 M ethanolamine at room temperature for 4 h. The resin was further equilibrated with 0.1 M sodium acetate buffer containing 0.5 M KCl, pH 4.0 followed by 0.1 M sodium borate buffer containing 0.5 M KCl, pH 8.0 and coupling buffer in order to obtain the optimum pH and ionic strength to facilitate the binding of Ralbp1 with the attached DNP-SG groups on the resin.

2.4.7 Purification of recombinant Ralbp1 from E. coli BL21(DE3)

Recombinant Ralbp1 protein was purified using a prokaryotic expression system *E. coli* BL21(DE3) (Invitrogen, CA). An aliquot of *E. coli* BL21(DE3) was transformed with 1 μL of pET30a(+) cloned with Ralbp1. Transformed colonies were

screened using antibiotic kanamycin (50 μg/mL) resistance since plasmid pET30a(+) consists of kanamycin resistance.

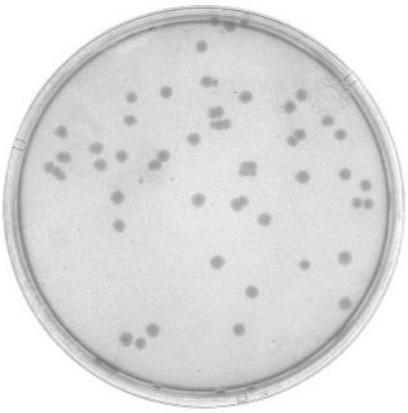

Figure 2.9 *E. coli* BL21(DE3) transformed with pET30a(+)/ Ralbp1 cultured on LB agar containing kanamycin (50 μg/mL)

Recombinant Ralbp1 was purified by forming a primary culture by inoculating a single *E. coli* BL21(DE3) colony in 3 mL of LB media containing kanamycin (50 μg/mL) and incubating at 37 ^{o}C, over night shaking at ~225 rpm. Primary culture was then diluted 100 fold, to obtain a secondary culture. During the construction of pET30a(+)/ Ralbp1, recombinant Ralbp1 was cloned under the lac operon. Therefore the expression of the recombinant Ralbp1 was induced by addition of isopropyl β-D-1-thiogalactopyronoside (IPTG) (0.4 mM), when the absorbance at 600 nm reached 0.6.

Upon induction the protein was allowed to express for 18 h by incubating at 37 ^{o}C shaking at ~225 rpm. *E. coli* BL21(DE3) cells were then collected by centrifugation at 2,000 x g for 10 min at 4 ^{o}C. Cells were then lysed in the lysis buffer containing detergent polidocanol (1 %) and EDTA (0.2 mM) by sonication at 50 W for 30 s each time. The cell lysate was incubated with lysis buffer over night at 4 ^{o}C in order to

extract the protein from the membrane. Upon completion the cell debris were separated by centrifugation at 28,000 x g for 40 min at 4 ^{o}C. Extracted Ralbp1 protein in the supernatant fraction was purified by affinity chromatography with cyanogen bromide (BrCN) activated Sepharose 4B resin coated with DNP-SG. Nonspecifically bound proteins were removed by washing with wash buffer followed by lysis buffer containing 0.01 % sodium dodecyl sulfate (SDS). Finally the protein was eluted with elution buffer. The eluted protein was dialyzed against dialysis buffer containing 0.01 % SDS and 1 % DE-52 (v/v), over night at 4 ^{o}C. Purified Ralbp1 protein was then lyophilized and stored at 0 ^{o}C until further used.

Purity of the protein was determined by carrying out SDS-PAGE as well as by western blotting with polyclonal antibodies against human Ralbp1. Also purification fold at each step was analyzed by carrying out SDS-PAGE with an aliquot at each purification step.

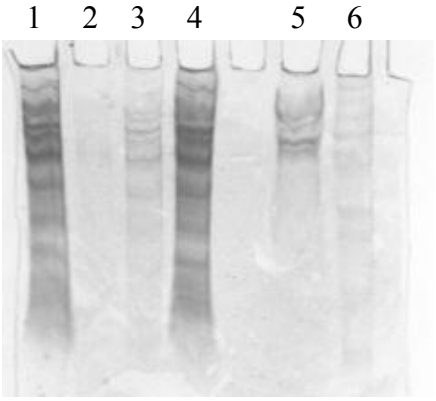

Figure 2.10 SDS-PAGE of samples at different purification steps

Smaples loaded in the gel are as follows; crude sample (lane 1), sample from second washing (lane 2), sample from first washing (lane 3), sample from unabsorbed fraction (lane 5) and broad range fraction (lane 6)

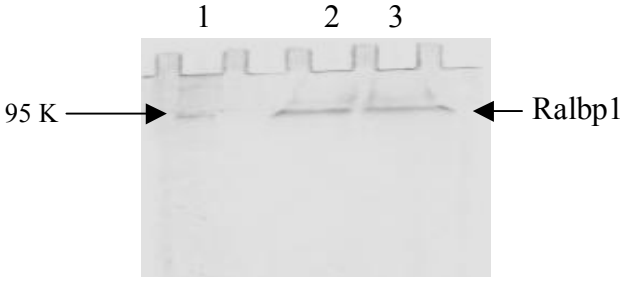

Figure 2.11 SDS-PAGE of purified recombinant Ralbp1

Broad range protein ladder (lane 1) and purified Ralbp1 sample 1 and 2 (lane 2 and 3)

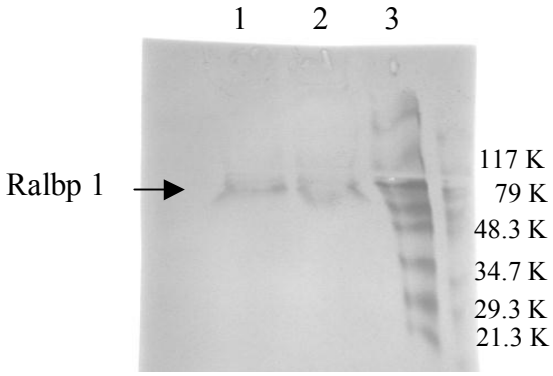

Figure 2.12 Western blot of purified recombinant Ralbp1 using polyclonal antibodies

Lane 1-2 indiate purified Ralbp1 sample 1 and 2 while lane 3: Broad range protein ladder

2.4.8 Purification of rec-Ralbp1 by Ni-NTA affinity chromatography

Recombinant full length and the deletion mutant Ralbp1 was purified from a bacterial culture by affinity chromatography using Ni-NTA superflow resin from Qiagen, CA. *E. coli* BL21(DE3) transformed with pET-30a(+) vector containing full length Ralbp1 cDNA clone with a 6X-histidine tag at the N-terminal domain were grown at 37 °C until optical density at 600 nm reached 0.6. Expression of Ralbp1 was induced by the addition of IPTG to obtain a final concentration of 0.4 mM and the culture was further incubated at 37 °C overnight shaking ~225 rpm. The bacterial cell pellet was obtained by centrifuging the culture at 1,400 x g for 10 min. The bacterial cells were lysed by resuspending in 5 ml of lysis buffer followed by sonicating at 50 W for 15 s, 3 times on ice. The protein was extracted from the membrane by incubating the cell lysate with lysis buffer for 2 h at 4 °C with gentle shaking. Afterwards the cell

lysate was centrifuged at 28,000 x *g* for 20 min at 4 °C and the supernatant liquid was applied on Ni-NTA superflow resin pre-equilibrated with lysis buffer. The resin was incubated for 2 h at 4 °C with gentle shaking followed by washing with wash buffer until optical density at 280 nm reached zero in order to remove none specifically bound proteins. The protein bound to the resin was eluted with elution buffer, dialyzed against dialysis buffer and concentrated using an Amicon Centriprep concentrators and stored at 4 °C until further used.

The purified protein was subjected to SDS-PAGE followed by western blot analysis with polyclonal anti-Ralbp1 antibodies raised in rabbit followed by horseradish peroxidase conjugated goat anti-rabbit secondary antibodies.

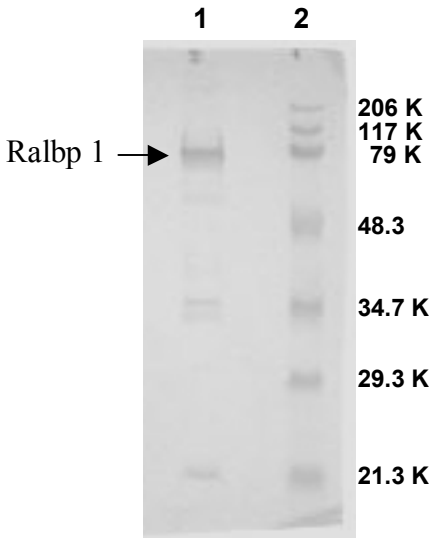

Figure 2.13 Western blot: Ni-NTA affinity purified rec-Ralbp1

Lane 1 indicates Ni-NTA purified rec-Ralbp1 while lane 2: broad range protein marker

A major peptide at the expected molecular weight 95 kDa was seen along with several low molecular weight peptides at 35 kDa and 21 kDa. The existence of these internal peptide sequences has being reported from our previous studies as well (Awasthi et al. 2000; Awasthi et al. 2001).

2.4.9 Transformation

Transformation of competent *E. coli* DH5α is an in-vivo method of amplifying selected DNA using a biological system. Transformation is a procedure by which a foreign DNA is introduced in to a bacterial cell. There are different types of transformation methods such as $CaCl_2$ induced cell membrane permeabilization, electroporation etc. The choice of the method depends on the type of cells used in the transformation as well as the DNA to be introduced.

During the study plasmid vectors pET30a(+) and pcDNA3.1 cloned with recombinant human Ralbp1 was transformed into *E. coli* DH5α by $CaCl_2$ induced pathway. Transformation of competent *E. coli* DH5α, was carried out using ligation mixtures as well as purified plasmids. When using ligation mixtures for transformations 2 µL was used while 1 µL of the purified plasmid was sufficient. Fifty µL of competent *E. coli* DH5α was thawed on ice, mixed with DNA and incubated on ice for 20 min. In the presence of divalent cations such as Ca^{+2} bacterial cell walls become permeable to DNA when the cells are chilled in ice. Afterwards the bacterial cells were heat shocked by incubating at 42 ^{o}C for 40 s followed by incubating on ice for 5 min. The heat shock causes the DNA to enter the cell. To each transformation mixture 600 µL of SOC media

(which has being previously warmed to 37 ^{o}C) was added and incubated at 37 ^{o}C for 15 min with gentle shaking (~140 rpm).

When transforming ligation mixtures, 150 µL and 450 µL were plated on LB agar plates containing the selective antibiotic. Since plasmid vector pET30a(+) consists of kanamycin resistance, transformation mixtures of pET30a(+) were plated on LB agar plates containing kanamycin (50 µg/mL) resistance while transformation mixtures of plasmid vector pcDNA 3.1 which encoded ampicillin resistance gene were plated on LB agar plates with ampicillin (70 µg/mL). When pure plasmids were used for the transformation, 5 µL and 100 µL of the transformation mixtures were plated on the LB agar plates with selective antibiotic. Upon overnight incubation at 37 ^{o}C, the transformed *E. coli* colonies were assessed for the presence of the plasmid by PCR as well as plasmid DNA purification.

2.4.10 Plasmid DNA purification (Mini prep)

Transformation of competent *E. coli* is a method by which extraneous DNA could be amplified by using a live system. However in purifying DNA from bacterial cells it is necessary to lyse the bacterial cell membranes while keeping the activity of degradative enzymes such as nuclease and proteases released during the cell disruption a minimum. Afterwards it is necessary to isolate the DNA of interest from other macro molecules present in the cells including genomic DNA by employing a fractionating procedure (Switzer RL 2001).

During the study, plasmid DNA was purified from *E. coli* DH5α cells using QIAprep miniprep kits. According to the procedure, the bacterial cell walls disrupted by alkaline lysis followed by isolation of plasmid DNA by adsorption on to silica.

Randomly selected several transformed *E. coli* colonies were inoculated in 5 mL of LB media containing the selective antibiotic and incubated at 37 ^{o}C overnight, shaking at ~ 225 rpm. Bacterial pellets from several cultures were used to purify plasmid DNA. The bacterial pellet was re-suspended in 250 µL of buffer P1. Then 250 µL of buffer P2 was added in order to lyse the cells. The reagents were mixed thoroughly by inverting the tube several times. Afterwards 350 µL of the neutralizing buffer N3 was added to the reaction mixture and mixed thoroughly by inverting the tube several times. By centrifugation at 17,900 x g for 10 min genomic DNA was separated from plasmid DNA. Bacterial genomic DNA forms a white clump while plasmid DNA was collected in the supernatant, which was applied on the QIAprep spin column. The supernatant was applied on to QIAprep column and centrifuged for 1 min and the flow-through fraction was discarded. Plasmid DNA was absorbed onto silica columns under high salt conditions while the protein and RNA are passed onto the flow through. Endonucleases were removed by washing the column with 0.5 mL of buffer PB followed by washing with 0.75 mL of buffer PE to remove the salts. The flow-through fraction was discarded upon completion of washing with buffer PB and PE. The remaining ethanol from the washing buffers was removed by centrifuging for an additional minute. The column was transferred on to a fresh collection tube and the plasmid DNA was eluted by addition of de-ionized water onto the center of the column

followed by centrifugation for a minute. The DNA was then stored at -20 ^{o}C until further used.

2.4.11 Restriction endonuclease digestion

Restriction endonucleases catalyze the hydrolysis of phosphodiester bonds at highly specific sequences, on both strands of DNA. These are formed in prokaryotes as a defense mechanism against foreign DNA. DNA methylation protects the cellular DNA from digestion by endonucleases.

In the process of cloning recombinant human Ralbp1 into prokaryotic vector pET30a(+) and eukaryotic vector pcDNA 3.1, the insert DNA was cloned onto a site flanked by restriction endonucleases BamH I and Xho I. Both vector and insert DNA (amplified PCR product) were digested with restriction endonuclease BamH I and Xho I to make the ends compatible with each other.

The composition of the digestion mixture consisted of NE buffer 2 (1X), BSA (1X), 2 µL of each restriction endonuclease BamH I and Xho I, DNA (plasmid vector/ insert gene) and de-ionized water to make the reaction volume of 100 µL. Vector digestions were carried out at 37 ^{o}C for 3 h while digestion reaction of the insert gene was carried out at 37 ^{o}C overnight. Upon completion the linearized DNA with cohesive ends was separated by 1 % agarose gel electrophoresis and gel purified.

2.4.12 Agarose gel electrophoresis

Agarose is a polymer of galactose and 3,6-anhydro galactose connected together by α (1 – 4) glycosidic bonds, isolated from sea weed. Due to it's ability to form a rigid gel with uniform pore size upon solidifying after dissolving in buffer, agarose gel electrophoresis is a technique widely used for the separation of DNA molecules according to the molecular weight. Depending on the size of the DNA molecule to be separated the pore size of the gelling material can be controlled by varying the concentration of agarose. More concentrated gels give rise to smaller pore sizes and hence are used for the separation of smaller DNA molecules while less concentrated gels with larger pore sizes are used for the separation of DNA molecules with higher molecular weight (Switzer RL 2001).

During this study, separation of DNA molecules by agarose gel electrophoresis was carried out according to the protocol described by Sambrook et al. (Sambrook J 1989). Since the gene encompassing recombinant Ralbp1 is 1968 bps and the plasmid vectors used for the cloning, pET30a (+) and pcDNA3.1 both are 5422 bps and 5428 bps respectively, 1 % (w/v) agarose gels were used for the separation. 1 g of agarose (lyophilized white powder) was dissolved in 100 mL of Tris-acetic acid-EDTA buffer, pH 8.3 (TAE) and was heated until a clear solution was obtained. Afterwards, the solution was cooled down ~50 ^{o}C and mixed with 3 µL of ethidium bromide (EtBr) and poured on to a tray with a matching comb inserted on it. When the gel solidified the comb was removed to obtain the wells and the gel was kept in a tank with buffer TAE, pH 8.3, covering the gel. The DNA samples mixed with the DNA loading sample buffer

containing bromophenol blue were then loaded onto the wells along with 1 kB DNA ladder, which consists of several DNA fragments of known molecular weight. A voltage difference of 80 V was applied across the gel for approximately 1 h, in order to separate the DNA. The DNA fragments were visualized by the fluorescence emitted by ethidium bromide, which has intercalated with the DNA, by exposing the gel to UV light (256 nm – 300 nm).

2.4.13 Gel purification of DNA from agarose gels using QIAquick gel extraction kit

Agarose gel electrophoresis is used to separate DNA samples following a PCR amplification or restriction endonuclease digestion. Once the separation is achieved the DNA of interest needs to be extracted from the agarose gel, to be used in down stream applications. Throughout this study the extraction of DNA from agarose gels were carried out using QIAquick gel extraction kits from Qiagen, where binding and elution of DNA to an optimize silica gel membrane occur by varying the ionic strength and pH of different buffers.

The agarose gel piece containing the DNA of interest was excised from the gel using a sharp scalpel under UV light and the weight was measured. Care was taken to minimize the amount of agarose. The gel piece was dissolved by the addition of buffer QG, 3 times the volume of the gel piece and keeping in a water bath at 50 ^{o}C for 10 min. Vortexing was carried in between to facilitate the solubilization of the gel piece. Afterwards the solution was checked for any changes in the color due to alterations of pH caused by dissolving the gel piece. Buffer QG contains a pH indicator which is

yellow during lower pH values and becomes violet at higher pH values. This was mandatory since binding of the DNA with the silica gel membrane occurs at low pH.

Equal volume of isopropanol was added to the sample and mixed gently. The sample was then applied onto the QIAquick spin column, centrifuged and discarded the supernatant fluid. Under the high salt, low pH conditions provided by buffer QG, DNA binds to the silica gel membrane while agarose, dye, ethidium bromide, etc get collected in the flow through. Additional 0.5 mL of buffer QG was applied onto the column to remove any remaining traces of agarose. The salts were removed by washing the column with buffer PE. Residual ethanol remaining on the column was removed by centrifugation of the column for an additional minute. Afterwards the DNA was eluted with de-ionized water. The DNA was stored at -20 ^{o}C until further used. (QIAquick Spin Handbook, Qiagen, CA)

2.4.14 Determination of the DNA concentration

DNA samples were diluted in de-ionized water and the absorbance at 260 nm was measured using de-ionized water as a blank. It has being experimentally determined that 50 µg/mL of duplex DNA accounts for 1 U of absorbance in a cell with a 1 cm light path. Therefore the concentration of a DNA sample was calculated as below.

Concentration of DNA µg/mL = A_{260nm} x dilution x 50 µg/mL

2.4.15 Preparation of competent E. coli DH5α

Competent *E. coli* are used for *in-vivo* amplification of DNA. In order to introduce foreign DNA to a bacterial cell, it is necessary to permeabilize the cell membrane. This is achieved in chemically competent *E. coli* by exposing the bacterial cells to divalent cations followed by giving a heat shock.

A primary culture of 3 mL of SOB medium was inoculated with 10 µL of *E. coli* DH5α and incubated at 37 ^{o}C over night with shaking at ~225 rpm. Afterwards the primary culture was diluted 100 fold by addition of 300 mL of SOB and incubated at 37 ^{o}C until the optical density at 600 nm reached 0.6. Then the culture was kept at 4 ^{o}C for 20 min, and the bacterial cell pellet was collected by centrifugation at 1,400 x g for 5 min. The bacterial cell pellet was re-suspended in $CaCl_2$ solution and incubated at 4 ^{o}C for 20 min. Afterwards the supernatant fluid was discarded after centrifugation at 1,400 x g for 5 min at 4 ^{o}C. Repeated washing with $CaCl_2$ solution. The cells were then re-suspended in $CaCl_2$, aliquoted in to 50 µL fractions and stored at -70 ^{o}C, until further use.

2.4.16 Preparation of competent E. coli BL21(DE3)

E. coli BL21(DE3) are widely used prokaryotic expression systems for the expression of recombinant proteins.

A primary culture of 3 mL of SOB media was inoculated with 10 µL of *E. coli* BL21(DE3) and incubated at 37 ^{o}C overnight with shaking ~225 rpm. Afterwards the primary culture was diluted 100 fold by addition of 300 mL of SOB and incubated at 37

^{o}C until the optical density at 600 nm reached 0.6. Then the culture was kept at 4 ^{o}C for 20 min, and the bacterial cell pellet was collected by centrifugation at 1,400 x g for 10 min. The bacterial cell pellet was re-suspended in ice cold TB solution and incubated at 4 ^{o}C for 10 min. Afterwards the supernatant was discarded after centrifugation at 1,400 x g for 10 min at 4 ^{o}C. Repeated washing with TB solution. The cells were then re-suspended in 5 mL of TB solution containing 7 % DMSO and incubated at 4 ^{o}C for another 10 min. Meanwhile, 10 mM potassium acetate (KAc) solution, pH 6.0 containing 2.2 M DTT was prepared and added to obtain 3.5 % v/v to the re-suspended bacteria in TB and further incubated for 10 min. The bacterial suspension was aliquoted in to 50 µL fractions and stored at -70 ^{o}C, until further use.

2.4.17 Determination of protein concentration – Bradford assay

Determination of concentration of proteins by Bradford assay is a colorimetric assay introduced by M. M. Bradford (Bradford 1976). The key component in the Bradford reagent Coomassie Brilliant Blue G-250 is a dye which in its free form exists in red color, with maximal absorbance at 470 nm. It has a strong tendency to interact with basic amino acids such as arginine and aromatic amino acids of proteins. Upon binding with the proteins the color of the dye becomes blue with a shift in the maximal absorbance to 595 nm. Therefore by measuring the absorbance at 595 nm, the amount of bound form of the dye and hence the concentration of the protein present in the solution can be determined by a simple spectrophotometric assay using the Beer-Lambert law. Bradford assay is most sensitive in the concentration range 2 µg/mL to

200 μg/mL. A major drawback associated with the method is the interferences caused by salts and the detergents present in the protein samples.

A series of protein standard solutions of bovine serum albumin (BSA) with concentrations ranging from 0.2 mg/mL to 1.4 mg/mL were prepared according to the manufacturer's protocol. Reaction mixtures for protein determination by absorbance were prepared by addition of 20 μL of each sample and 80 μL of de-ionized water in 1 mL of Bradford assay reagent. The solutions were mixed by vortexing and incubated at room temperature for 5 min, upon which the absorbance was measured at 595 nm against a blank of 1 mL of Bradford reagent containing 100 μL of de-ionized water. A standard curve was prepared by plotting absorbance (y axis) against concentration (x axis). Unknown protein solutions were prepared according to the same method and the concentration was determined by the standard curve. The standard curve used during the protein estimations is given bellow.

Table 2.4 Concentration and absorbance values of BSA standard solutions

Standard solution	Concentration mg/mL	Absorbance
1	0	0
2	0.25	0.08
3	0.5	0.18
4	1.0	0.37
5	1.4	0.52

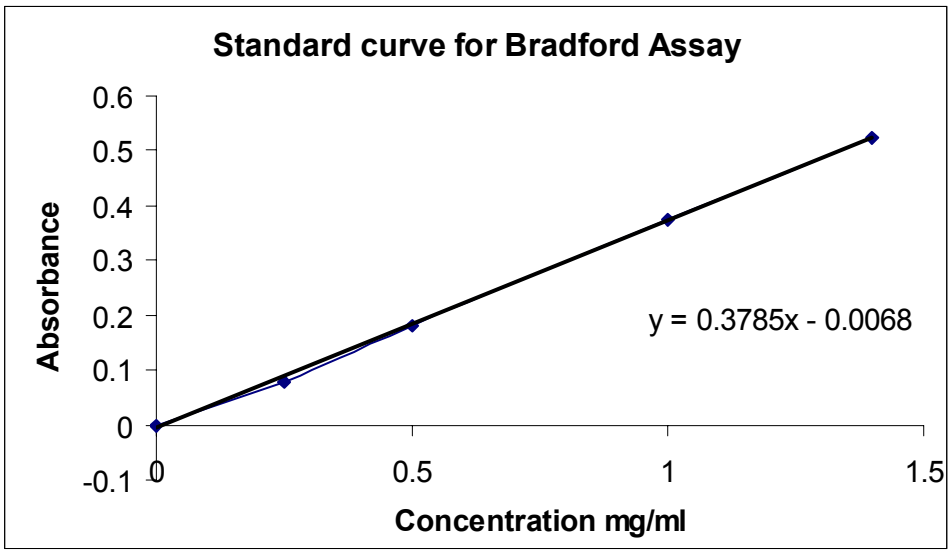

Figure 2.14 Standard curve for Bradford assay

2.4.18 Sodium dodecyl sulfate-polyacrylamide gel electrophoresis (SDS-PAGE)

Sodium dodecyl sulfate-polyacrylamide gel electrophoresis, (SDS-PAGE) is a technique by which proteins and small nucleic acid fragments are separated according to the molecular weight, that has being first introduced by Laemmli in 1970 (Laemmli 1970). Polyacrylamide is a polymer formed by the monomer unit acrylamide and the cross linker N,N'-methylene-bis-acrylamide. Polymerization is induced by free radical generators ammonium persulfate and N,N,N',N'-tetramethylethylenediamine (TEMED).

The protein samples were heated for 5 min in sample buffer containing SDS and a reducing agent such as β-mercaptoethanol. The disulfide bonds present between the peptides were reduced by β-mercaptoethanol and the detergent disrupts the non covalent

attractions, giving rise to totally denatured protein. Binding of large number of SDS molecules with the protein (one SDS molecule per every two amino acids) yield a highly negatively charged molecule regardless of the any intrinsic charges that might have being present on the protein. SDS-PAGE essentially separates the proteins according to the molecular weight since the variations caused by secondary and tertiary structures are eliminated by protein denaturing. A single SDS-PAGE gel consists of two layers with different acrylamide compositions, the stacking gel and the resolving gel.

Table 2.5 Composition of stacking gel and resolving gel during SDS-PAGE

Component	Stacking gel (for 2 gels)	Resolving gel (for 2 gels)
Water	3.07 mL	7.25 mL
Acrylamide-bis acrylamide (60 g: 1.6 g)	0.6 mL	2.34 mL
10 % SDS	0.05 mL	0.112 mL
14.3 M β-mercaptoethanol		1.87 µL
3 M Tris HCl, pH 8.8		1.4 mL
0.5 M Tris HCl, pH 6.8	1.3 mL	
5 % Ammonium persulfate (APS)	50 µL	0.112 µL
TEMED	11.2 µL	11.2 µL

The concentration of acrylamide in the stacking gel is 7 % yielding larger pore sizes compared to the resolving gel which consists of 12.5 % acrylamide. The protein samples were loaded on to the wells created in the stacking gel. The electrophoresis was initiated by applying a voltage difference of 200 V and due to the negative charge imposed by binding of SDS molecules, the proteins migrated towards the anode. Initially due to the large pore sizes in the stacking gel the friction was less and the protein molecules stacked together at the stacking gel-resolving gel interface.

Afterwards on the resolving gel, the protein molecules were separated according to the molecular weight.

Once the gel electrophoresis was completed, the separated proteins were visualized by staining the gel with 0.2 % Coomassie Brilliant Blue R-250. It is a dye that binds with the proteins by mainly interacting with arginine residues and also with tryptophan, tyrosine, phenylalanine, lysine and histidine to a lesser extent. Afterwards the unbound dye was removed by washing the gel with de-staining solution, composed of, acetic acid (10 %) and methanol (20 %). The proteins were identified according to the size by using a protein molecular weight maker which consists of various peptides of known molecular weight.

Staining with Coomassie Brilliant Blue R-250 is sensitive for protein concentration range 0.1 to 0.5 µg. Silver staining which has a higher sensitivity can be used to identify proteins up to 10 ng proteins.

2.4.19 Western blotting

Western blotting or immuno-blotting was introduced by Harry Towbin in 1979 as a technique that could be used to identify a protein from a heterogeneous protein mixture (Towbin et al. 1979).

The protein samples or crude cell extracts were separated by SDS-PAGE. Afterwards the gel was equilibrated with blotting buffer for 10 min each time, thrice, in order to remove the SDS present in the running buffer. This was mandatory since SDS interfere with the transfer of proteins on to the membrane. Then the proteins from the

gel were transferred to the nitrocellulose membrane by electro blotting. The membrane was placed next to the gel and two layers of tissue papers were stacked on either side in a plastic cassette. The cassette was dipped in blotting buffer and subjected to electric current of 240 mA for 4 h.

Following electro blotting the nitrocellulose membrane was incubated in 5 % non fat dry milk (NFDM) for 10 min each time, thrice, in order to block the non specific sites. This is essential to reduce the back ground caused by binding of the antibodies with non specific sites on the membrane. Upon completion the membrane was incubated with primary antibodies in 5 % milk solution in TBS, over night at room temperature. During this study the nitrocellulose membrane was incubated with polyclonal rabbit anti-human rec-Ralbp1 IgG as the primary antibody. Afterwards the unbound anti bodies were removed by washing with 5 % milk in TBS, three times, with each time for 10 min.

Nitrocellulose membrane was then incubated with the horseradish peroxidase-conjugated goat anti-rabbit secondary antibodies in 5 % milk in TBS for 4 h at room temperature. The unbound secondary antibodies were then rinsed away by washing the membrane with TBS three times, time 10 min each. Afterwards the membrane were developed using developing solution containing 4-chloro1-napthol and hydrogen peroxide.

2.4.20 Reconstitution of rec-Ralbp1 into proteoliposomes

Reconstitution of the purified protein into proteoliposomes was performed according to the previously established procedure by S. Awasthi (Awasthi et al. 2000). The protein was dialyzed against reconstitution buffer. A mixture of soybean asolectin (40 mg/mL) and cholesterol (10 mg/mL) was prepared in reconstitution buffer by sonication. An aliquot of protein (0.9 mL) containing 10 µg protein was mixed with 100 µL of the lipid mixture to obtain a final lipid constitution 5 mg/mL for 10 µg protein. The reaction mixture was sonicated for 15 s at 50 W. After wards 200 mg of SM-2 BioBeads pre-equilibrated with reconstitution buffer (without polydoconol) were added to the reaction mixture to initiate the vesiculation by removal of detergent. Upon incubation of the reaction mixture at 4 ^{o}C, SM-2 beads were removed by centrifugation at 3620 x g. Control liposomes were prepared by using same amount of crude *E. coli* protein in place of purified rec-Ralbp1.

Analysis of the percentage incorporation of Ralbp1 into liposomes, were studied by carrying out western blot analysis of 104,000 x g pellet which contains liposomes vs supernatant. It has being observed that > 95 % Ralbp1 to be incorporated into the liposomal fraction.

2.4.21 Transport studies using proteoliposomes of rec-Ralbp1

ATP dependent transport by Ralbp1 was studied using proteoliposomes reconstitute with rec-protein according to the procedure given in section 2.4.20.

Transport studies were carried out according to the rapid filtration technique which has being previously published (Awasthi et al. 2000; Awasthi et al. 1994).

The transport assay when [^{14}C]-DOX was used as the substrate is as follows. Proteoliposomes in reconstitution buffer (250 ng protein) were diluted with transport buffer containing [^{14}C]-DOX (specific activity 85 cpm/pmol). The reaction mixture was incubated at 37 ^{o}C for 5 min. Transport activity was measured in the presence as well as in the absence of ATP, by preparing reaction mixtures with ATP (experimental) and without ATP (control). To each reaction mixture, transport buffer containing ATP/NaCl was added to obtain a final concentration of 3.6 μM DOX, 4 mM ATP/ 6 mM NaCl, 4 mM $MgCl_2$. Upon addition of ATP (to the experimental) or NaCl (to the control), each reaction mixture was incubated at 37 ^{o}C for 5 min.

Samples of equal volume (30 μL) from each reaction mixture were added on to 96 well plate filtration system from Millipore which has being previously equilibrated with DOX and washed with transport buffer. The reaction mixtures were filtered rapidly by vacuum filtration. The filters were punched off and dissolved in scintillation fluid and the radioactivity was measured. The residual counts in control reactions which contained NaCl in place of ATP were subtracted from the counts obtained for experimental samples which contained ATP. Each determination was carried out in triplicate.

Transport assay was also performed with 100 μM [^{3}H]-DNP-SG (specific activity 3 600 cpm/nmol) and 300 nM [^{3}H]-LTC_4 (specific activity 1 400 cpm/pmol) as

substrates. The composition of the reaction mixtures and the reaction conditions were same for all 3 substrates.

2.4.22 Transient transfection

Transfection is a procedure by which foreign molecules are introduced to animal cells. Of the several methods available, lipofectamine is a very widely used method due to its relative simplicity as well as the efficiency in transfecting wide range of cell lines. Lipofectamine is based on formation of lipid complexes of DNA which can penetrate the cell membrane.

In a 6 well plate, 0.6 x 10^6 cells were plated in each well with 2 mL of RPMI-1640 medium containing 10 % fetal bovine serum (FBS), 1 % penicillin-streptomycin (P/S), 1 % sodium pyruvate (100 mM), 10 mM HEPES, 4.5 g/L glucose and 1.5 g/L sodium bicarbonate. Following incubation of the cells at 37 ^oC in a CO_2 incubator (5 % CO_2) for 24 h, transient transfection was carried out using lipofectamine 2000 reagent, according to the manufacture's protocol. Plasmid DNA (2.0 µg) were diluted with 250 µL of DMEM medium without serum. Lipofectamine reagent was gently mixed and diluted 10 µL in to 250 µL of DMEM medium without serum and incubated at room temperature for 5 min. Diluted lipofectamine and DNA were mixed thoroughly and incubated at room temperature for 30 min. DNA-lipofectamine complexes (500 µL) were added to each well containing 2 mL of RPMI-1640 media, gently mixed and incubated at 37 ^oC in a CO_2 incubator. Expression of the transgene was checked after 48 h following transfection.

2.4.23 Determination of antibiotic concentration lethal to cells

Cells were counted using trypan blue stain and plated 0.5 x 10^6 in each well of a 6 well plate. Two ml of RPMI-1640 medium containing 10 % fetal bovine serum (FBS), 1 % penicillin-streptomycin, 1 % sodium pyruvate (100 mM), 10 mM HEPES, 4.5 g/L glucose and 1.5 g/L sodium bicarbonate was added and the cells were incubated 24 h at 37 ^oC in a CO_2 (5 % CO_2) incubator. Upon incubation, the medium was replaced by a series of RPMI-1640 medium containing 0 µg/mL, 50 µg/mL, 100 µg/mL, 200 µg/mL, 400 µg/mL, 600 µg/mL, 800 µg/mL, 1000 µg/mL antibiotic G418. Each experiment was carried out in duplicate. Medium was refreshed every 48 h for 2 weeks. The effect of G418 on cells was being closely observed using light microscope.

2.4.24 Stable transfection

During stable transfection the foreign DNA integrates with the host genetic material and hence does not get lost during cell division. The most widely used selective method for the identification of stably transfected cells is the antibiotic resistance provided by the foreign DNA material. The host cells become resistant to the selective antibiotic due to the expression of the genes from integrated DNA.

In a 6 well plate, 0.6 x 10^6 cells were plated in each well with 2 mL of RPMI-1640 containing 10 % fetal bovine serum (FBS), 1 % penicillin-streptomycin, 1 % sodium pyruvate (100 mM), 10 mM HEPES, 4.5 g/L glucose and 1.5 g/L sodium bicarbonate. Following incubation of the cells at 37 ^oC in a CO_2 incubator (5 % CO_2) for 24 h, stable transfection was carried out using lipofectamine 2000 reagent, according

to the manufacture's protocol. Plasmid DNA (2.0 μg) were diluted with 250 μL of DMEM medium without serum. Lipofectamine reagent was gently mixed and diluted 10 μL in to 250 μL of DMEM medium without serum and incubated at room temperature for 5 min. Diluted lipofectamine and DNA were mixed thoroughly and incubated at room temperature for 30 min. DNA-lipofectamine complexes (500 μL) were added to each well containing 2 mL of RPMI-1640 media, gently mixed and incubated at 37 ^{o}C in a CO_2 incubator.

The following day, the medium was changed with RPMI-1640 medium containing antibiotic G418 (600 μg/mL). Every 48 h the media were refreshed with RPMI-1640 containing G418 (600 μg/mL) for two weeks. Individual G418 resistant colonies were trypsinized, isolated and cultured separately in RPMI-1640 medium containing 600 μg/mL of G418. The expression of the transgene was assessed by reverse transcriptase polymerase chain reaction (RT-PCR).

2.4.25 Purification of RNA

Purification of total RNA from different cell lines was performed with the aid of RNeasy mini kit from Qiagen, CA, according to the manufacturer's protocol. The RNeasy procedure combines the selective binding properties of RNA with the silica-based membrane with the speed of microspin technology. RNeasy silica-based membrane has the capacity to bind up to 100 μg of RNA longer than 200 bases under the high salt conditions of the buffer. Guanidine thiocyanate contained in the buffer ensures the RNA to be intact by inactivation of the RNases during lysis and

homogenization of the biological samples. Upon application of the sample on to the RNeasy column, all RNA molecules longer than 200 base pairs get efficiently bound to the membrane while the contaminants are removed. This phenomenon helps in enrichment of mRNA as 15-20 % of cellular RNA, which comprise of 5.8S rRNA, 5S rRNA and tRNAs are smaller than 200 bps and hence could be selectively excluded.

Cells were collected in an RNase free eppendorf tube and lysed by addition of 600 µL of RLT buffer in to which β-mercaptoethanol was added (10 µL of β-mercaptoethanol/ 1 mL of RLT buffer) followed by mixing. Sample was homogenized by adding on to a QIA-shredder spin column followed by centrifugation for 2 min at 14 000 rpm. An equal volume (~600 µL) of 70 % ethanol was added to the flow through and the sample was added on to a RNeasy column. The flow through was discarded after centrifugation at 8,000 x g. RNeasy column was washed with 700 µL of buffer RW1 followed by 500 µL of buffer RPE twice, each time centrifuging at 8,000 x g for 15 s. The residual ethanol on the column was removed by centrifuging the column at 8 ,000 x g for 2 min. The RNA was eluted from the column with 50 µL of RNase free DEPC water by centrifuging at 8,000 x g for 1 min. Purified RNA samples were stored at -80 ^{o}C until further used. The concentration of the RNA was determined by absorbance at 260 nm as well as by conducting agarose gel electrophoresis on a 1 % agarose gel. When carrying out gel electrophoresis RNA samples were denatured after mixing with the sample buffer, by heating to 60 ^{o}C for 10 min followed by cooling on ice for 5 min. Gel electrophoresis was carried out at 70 V for 2 h.

Concentration of RNA, 1 $OD_{260\ nm}$ = 40 µg/mL

2.4.26 Reverse transcriptase polymerase chain reaction (RT-PCR)

Reverse transcription polymerase chain reaction is a technique by which a selected RNA strand can be amplified to produce its complimentary cDNA. Reverse transcriptase enzyme which is a RNA-dependent DNA polymerase, synthesizes the complementary DNA from the RNA by reverse transcription. Afterwards the DNA was amplified by polymerase chain reaction.

Transgene expression in stably transfected cells were assessed by carrying out RT-PCR using RNA purified from wild type untransfected cells as well as stably transfected cells. Equal concentration of total RNA was used from both types of cells. Each 25 µL reaction mixture consisted of de-ionized water, 5 µL of reverse transcriptase buffer, 0.5 mL of dNTPs, forward and reverse primers, 1 µL of each, RNA and reverse transcriptase enzyme. Reaction conditions consisted of an initial reverse transcription time of 30 min at 42 ^{o}C followed by denaturation of the double stranded DNA by heating up to 95 ^{o}C for 5 min. This was followed by 45 cycles of 30 s at 95 ^{o}C, 30 s at 60 ^{o}C and one min at 72 ^{o}C. The final extension step consisted of 7 min at 72 ^{o}C.

The differential expression of the transgene in the untransfected and stably transfected cells were assessed by conduction agarose gel electrophoresis (1 %).

2.4.27 Drug sensitivity assay

Ralbp1 mediated drug sensitivity was assayed by determination of the IC_{50} of the drugs, according to a colorimetric assay for determination of cell proliferation described by Mosmann in 1983 (Mosmann 1983; Wilson 2000). Yellow colored 3-(4,5-

dimethylthiazol-2-yl)-2,5-diphenyltetrazolium bromide (MTT), a tetrazol is reduced to insoluble purple formazan by the reductase enzymes in mitochondria of living cells. Solublization of formazan in a suitable solvent (dimethyl sulfoxide (DMSO) or a solution of the detergent sodium dodecyl sulfate in dilute hydrochloride) allows the quantification by measuring the absorbance at 570 nm, which is directly proportional to the viable cells present.

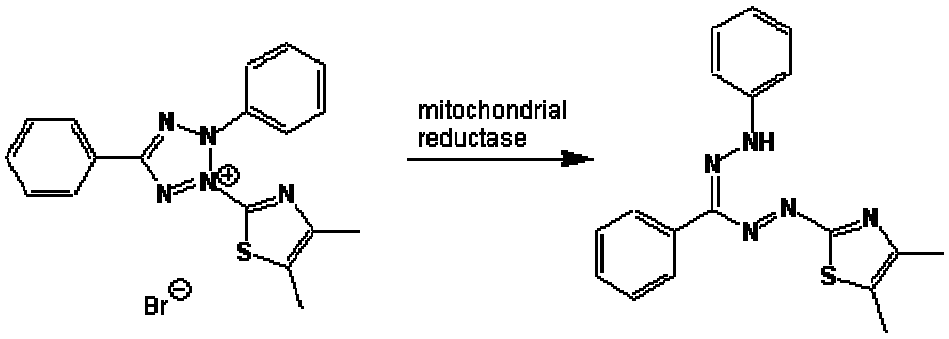

Figure 2.15 Reduction of MTT into purple formazan

Cell density was measured by trypan blue dye exclusion assay. Approximately 20,000 cells were seeded into each well from lane 2-12 of a 96-well flat-bottomed microtiter plate containing 160 µL RPMI medium. First lane which is used as a blank contained only RPMI media. Following 24-hour incubation at 37 ^{o}C in 5 % CO_2 incubator, 40 µL aliquots of drug concentrations ranging from 1 to 10,000 nm were added to wells ranging from lane 3-12. Lane 2 is used a positive control to asses the cell proliferation without any drugs. Eight replicate wells were used to assess the effect for each concentration of the drug. Following 96 h of incubation, 20 µL of 5 mg/mL MTT in PBS was added to each well and incubated for 2 h of at 37 ^{o}C in 5 % CO_2 incubator.

The plates were centrifuged and medium was decanted. Subsequently, the cells were dissolved in 100 µL DMSO by gentle shaking for 2 h at room temperature, Formation of formazan was determined by measuring the absorbance at 570 nm (Awasthi et al. 1996).

2.4.28 siRNA Trasfection

The cells were transfected with siRNA using TransMessenger transfection kit from Qiagen which is based on lipid formulation together with condensation of RNA. Initially RNA to be transfected is condensed by the dual activity of specific RNA condensing agent Enhancer R and RNA condensing buffer, buffer ECR. Then the addition of TransMessenger transfection reagent produces TransMessenger-RNA complexes which can enter the cells through cell membrane.

Transfection of cells with siRNA using TransMessenger transfection kit from Qiagen was performed according to the manufacturers protocol, which has being developed based on the standard transfection protocol as well as results of the RNAi studies by Elbashir et al. (Elbashir et al. 2001).

Depending on the growth rate of the cell type, 50 000 to 100 000 cells were seeded in each well of a 24-well plate and incubated with 0.5 mL of RPMI medium containing 10 % FBS and 2 % P/S for 24 h at 37 ^{o}C with 5 % CO_2. Enhancer R (1.6 µL) was diluted with buffer ECR. Maintaining the ratio of enhancer to siRNA, 2:1, 0.8 µg of siRNA was added to the mixture diluted with buffer ECR to obtain a final volume of 100 µL and mixed by vortexing. The siRNA-Enhancer R mixture was incubated at

room temperature for 5 min. TransMessenger transfection reagent (4 µL) was added to the reaction mixture, mixed by pipetting up and down several times and incubated at room temperature for 15-25 min to allow the TransMessnger-RNA complex formation. Mean while the growth media from the plate was removed and the cells were washed with PBS. Upon incubation for 15-25 min, 300 µL of RPMI medium with out FBS or antibiotics was added on to the transfection reagent mixture, mixed by pipetting up and down twice and added on the cells and swirled to ensure uniform distribution. The cells were incubated with the transfection complexes for 3 h at 37 ^{o}C with 5 % CO_2. Afterwards the complexes were removed and the cells were washed with PBS and supplied with 500 µL of RPMI medium containing 10 % FBS and 2 % P/S and allowed to grow at 37 ^{o}C with 5 % CO_2. Gene silencing was monitored after sufficient incubation time.

2.4.29 In vitro site directed mutagenesis – substitution mutations

Single amino acid substitutions were carried out using QuickChange II site directed mutagenesis kit from Stratagene, CA according to the manufacturer's protocol.

During the procedure two oligonucleotide primers, both containing the desired mutation and each complementary to the opposite strands of the double stranded vector were used to anneal and extend by PfuUltra high fidelity DNA polymerase. Extension of the primers generates a mutated plasmid. PCR products are subjected to Dpn I endonuclease digestion, where methylated parental DNA strands are selectively digested at targeted sequence 5'-Gm^{6}ATC-3'. The newly synthesized plasmid

containing the desired mutation was then transformed into XL-1 Blue supercompetent cells. A schematic diagram of the procedure is given below.

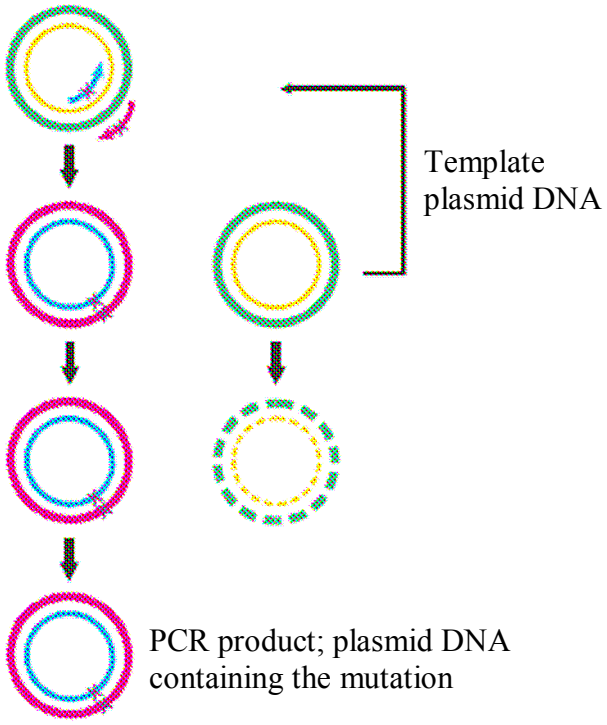

Figure 2.16 Over view: site directed mutagenesis (www.stratagene.com)

The nucleotide sequence of the mutagenic primers with the respective substitution mutations were as follows. Substitution of amino acid tyrosine 231 with alanine (Y231A), 5'-GTGAAGGCATCGCAAGAGTATCAGGA-3' (with its reverse complement), serine 234 with alanine (S234A), 5'-CATCTACAGAGTAGCAGGAAT TAAATC-3' (with its reverse complement), lysine 237 with alanine (K237A), 5'-GTATCAGGAATTGCATCAAAGGTGGATG-3' (with its reverse complement), lysine 244 with alanine (K244A), 5'-TGGATGAGCTAGCAGCAGCCTATGACC-3'

(with its reverse complement), tyrosine 247 with alanine (Y247A), 5'CTAAAAGCA GCCGCAGACCGGGAGGAGT-3' (with its reverse complement) and substitution of both serine 234 and lysine 237 with alanine (S234A K237A), 5'-CTACAGAGTAGC AGGAATTGCATCAAAG-3' (with its reverse complement).

Reaction mixtures were prepared by mixing 5 µL of 10X reaction buffer, 5-50 ng of double stranded DNA, 125 ng of forward and reverse primers, 1 µL of dNTP mix and 1 µL of PfuUltra HF DNA polymerase (2.5 U/µL). Two reaction mixtures each containing 5 ng and 50 ng of template DNA was prepared for each substitution mutation. PCR cycling parameters consisted of an initial denaturation step of 30 seconds at 95 ^{o}C followed by 16 cycles of 30 s at 95 ^{o}C, 1 min at 55 ^{o}C followed by 7 min at 68 ^{o}C. The reaction mixtures were cooled down < 37 ^{o}C by keeping in ice for 2 min.

Dpn I restriction endonuclease (1 µL from 10 U/µL stock) was added to each reaction mixture and incubated at 37 ^{o}C for one hour in order to digest the methylated parental DNA. *E. coli* XL1 blue supercompetent cells were gently thawed on ice and transformed with 1 µL of the PCR product. The cells were incubated on ice after the addition of the PCR product followed by being subjected to heat pulse for 45 s at 42 ^{o}C and incubation on ice for 2 min. Afterwards 0.5 mL of NZY^{+} broth pre heated to 42 ^{o}C was added on to the transformation mixture and further incubated at 37 ^{o}C for 1 h, shaking ~ 225 rpm. Transformation mixture was then plated on LB agar plates containing antibiotic kanamycin (250 µL on each plate) and incubated at 37 ^{o}C over

night. Plasmid DNA was purified from randomly selected individual colonies and screened for the mutation by sequencing.

2.4.30 Ralbp1 mediated uptake studies

Ralbp1 mediated uptake of glutathione conjugates (GS-E) was studied according to the previously published method (Stuckler et al. 2005). Wild type mouse embryonic fibroblast cells ($MEFs^{+/+}$), Ralbp1 gene knockout mouse embryonic fibroblast cells ($MEFs^{-/-}$), Ralbp1 gene knockout embryonic fibroblast cells ($MEFs^{-/-}$) transfected with empty pcDNA3.1 vector or full length Ralbp1-pcDNA3.1 or a mutant Ralbp1-pcDNA3.1, were harvested and aliquots containing 5×10^6 cells (in triplicate) were pelleted and resuspended in 80 µL medium. [^{14}C]-Melphalan (20 µM; specific activity, 92.5 cpm/pmol) 20 µL was then added to the medium and incubated for 20 min at 37 °C. Drug uptake was stopped by rapid cooling on ice. Cells were centrifuged at 2,000 x *g* for 2 min at 4 °C and medium was completely decanted. Radioactivity was determined in the cell pellet after washing twice with ice-cold PBS and resuspending in scintillation fluid.

2.4.31 Ralbp1 mediated endocytosis

Endocytosis of the epidermal growth factor (EGF) was studied in Ralbp1 gene knockout mouse embryonic fibroblast cells transfected with wild type full length as well as transport deficient mutants of Ralbp1. Wild type mouse embryonic fibroblast cells and untransfected knockout fibroblast cells were used as controls.

MEFs$^{-/-}$ 0.2 x 10^6 cells/mL cells or MEFs$^{+/+}$ 0.1 x 10^6 cells/mL were grown on sterilized glass cover slips (18 mm size) in RPMI 1640 medium in tissue culture treated 12 well plates for overnight. Afterwards the cells were washed with HBSS several times. Then the cells were incubated with 100 µL of rhodamine red conjugated EGF (40 ng/ml prepared in DMEM medium containing 1 % BSA) for 60 min at 4 ^oC followed by incubation at 37 ^oC in humidified chamber for 10 min. The cells were then fixed with 4 % paraformaldehyde in HBBS. The cover slips were mounted on slides upside down with vectashield mounting medium The Slides were analyzed using confocal laser scanning microscopy with Zeiss 510-meta system at 40X magnification with excitation wave length at 488 nm and emission 580 nm.

2.4.32 Immunohistochemical localization of Ralbp1

Immunohistochemical localization of Ralbp1 was carried out in H358 cells as well as mouse embryonic fibroblast cells. In addition Ralbp1 in H358 cells was co localized with herceptin (a protein known to have cell surface epitopes) to asses for the cell surface epitopes. MEF$^{-/-}$ cells transfected with transport deficient mutants Ralbp1 was used to assess the effects of mutations on localization of the protein.

The cells (1 x 10^6) were grown on sterilized cover slips for 24 h. The cells were washed with PBS several times to remove the growth media. MEF cells were fixed by methanol and acetic acid mixture (3:1) for 5 min followed by washing 2-3 times with PBS to remove the left over fixing media. Nonspecific antibody interactions were minimized by pre-treating both fixed MEF cells and H358 cells with 10 % goat serum

in PBS for 60 min at room temperature. The cells were then incubated with primary antibodies, anti-Ralbp1 IgG, anti-her2/neu IgG or pre immune IgG for 2 h at room temperature in a humidified chamber. Excess primary antibodies were washed away with PBS (5 times, 3 min each).

After wards the cells were incubated with the secondary antibodies. In the study of effects of mutations on localization of Ralbp1 fluorescein isothicyanate (FITC) conjugated goat anti-rabbit IgG was used as the secondary antibody. During co-localization with Herceptin, rhodamine red-x-conjugated goat anti-rabbit IgG was used as the secondary antibody for Ralbp1 while fluorescein isothiocyanate (FITC) conjugated goat anti-human IgG was used as the secondary antibody for Herceptin. All the secondary antibodies were diluted 50 fold in PBS. The cells were incubated with secondary antibodies for 1 h at room temperature in a humidified chamber. The unbound secondary antibodies were removed by washing with PBS (7 times, 3 min each). The nucleus of the MEF cells was stained with DAPI for 3-5 min followed rinsing with PBS to remove the excess. The cover slips were air-dried and mounted on the slides with Vectashield mounting medium for fluorescence (Vector Laboratories). The images of localization studies using MEFs were carried out at 40X magnification while H358 cells were photographed at 400X magnifications using a LEICA DMLB confocal microscope.

2.4.33 In vitro site directed mutagenesis – deletion mutations

A PCR based method was used to create a series of 15 amino acid deletion mutants of Ralbp1 using full length Ralbp1 cloned in pET30a(+) expression vector as the template. The sequences of the full length upstream and down stream primers respectively were as follows, 5'-GGCGGATCCATGACTGAGTGCTTCCT-3' (BamH I restriction endonuclease site underlined) and 5'-CCGCTCGAGTAGATGGACG TCTCCTTCCTATCCC-3' (Xho I restriction endonuclease site underlined). The sequence of the each mutagenic primer with the respective deletion mutation was as follows. Deletion of amino acids 203-219 (del 203-219), 5'-GTAGAGAGGACCATG GTAGAG AAGTATGGC-3' (with its reverse complement), deletion of amino acids 154-170 (del 154-170), 5'-GAAGAAGTCAAAAGACAAGCCAATTCAGGAG-3' (with its reverse complement), deletion of amino acids 171-185 (del 171-185), 5'-GAAGAAAAAGAAACTCAAACCCATTTTT-3' (with its reverse complement) and deletion of amino acids 154-219 (del 154 -219), 5'-GAAGAAGTCAAAAGACGTAG GAAGTATGGC-3' (with its reverse complement).

During PCR 1 two "halves" flanking from the regions to be deleted were amplified by PCR. The reaction mixture consisted of 500 ng of template DNA, forward and the reverse primers (with a final concentration of 30 pmol each), dNTPs with a final concentration of 2.5 μM each, thermopol buffer (1X), BSA (1X) and 2.5 U of vent DNA polymerase. PCR reaction conditions included an initial denaturation step of 5 min at 94 ^{o}C followed by 30 cycles of 94 ^{o}C, 30 s at 60 ^{o}C and 1 min at 72 ^{o}C. The final

extension step was 7 min at 72 ^{o}C. The PCR products were separated by 1 % agarose gel electrophoresis and gel purified with the aid of gel purification kit from Qiagen.

During second PCR, the products of the first PCR which included two halves of each mutation, were ligated and extended giving rise to the full length deletion mutants of Ralbp1. The 100 µL reaction mixture consisted of equal amount of PCR 1 product for each mutation, 10 µL of thermopile buffer (10X), 1.5 µL of dNTPs (10 mM each), 1 µL of BSA (100X), 1 µL of vent DNA polymerase (2.5 U), 1 µL of $MgCl_2$ and de-ionized water. The reaction conditions were, initial denaturation step of 5 min at 94 ^{o}C followed by 12 cycles of 30 s at 94 ^{o}C, 1 min at 50 ^{o}C and 2 min at 72 ^{o}C with a final extension step of 7 min at 72 ^{o}C.

The PCR products were separated by agarose gel electrophoresis, gel purified with the aid of gel purification kit from Qiagen and digested with restriction endonuclease BamH I and Xho I over night at 37 ^{o}C. The BamH I and Xho I cleaved PCR products were gel purified and ligated with plasmid vector pET30a(+) previously digested with the same restriction endonucleases. The ligated products were transformed in to *E. coli* DH5α. Plasmid DNA was purified from an over night culture of a single colony and the mutation was confirmed by DNA sequencing. Techniques for restriction enzyme digestion, ligation, transformation and other standard molecular biological manipulations were performed according to the protocols described in Sambrook et al., (Sambrook J 1989).

CHAPTER 3

Ralbp1 AS AN ARBITRATOR OF PKCα MEDIATED DRUG RESISTANCE SIGNALING

3.1 Abstract

NSCLC cells are inherently more resistant to chemotherapeutic agent doxorubicin (DOX) as compared to SCLC. Since Ralbp1 is a key transporter responsible for drug accumulation defect consisting of several PKCα phosphorylation sites we investigated the role of PKCα activity on transport properties of Ralbp1. The enhanced transport activity of Ralbp1 by PKCα mediated phosphorylation, lead us to the hypothesis, differential PKCα mediated phosphorylation as a cause for the variations of drug resistance observed in NSCLC and SCLC. Higher expression of PKCα in NSCLC as compared to SCLC as well as, the decrease of IC_{50} value of NSCLC for DOX, to the level of SCLC, by depletion of PKCα confirmed our hypothesis to be true. Although $Ralbp^{-/-}$ MEFs were significantly more sensitive to DOX as compared to $Ralbp^{+/+}$ MEFs (IC_{50} 25 vs 125 nM), depletion of PKCα only affected the DOX sensitivity of $Ralbp^{+/+}$ MEFs. These experimental data confirmed that Ralbp1 in necessary for the PKCα mediated drug resistance signaling.

3.2 Introduction and background

NSCLC indicate a lower drug accumulation and hence greater resistance as compared to SCLC, implicating a fundamental difference in the drug efflux mechanisms (Ahmad et al. 1992; Clark et al. 2003; Ding et al. 2002). The resistance mechanisms responsible for the inherent doxorubicin resistance of NSCLC and acquired DOX resistance in SCLC have being the subject of numerous investigations (Volm et al. 2003). By looking at the possible post translational modifications that can occur differentially between NSCLC and SCLC, it is being observed that increased protein kinase-C (PKC) activity to be closely link with the greater drug accumulation defect in NSCLC (Ahmad et al. 1992; Clark et al. 2003; Ding et al. 2002) as compared to SCLC. According to the literature, MRP is not regulated by PKC while Pgp is phosphorylated. Nevertheless phosphorylation of Pgp does not seem to affect its transport of DOX (Ahmad et al. 1994; Spitaler et al. 1998). The primary structure of Ralbp1 consists of several PKCα mediated phosphorylation sites. Several of these sites have been experimentally confirmed through point mutations (Singhal et al. 2005).

Hence the work described in this chapter depicts our attempts to test the hypothesis that cellular Ralbp1 levels and transport activity and the regulation of Ralbp1 by PKCα is a significant determinant of inherent DOX resistance in NSCLC.

3.3 Results and Discussion

3.3.1 Phosphorylation of Ralbp1 by PKCα

From previous studies by Pikula et al., it has being reported that the activity of Ralbp1, rat homolog of Ralbp1, had increased several fold by phosphorylation mediated by PKCα (Pikula et al. 1994a). Also the primary structure of the Ralbp1 consisted of several putative sequences for PKCα mediated phosphorylation (Awasthi et al. 2002). Hence among the possible post-translational modifications which could have an effect towards the substrate stimulated ATPase activity of Ralbp1 we decided to analyze the effects of PKCα mediated phosphorylation as a starting point.

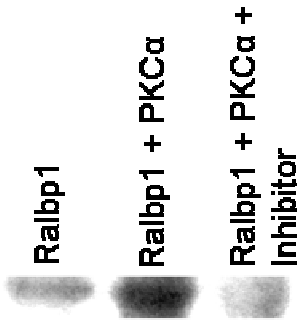

Figure 3.1 PKCα mediated phosphorylation of rec-Ralbp1 (Sharma, Wickramarachchi, et al., 2004)

Bacterially expressed purified rec-Ralbp1 protein, by itself, together with PKCα (0.25 μg per 5 μg Ralbp1 protein) and together with PKCα (0.25 μg per 5 μg Ralbp1 protein) and an inhibitor of PKCα (10 nM Bis-indolylmalemide) was incubated with for 30 min at 37 ^{o}C along with [γ-^{32}P] ATP (specific activity 1 μCi/mmol). The protein mixtures were subjected to SDS-PAGE using 12.5 % polyacrylamide gels and the

associated radio activity was determined by autoradiography for 48 h. Fold increase in phosphorylation was determined by scanning densitometry using phosphorimager.

Rec-Ralbp1 protein indicated basal level of radio activity possibly due to the presence of the two ATP binding sites. The association of the radioactivity was significantly increased by incubating the protein with PKCα. The presence of the PKCα inhibitor bis-indolylmaleimide decreased the association of radiation to the basal level. Thus increase in radioactivity has being due to the phosphorylation effect of PKCα.

3.3.2 Effects of PKCα mediated phosphorylation on transport function of rec-Ralbp1

The effect of phosphorylation on transport activity was determined by comparing the ATP dependent uptake of two glutathione conjugates, [^{3}H]-DNP-SG and [^{3}H]-LTC_4 by proteoliposomes formed of phosphorylated (Ralbp1 with PKCα) and unphosphorylated (Ralbp1 with PKCα and the inhibitor of PKCα) protein and control liposomes.

Proteoliposomes are formed using 50 ng of phosphorylated/ unphosphorylated protein. Liposomes in transport buffer were incubated with each substrate, [^{3}H]-DNP-SG or [^{3}H]-LTC_4 with a final concentration, 100 μM and 0.1 μM respectively for 5 min at 37 ^{o}C. The transport was initiated by the addition of ATP (experimental) or AMP (control) to obtain a 4 mM concentration in a final reaction volume of 120 μL. Following 5 min incubation at 37 ^{o}C with ATP/ AMP, 30 μL aliquots of the reaction mixture were filtered in triplicate using a nitrocellulose filters in a 96 well plate by rapid

filtration method as described before. The radioactivity retained on the membrane was considered as the liposomal uptake of each substrate.

Compared to the control liposomes, Ralbp1 proteoliposomes showed a markedly increase in the uptake of both [^{3}H]-DNP-SG as well as [^{3}H]-LTC_4. When the uptake of unphosphorylated and phosphorylated protein was compared phosphorylation increased the uptake of [^{3}H]-DNP-SG by 3.5 fold while uptake of [^{3}H]-LTC_4 was increased by 2.1 fold. These findings strongly suggest that phosphorylation by PKCα as a positive modulator of transport function of Ralbp1.

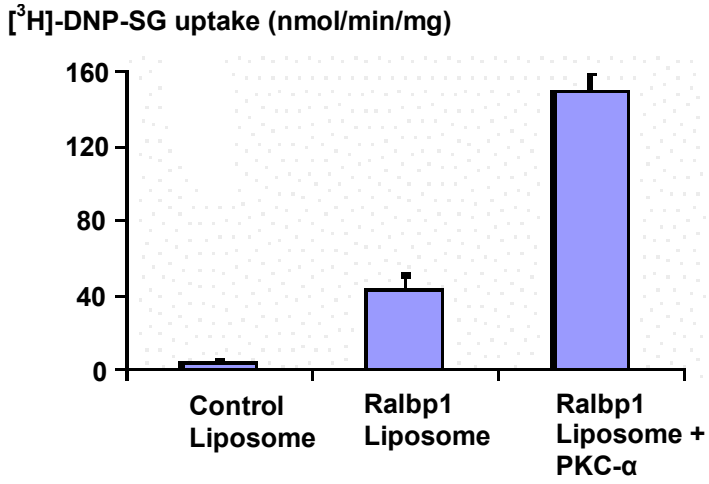

Figure 3.2 Effect of PKCα phosphorylation on uptake of [^{3}H]-DNP-SG (Sharma, Wickramatachchi, et al., 2004)

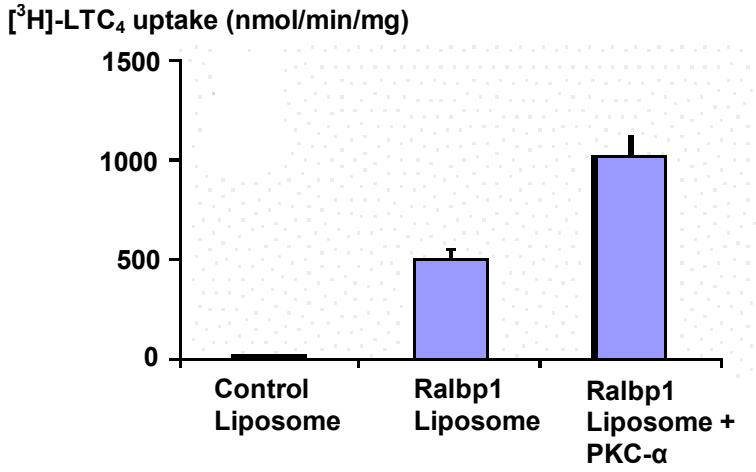

Figure 3.3 Effect of PKCα phosphorylation on uptake of [^{3}H]-LTC$_4$ (Sharma, Wickramatachchi, et al., 2004)

3.3.3 Differential expression of PKCα in SCLC and NSCLC cell lines and suppression by siRNA

Drug accumulation defects are a major cause for the failure of chemotherapy for SCLCs as well as NSCLCs (Samuelsson et al. 1987). It has being reported from numerous studies that in NSCLCs the drug accumulation is inherently lower than in SCLCs. Based on our previous observations that Ralbp1 is a major transporter of unconjugated and glutathione conjugates of wide range of xeno/ endobiotics (Awasthi et al. 2000) and that its activity is increased by PKCα mediated phosphorylation of rec-protein (Sharma et al. 2004) as well as the identification of PKCα phosphorylation sites by site directed mutagenesis (Singhal et al. 2005a), we hypothesize that, increased PKCα activity may be one mechanism that is responsible for the increased efflux of chemotherapeutic agents from NSCLCs as compared to SCLCs.

In order to test whether PKCα is differentially expressed in NSCLC and SCLC, we carried out western blot analysis with an equal amount of crude protein (100 μg) from several SCLC cell lines as well as NSCLC cell lines. Also suppression of PKCα was analyzed by using siRNA, targeted towards the nucleotides 1960–1978 (GAAGGGTTCTCGTATGTCA) of PKCα cDNA. The corresponding sense and the antisense siRNA sequences are 5'-GAAGGGUUCUCGUAUGUCAdTdT-3' and 5'-UG ACAUACGAGAACCCUUCdTdT-3' respectively. The sense and the antisense siRNA sequences of the non silencing control siRNA termed scramble siRNA were as follows, 5'-UUCUCCGAACGUGUCACGUdTdT-3' (sense) and 5'-ACGUGACACGUUCGG AGAAdTdT-3' (antisense).

SCLC H182, H1417, and H1618 and NSCLC H226, H358, H1395 and H 2347 were transfected with double stranded PKCα siRNA with the aid of Transmessenger transfection reagent kit from Qiagen for 3 h. Afterwards the cells were washed with phosphate buffer saline (PBS) and allowed to grow in fresh complete medium for 48 h. A homogenate was prepared in lysis buffer and 100 μg of protein from each sample was used for the SDS-PAGE followed by western blotting with rabbit-anti-human PKCα primary antibodies and HRP conjugated goat-anti-rabbit secondary antibodies. Chromogenic substrate 4-chloro-1-napthol was used to visualize the bands. β-actin was used as an internal control to asses the uniformity of the loading.

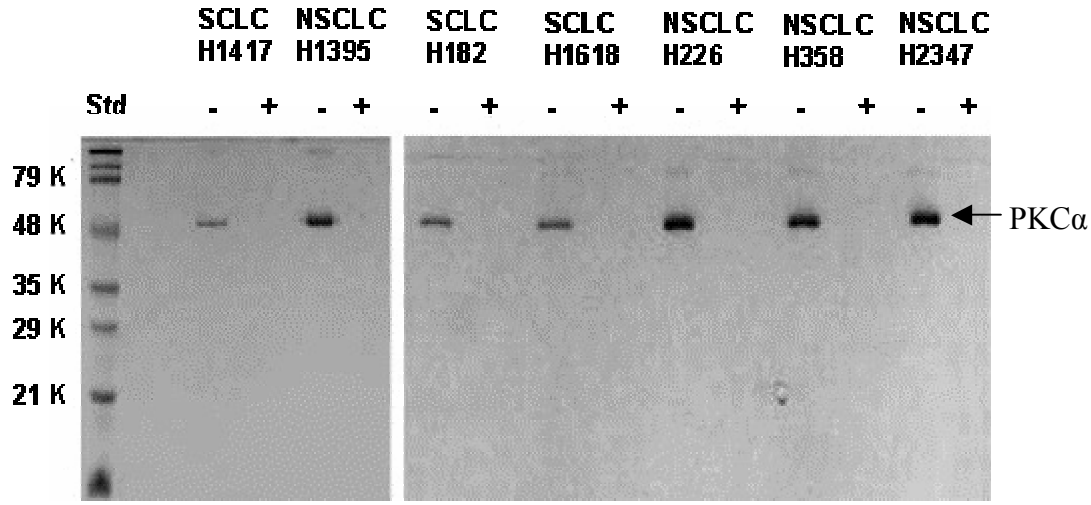

Figure 3.4 Western blot with anti-PKCα IgG (Singhal, Wickramarachchi, et al., 2006)

The western blot analysis indicated the expression of PKCα to be higher in NSCLC as compared to that of SCLC. Also it is evident that siRNA against nucleotides 1960–1978, successfully suppresses the expression of PKCα.

3.3.4 PKCα depletion, effects on doxorubicin transport activity of Ralbp1 in SCLC and NSCLC

The observed PKCα mediated enhancing effect on the transport function of Ralbp1 was studied *in vitro* by comparing the transport of doxorubicin from phosphorylated and unphosphorylated (by depletion of PKCα) Ralbp1 from several SCLC, H182, H1417, H1618 and NSCLC H226, H358, H1395 and H2347 cell lines.

The expression of the PKCα was suppressed by PKCα-siRNA with the aid of Transmessenger trasfection reagent from Qiagen as described in section 2.4.28. Scrambled siRNA was used as a control. Following 3 h the cells were washed with PBS and were allowed to grow in fresh complete media for 48 h. Ralbp1 was purified to

homogeneity from cells by DNP-SG affinity chromatography as described in 2.4.7. Purified protein was reconstituted in to proteoliposomes with cholesterol and asolectin according the procedure described in section 2.4.20. The transport studies with ^{14}C-DOX were carried out as previously described in section 2.4.21.

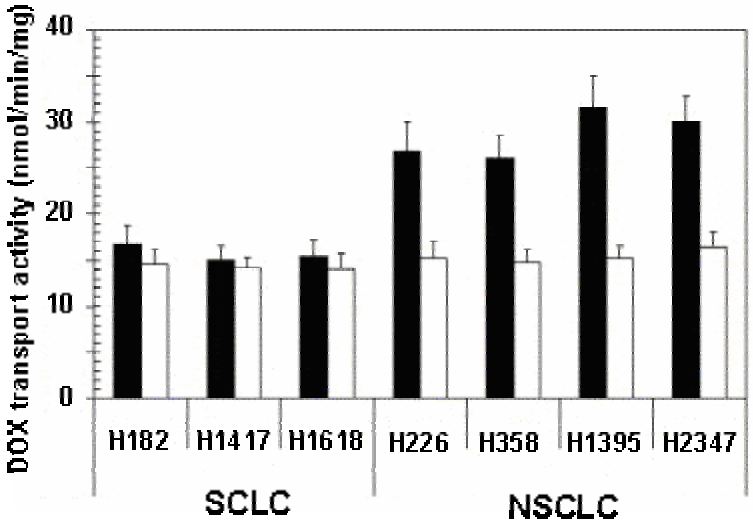

Figure 3.5 PKCα depletion, effects on transport function of Ralbp1 (*in vitro*) (Singhal, Wickramarachchi et al., 2006)

Scrambled siRNA (control) transfected cells are indicated by black color while PKCα-siRNA (experimental) transfected cells are indicated by white color

Results of the doxorubicin transport activity indicated that NSCLC has a higher transport activity as compared to SCLC, in compliance with the higher multi drug accumulation defect. Depletion of PKCα by siRNA decreased the transport function of NSCLC to the level observed with SCLC indicating that the differences of the transport activity is caused by PKCα mediated phosphorylation. Depletion of PKCα in SCLC slightly reduced the transport activity in SCLC presumably through other pathways regulated by PKCα.

3.3.5 The effect of PKCα depletion on cell survival of SCLC and NSCLC

The effect of depletion of PKCα mediated phosphorylation on cell survival and growth was studied by determining the viable cell density by MTT assay.

Several SCLC H182, H1417, H1618 and NSCLC H226, H358, H1395, H2347 cell lines were transfected with PKCα-siRNA or scrambled siRNA (control) as before. The cells were then seeded 20,000 cells/ well in a 96 well plate. After 96 h incubation at 37 ^{o}C, the viable cell density was determined by MTT assay as described in section 2.4.29.

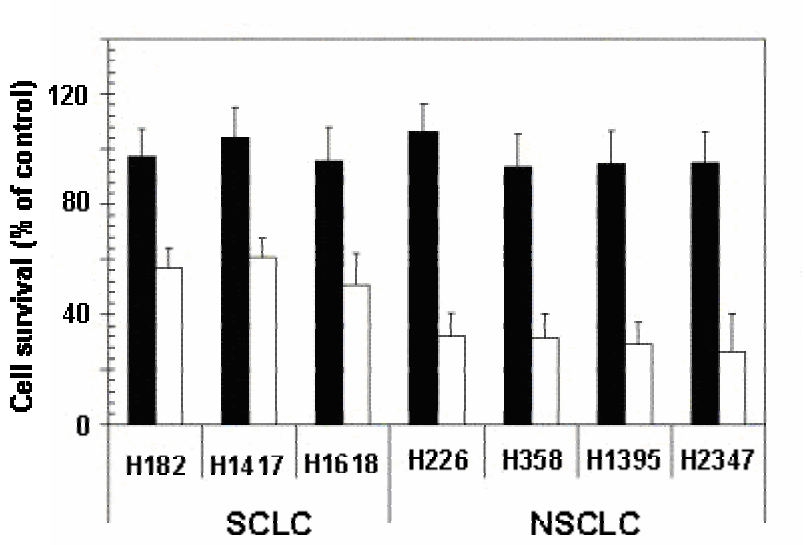

Figure 3.6 Depletion of PKCα mediated phosphorylation, effects on cell survival of SCLC and NSCLC (Singhal, Wickramarachchi et al., 2006)

Scrambled siRNA (control) transfected cells are indicated by black color while PKCα-siRNA (experimental) transfected cells are indicated by white color

According to the results, depletion of PKCα affected the growth and survival of both SCLC as well as NSCLC indicating its key role in cell proliferation and/ or differentiation. The decrease of growth rate in SCLC (43 ± 5%, n = 3) was less as compared to that of NSCLC (~ 70 ± 3%, n = 4). These findings indicate that PKCα mediated phosphorylation plays a major role in NSCLC during growth differentiation as well as in xeno/ endobiotic efflux.

3.3.6 Effect of depletion of PKCα on resistance against doxorubicin mediated cytotoxity

The effect of depletion of PKCα on resistance against doxorubicin mediated cytotoxity was studied by comparing the IC_{50} values of several SCLC and NSCLC cell lines. SCLC H182, H1417, H1618 and NSCLC H226, H358, H1395 and H2347 cell lines were transfected with PKCα-siRNA (experimental) or scrambled siRNA (control) as before. The cells were then seeded 20,000 cells/ well in a 96 well plate. Following incubation for 96 h at 37 ^{o}C, with varying concentrations of doxorubicin from 0.01 μM to 2 μM, the viable cell density was determined by MTT assay as described in section 2.4.29. Eight replicates were carried out for each concentration.

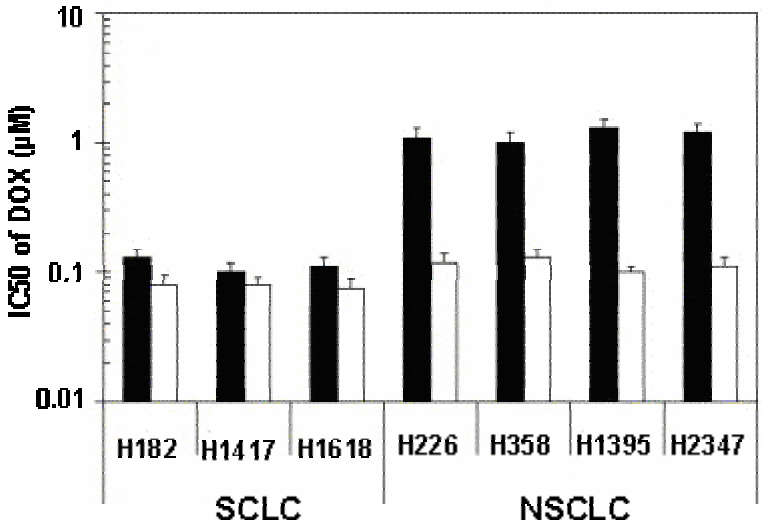

Figure 3.7 Depletion of PKCα on resistance against doxorubicin mediated cytotoxity in SCLC and NSCLC (Singhal, Wickramarachchi et al., 2006)

Scrambled siRNA (control) transfected cells are indicated by black color while PKCα-siRNA (experimental) transfected cells are indicated by white color

In agreement with the studies done by others, IC_{50} value for doxorubicin with NSCLC was much higher than that is seen with SCLC. As seen with the transport studies, the effect of depletion of PKCα was greater in NSCLC as compared to SCLC. Depletion of PKCα in SCLC lowered the IC_{50} of doxorubicin slightly in SCLC most likely through other pathways regulated by PKCα.

3.3.7 Requirement of Ralbp1 for PKCα attributed resistance against doxorubicin mediated cytotoxity

In order to asses that PKCα mediated doxorubicin resistance was mediated mainly through phosphorylation of Ralbp1 or whether some other proteins are also involved, we studied the effect of depletion of PKCα on doxorubicin resistance, in cells that do not express Ralbp1. This was carried out by comparing the effect of depletion of PKCα IC_{50} towards doxorubicin in Ralbp1 gene knockout mouse embryonic fibroblast cells ($MEFs^{-/-}$) with that of wild type mouse embryonic fibroblast cells ($MEFs^{+/+}$).

$MEFs^{+/+}$ and $MEFs^{-/-}$ were transfected with PKCα-siRNA (experimental) or scrambled siRNA (control) using Transmessenger transfection kit from Qiagen. After 3 h of incubation at 37 ^{o}C, the cells were washed with PBS and incubated with fresh medium for 48 h at 37 ^{o}C. The cells were then seeded 20,000 cells/ well in a 96 well plate. Following incubation for 96 hours at 37 ^{o}C, with varying concentrations of doxorubicin from 0.01 μM to 2 μM, the viable cell density was determined by MTT assay as described in methods. Eight replicates were carried out for each concentration.

$Ralbp1^{-/-}$ MEFs are clearly more sensitive to doxorubicin as compared to $Ralbp1^{+/+}$ MEFs. Although depletion of PKCα sensitized $Ralbp1^{+/+}$ MEFs to

doxorubicin, they still are more resistant than the Ralbp1$^{-/-}$ MEF cells. Also according to the results, depletion of PKCα had no effect on the cytotoxicity of doxorubicin in Ralbp1$^{-/-}$ MEFs. This directly indicate that role of PKCα in drug accumulation defect mainly occur through the phosphorylation of Ralbp1.

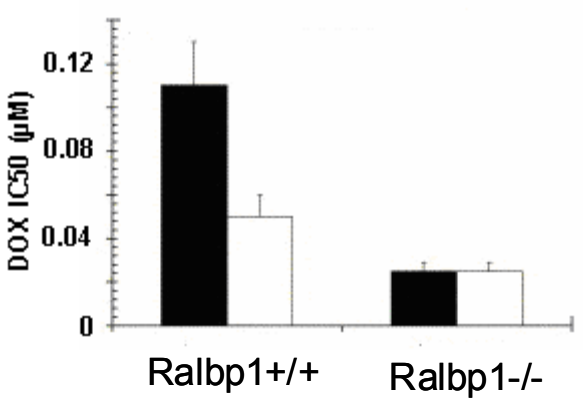

Figure 3.8 Effect of PKCα depletion on IC_{50} value of doxorubicin in Ralbp1$^{+/+}$ and Ralbp1$^{-/-}$ MEF cells (Singhal, Wickramarachchi et al., 2006)

Scrambled siRNA (control) transfected cells are indicated by black color while PKCα-siRNA (experimental) transfected cells are indicated by white color

3.4 Conclusions

The studies using rec-Ralbp1 proteoliposomes in the presence of PKCα indicated enhanced transport of both endobiotics (LTC_4) as well as xenobiotics (DNP-SG). In order to answer the question whether PKCα mediated phosphorylation of Ralbp1 as a cause for differential drug resistance observed in NSCLC and SCLC, we determined the expression of PKCα in several NSCLC and SCLC cell lines. Western blot analysis using antibodies against PKCα, with equal amount of crude protein from either cell lines indicated a higher expression of PKCα in all NSCLC cell lines as compared to SCLC cell lines. Depletion of PKCα by siRNA, in several NSCLC and SCLC cell lines, showed a decrease in the drug resistance (IC_{50} for DOX) of NSCLC cell lines to the level observed with SCLC cell lines. Same phenomenon was observed in DOX transport studies using proteoliposomes reconstituted with purified Ralbp1 from PKCα depleted NSCLC and SCLC. These results directly indicate that PKCα play a major role toward differential DOX resistance of NSCLC and SCLC.

The role of Ralbp1 in PKCα mediated resistance signaling was analyzed by determination of IC_{50} for DOX in $Ralbp1^{+/+}$ and $Ralbp^{-/-}$ MEFs in the presence and absence of PKCα. $Ralbp1^{-/-}$ MEFs were significantly sensitive to DOX as compared to $Ralbp^{+/+}$ MEFs. Depletion of PKCα did not affect the DOX sensitivity of $Ralbp1^{-/-}$ MEFs. On the other hand PKCα depletion sensitized $Ralbp^{+/+}$ MEFs by 2.2 fold. These results demonstrate that the effect of PKCα in mediated drug resistance requires the presence of functional Ralbp1; that is, the primary function of PKCα with respect to doxorubicin resistance in NSCLC is to keep Ralbp1 in its active phosphorylated state.

The complete reversion of the resistance phenotype from NSCLC to that of SCLC upon depletion of PKCα, and the complete inability of PKCα to affect resistance in Ralbp1$^{-/-}$ MEFs strongly support this conclusion.

CHAPTER 4

IDENTIFICATION OF MEMBRANE ANCHORING DOMAINS OF Ralbp1 AND CELLULAR LOCALIZATION

4.1 Abstract

The cellular distribution of Ralbp1 is of utmost importance due to its multi functional nature as an ATP dependent transporter, effector in Ras- Ral signal pathways, mitosis and receptor mediated endocytosis. Though our previous studies indicate Ralbp1 to be associated with the membrane, particularly N-terminal domain, other investigators suggest a cytosolic distribution attached to cytoskeleton (Hu & Mivechi 2003). In the absence of transmembrane helices in the primary structure of Ralbp1, we selected several regions with high sequence homology to vector peptides that are known to be capable of transmembrane transport of allocrites as candidate regions for membrane anchorage. A series of deletion mutants of Ralbp1 were constructed and effects of mutations on expression of the protein between cytosol and membrane as well as on transport properties were studied. The results of the study indicate aa 154–219 as important in membrane anchorage and that membrane anchorage is required for its transport function. Immunohistochemical co-localization of Ralbp1 with Herceptin in H358 lung cancer cells transfected with deletion mutant of aa 171-185, in which the wild type protein has being suppressed by siRNA indicate, aa 171-185 comprises a cell-surface epitope.

4.2 Introduction and background

Multiple roles of Ralbp1 such as ATP-dependent transporter, role as an effector protein in signaling pathways, mitosis, membrane ruffling and receptor mediated endocytosis all indicate Ralbp1 to be associated with the membrane. Previous studies have shown that N-terminal domain of Ralbp1 (N-Ralbp1$^{1-367}$) can be extracted only in the presence of a detergent indicating it to be associated with the membrane where as C-terminal domain of Ralbp1 (C-Ralbp1$^{410-655}$) is found in both aqueous and the detergent fractions. The rat and mouse homologues of Ralbp1, known as Ralbp1 and RIP1, respectively, appear to be associated with the membrane by our studies as well as studies by other investigators (Cheng et al. 2001; Drin et al. 2003; Letoha et al. 2003; Pikula et al. 1994a; Pikula et al. 1994b). Immunohistochemistry studies using antibodies against different regions of Ralbp1 in human lung cancer cells lines indicate the existence of cell surface epitopes (Minamide et al. 1990). Human lung cancer cells incubated with anti-Ralbp1 antibodies against various regions of Ralbp1 were checked for the sensitivity to doxorubicin (IC_{50} values for doxorubicin). Considerable decrease in IC_{50} values toward doxorubicin upon exposure to antibodies against particular regions suggest the existence of cell surface epitopes.

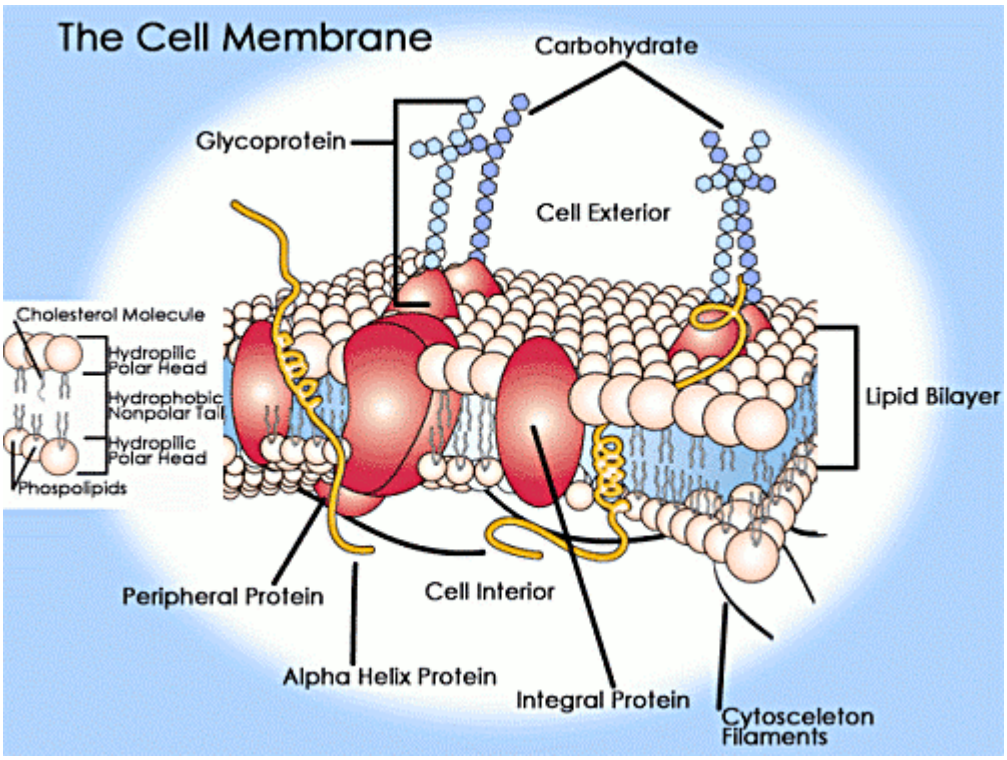

Figure 4.1 Membrane proteins (http://img.sparknotes.com/figures/A/a981208a1abd542364d5a13c08702881/cellmembrane.gif) (with permission)

Based on the attachment, membrane proteins are classified to two groups known as integral membrane proteins and peripheral membrane proteins. Peripheral proteins are associated with the membrane by non-covalent attachments such as electrostatic attractions with the integral proteins and could be de-attached simply by high salt concentrations (salting in) or by using solutions with elevated pH values. Integral proteins are more firmly attached to membrane by one or more trans-membrane amphipathic alpha helices with the hydrophobic side chains pointing outwards or by post-translational modifications such as addition of long chain fatty acid groups like myristoylation groups or by addition of glycosylation groups such as glycosyl

phosphatidylinositol that can interact with a single lipid bi-layer. Integral proteins require the use of a non ionic detergent to be disassociated from the membrane.

The N-terminal sequence analysis of Ralbp1 reveals that it does not have the necessary sequence required to be N-myristoylated although there are several potential sites with in the N-terminal domain which could be exposed upon proteolytic cleavage. Since post-translational modifications are essentially associated with eukaryotic systems and yet major fraction (~80 %) of recombinant Ralbp1 is found associated with the membrane even when expressed using bacterial systems, there should be other modes by which the protein is attached to the bi-lipid membrane apart from post-translational modifications.

The primary structure of Ralbp1 does not indicate the sequences of classical trans-membrane helices that are associated with ABC cassette of membrane transporters. Hydropathy plots reveal two regions of relatively high hydrophobicity, which could be potentially linked with the membrane. In order to identify some candidate sites for membrane anchorage we aligned the sequence of Ralbp1 with some vector peptides and some other known membrane associated proteins. Vector peptides are short 20 residue highly basic (rich in arginine) or amphipathic peptides that are capable of transporting substances across the cell membranes. Their polycationic nature as well as the amphipilicity facilitated the interactions with the cell membranes. Amino acid sequence analysis indicated that Ralbp1 has sequences with some degree of homology to vector peptides such as penetratin, Tat and MAP. Also it showed some degree of sequence homology to several other membrane associated proteins.

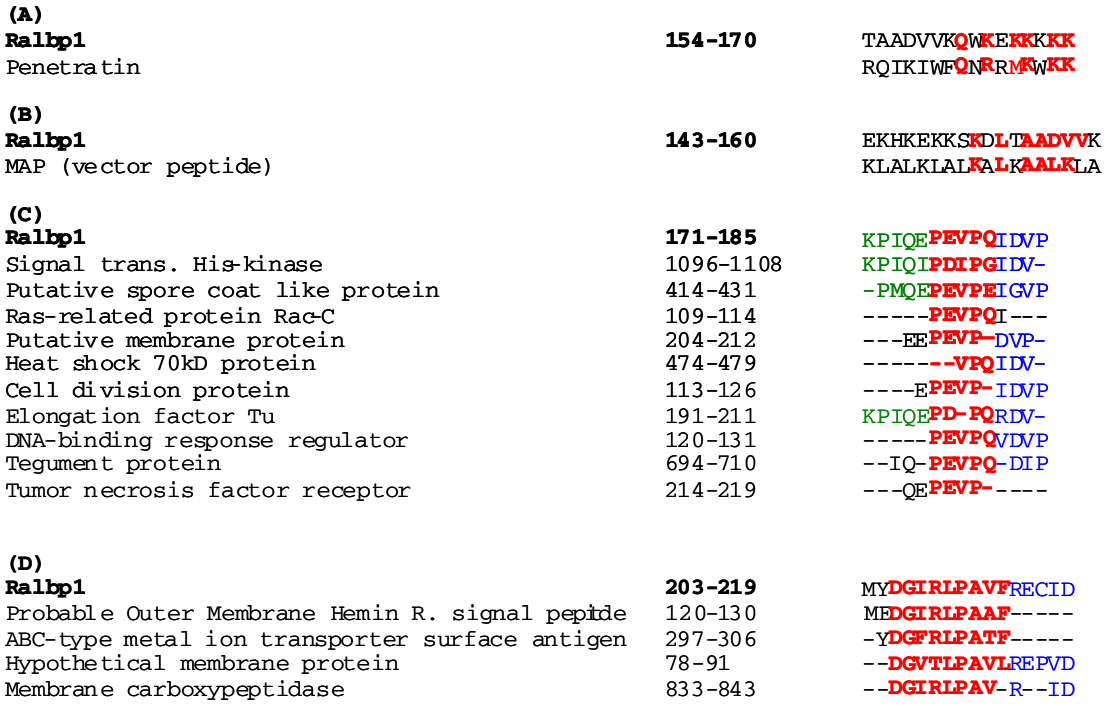

Figure 4.2 Sequence homology of Ralbp1 with vector peptides and membrane associated proteins (Yadav, Wickramarachchi et al 2004)

The chapter 4, describes about our attempts to identify the regions of Ralbp1 that could be important for membrane anchorage through a deletion mutant analysis. Depending on the sequence homology to vector peptides and several known membrane associated proteins, we constructed a series of deletion mutants and ascertained the effects of deletion mutations on distribution of the protein associated with the membrane and in cytosol as well as on transport.

4.3 Results and Discussion

4.3.1 Membrane localization of Ralbp1

Immunohistochemistry studies using antibodies against full length Ralbp1 on live unfixed H358 cells indicated a membrane associated pattern.

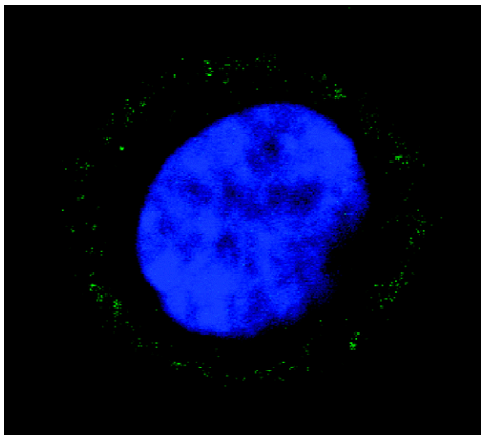

Figure 4.3 Cell surface localization of Ralbp1 (Yadav, Wickramarachchi et al., 2004)

NSCLC H358 cells grown on sterilized cover slips were incubated with poly clonal anti-Ralbp1 IgG primary antibodies followed by fluoroscene isothocyanate (FITC) conjugated goat anti-rabbit IgG secondary antibodies. The nucleus of the cell was stained with DAPI. The cells were analyzed by Zeiss LSM 510META laser scanning fluorescence microscopy.

4.3.2 Co-localization of Ralbp1 with a membrane associated protein

Her2/neu is a membrane associated protein which is over expressed in cancer cells. As further evidence for membrane association of Ralbp1, we co-localized Ralbp1 with her2/neu in NSCLC H358 cells. Rhodamine red-x-conjugated goat anti-rabbit antibodies were used as secondary antibodies for Ralbp1 while FITC conjugated goat anti-human antibodies were used as secondary antibodies for her2/neu.

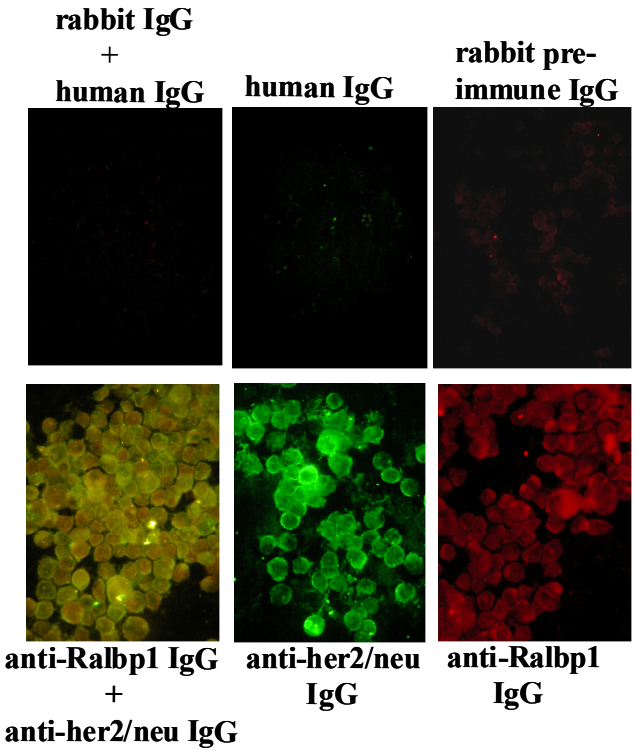

Figure 4.4 Co-localization of Ralbp1 with protein her2/neu (Yadav, Wickramarachchi et al., 2004)

Cell surface epitopes were recognized by both anti-Ralbp1 (red) and her2/neu antibodies (green), and these epitopes co-localized (yellow) in unfixed cells, indicating both her2/neu and Ralbp1 have cell surface epitope(s).

4.3.3 Identification of membrane associated domains of Ralbp1

Several of the regions that were identified as candidate regions for membrane association through sequence homology were deleted by the PCR-based method as described in methods. The effect of deletion mutations on cellular distribution of Ralbp1 was assessed by comparing the membrane associated and cytosolic fraction of wild type full length Ralbp1 and its deletion mutants, amino acids 154 -170, amino acids 171 -185, amino acids 203 -219 and amino acids 154 – 219.

Equal amount of protein (100 μg) from crude cell lysate of *E. coli* expressing wild type full length or deletion mutant Ralbp1, in lysis buffer with or with out 1 % non ionic detergent polydoconol ($C_{12}E_9$) was analyzed by Western blot analyses using anti-Ralbp1 antibodies.

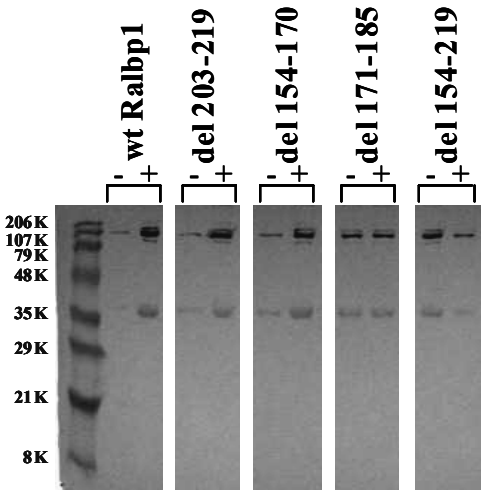

Figure 4.5 Effects of deletion mutations on cellular expression of Ralbp1 (Yadav, Wickramarachchi et al., 2004)

Sample extracted with 1 % polidocanol are indicated by (+) while samples extracted without polidocanol are indicated by (-)

When the ratio of membrane associated fraction to cytosolic fraction of each deletion mutant protein was compared with that of the wild type full length protein, deletion of amino acids 171-185 showed the greatest change in the ratio and hence in the cellular distribution. With the deletion of amino acids 171–185 more protein was seen in the cytosolic fraction. Deletion mutant of amino acids 154-170 also indicated a slight reduction in the membrane associated fraction while deletion of amino acids 203-219 did not affect the distribution of Ralbp1 significantly. Full length deletion mutant which include all three regions from amino acids 154-219 showed the greatest change in the distribution. There by it is evident from the results of the study that amino acids 154-219 contribute significantly towards membrane association of Ralbp1.

4.3.4 Effects of deletions on transport properties of Ralbp1

The effects of deletions on Ralbp1 as an ATP dependent transmembrane transporter was assessed by studying the [^{14}C]DOX and [^{3}H]DNP-SG as substrates. Purified full length rec-Ralbp1 or its deletion mutant proteins were reconstituted in to proteoliposomes and conducted the transport assay as described in methods. DOX was used as a cationic substrate while DNP-SG represented as an anionic GS-E.

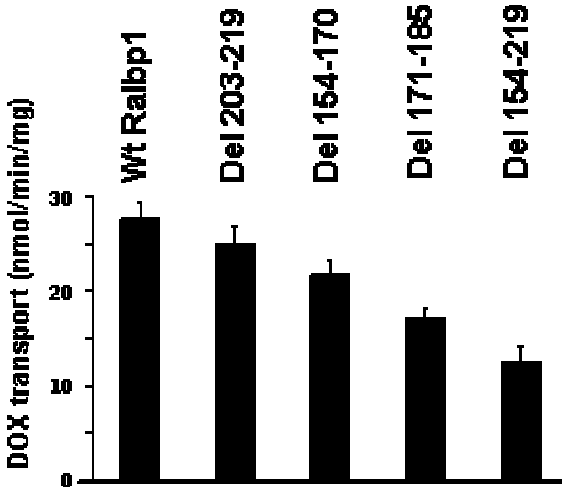

Figure 4.6 ATP dependent transport of DOX (Yadav, Wickramarachchi et al. 2004)

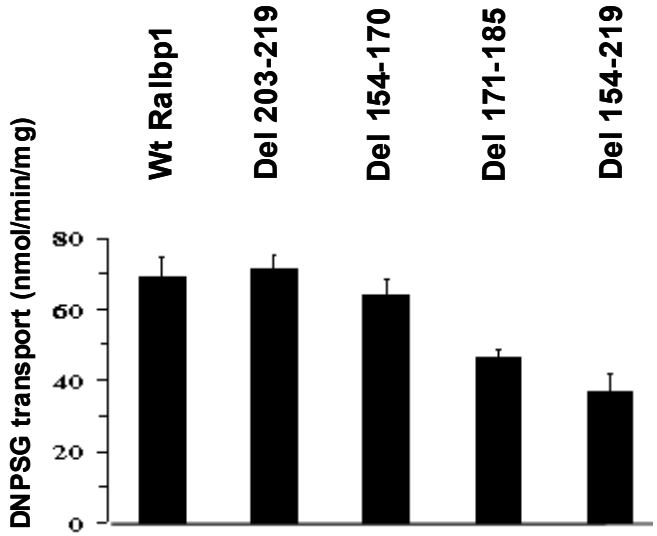

Figure 4.7 ATP dependent transport of DNP-SG (Yadav, Wickramarachchi et al. 2004)

The results of the transport study indicated a similar pattern with all the mutants for both DOX and DNP-SG regardless of the cationic/ anionic nature of the substrate. Deletion mutant of aa 203-219 indicated similar transport activity as wild type full length Ralbp1 for both DOX as well as DNP-SG. Small but significant decrease in transport activity was seen for both substrates for deletion mutant of aa 154-170. Deletion mutant of aa 171-185 resulted in an approximately 35-40 % loss of transport activity for both DOX as well as DNP-SG as compared to wild type full length protein. Deletion of entire region of aa 154-219 resulted in even further loss of transport activity (~50 %) for both substrates.

4.3.5 Identification of cell surface epitopes of Ralbp1

Cell surface epitopes of Ralbp1 are identified by expressing the mutant protein in H358 NSCLC cells. Study was conducted with aa 171-185 deletion mutant, based on the results of preliminary studies as well as being the most effective deletion mutant toward membrane association. The constitutively expressed wild type Ralbp1 in deletion mutant of aa 171-185 transfected, H358 cells were suppressed, by treating the cells with siRNA against region encoding aa 171-185. Non specific scrambled siRNA was used as the control.

Immunohistochemistry was performed using anti-del 171-185 antibodies as primary antibodies. The cell surface epitopes were identified by co-localizing with well known membrane associated protein her2/neu. Rhodamine red x-conjugated goat anti-

rabbit IgG and flurosceine (FITC) conjugated goat anti-human IgG were used as secondary antibodies for Ralbp1 and her2/neu primary antibodies, respectively.

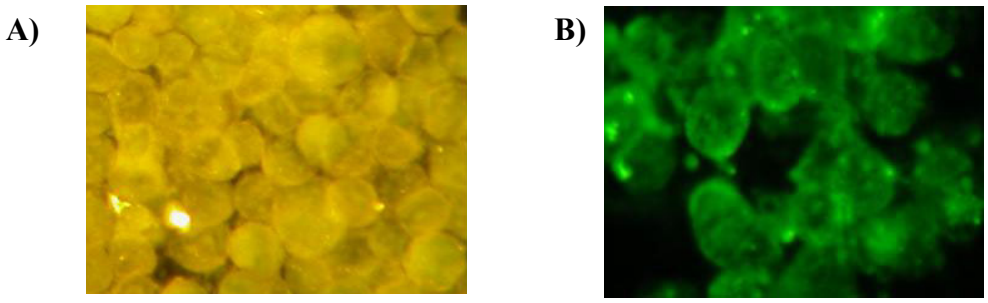

Figure 4.8 Identification cell surface epitopes of Ralbp1 (Yadav, Wickramarachchi et al. 2004)

Figure A indicates cells treated with scrambled siRNA while figure B indicates cells treated with anti- del 171-185 siRNA

On the cells where the control siRNA was used, both Ralbp1 and her2/neu proteins are co-localized as indicated by the yellow color resultant from the overlap of red and green fluorescence. Upon silencing with siRNA against aa 171-185, in aa 171-185 deletion mutant transfected cells, only the green fluorescence due to her2/neu was seen. These studies indicated that aa 171-185 is present at the cell surface.

4.4 Conclusions

In order to find an answer to the intriguing question about the distribution of the multifunctional protein, Ralbp1, the study discussed in chapter 4, aimed to identify the cell surface domains and to determine the importance of membrane anchorage in transport properties of Ralbp1. Several regions of potential candidates for membrane anchorage were selected based on the sequence homology to vector peptides and several other membrane associated proteins.

Out of the selected regions, aa 154-219 indicated the greatest effect towards membrane association as well as transport properties. Deletion mutant aa 154-219 showed almost a 50 % decrease in the transport of anionic substrate, DNP-SG as well as weakly cationic substrate, DOX with a concomitant decrease in association with the membrane. Through immunohistochemical studies it was evident that aa 171-185 possess cell surface epitopes. Nevertheless due to the fact that specific antibodies against the entire peptide encompassing aa 154-219 could not be raised, our findings leave open the possibility that the cell surface domain may not be limited to aa 171-185. Likewise, because the membrane anchorage or the transport, could not be completely abrogated by deletion of aa 154-219, other regions may play a role in membrane anchorage of Ralbp1.

CHAPTER 5

Ralbp1 AS A NOVEL LINK IN STRESS DEFENSE AND SIGNALING PATHWAYS

5.1 Abstract

Ralbp1 is bound to clathrin, the AP2 adaptor protein and is shown to play a vital role in endocytosis. However, its functional role in endocytosis had not been studied in Ralbp1-deficient cells or tissues. Herein, we report that Ralbp1 loss causes an almost complete cessation of clathrin-dependent endocytosis of epidermal growth factor receptor, which is restored fully by wild-type Ralbp1. Remarkably, mutant Ralbp1 proteins selected for decreased affinity for glutathione-conjugates displayed proportionately the same loss in endocytosis capacity as in other functional measures including substrate-stimulated transport activity, or the ability to confer drug-accumulation defect and drug-resistance phenotype. The rate of clathrin-dependent endocytosis was found to be directly proportional to the ATPase and transport activity of Ralbp1. These studies demonstrate that glutathione-conjugate transport activity of Ralbp1 is necessary for clathrin-dependent endocytosis. These fundamental observations give an insight about the functioning of the endocytosis apparatus, and its regulation by the mercapturic acid pathway.

5.2 Introduction and background

Although originally cloned as Ral effector, Ralbp1 has been linked with a diverse functions most prominently with the endocytosis and transport of glutathione conjugates. In order to test whether there is a link between the role of Ralbp1 in glutathione-conjugate transport and regulation of endocytosis, the potential glutathione-conjugate binding residues in Ralbp1 had to first be identified. Reasoning that the glutathione-moiety would bind at a site which resembled other known glutathione-binding proteins, we compared primary sequences and known glutathione-binding residues of glutathione *S*-transferases (GSTs) and crystallin with Ralbp1 (figure 5.3). Candidate residues of Ralbp1 were subjected to site-directed mutagenesis. The bacterially expressed mutants were purified and characterized with respect to DNP-SG affinity and transport-activity in artificial liposomes. These mutants were also cloned into eukaryotic expression vectors and transfected into Ralbp1-deficient ($Ralbp1^{-/-}$) mouse embryonic fibroblast cells in order to determine the effect of each mutation on transport-mediated drug-resistance as well as endocytosis. These studies demonstrated that DNP-SG affinity of Ralbp1 mutants correlated very well with transport activity, drug-resistance conferring activity, as well as with restoration of endocytosis in $Ralbp1^{-/-}$ MEFs, which are otherwise severely deficient in endocytosis. These findings have a fundamental implication in ligand-receptor signaling mechanisms, that the activity of a mercapturic-acid pathway efflux-protein directly regulates the crucial physiological process of clathrin-dependent endocytosis.

Glutathione *S*-transferases consist of 4 different classes; canonical soluble GSTs (Armstrong 1997), mitochondrial (kappa-class) GSTs (Jowsey et al. 2003; Ladner et al. 2004), microsomal GSTs (MAPEG-membrane associated proteins in eicosanoid and glutathione metabolism family) (Morgenstern et al. 1982), and the bacterial fosfomycin resistance proteins (Bernat et al. 1997). Substrate specificities and mechanisms are different between the families as well as between members of the same family although some commonalities do exist.

Among the 5 main classes of cytosolic GSTs; theta, sigma, alpha, mu and pi, GST alpha, mu and pi are more common among vertebrates. Broad substrate specificity of GSTs leads to less stringent structure at the active site and hence lower catalytic efficiency which is compensated by the abundance of GSTs.

Catalysis of conjugation of glutathione by GSTs comprise of binding and activation of glutathione as well as the electrophilic substrate. Although the binding and activation of glutathione is common to all the classes of GSTs and bears some general characteristics, binding of the substrate depends on the nature of the substrate as well as the enzyme. Availability of crystal structures of numerous GSTs and related proteins have provided a wealth of structural as well as mechanistic information about these enzymes (Hitchens et al. 2001). Cytosolic GSTs are dimeric proteins with an active site in each monomer. The GSH binding site known as G-site is located in N-terminal domain.

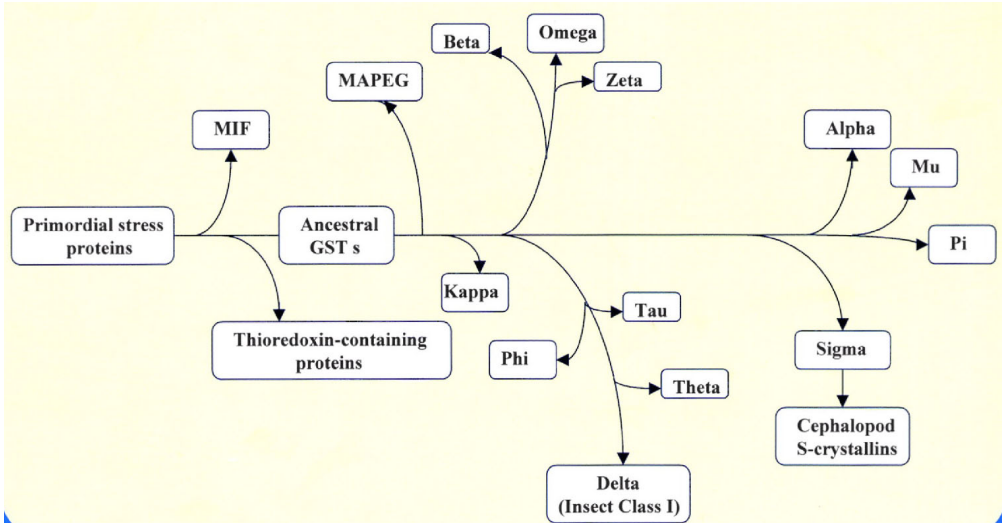

Figure 5.1 Evolution of glutathione *S*-transferases (Sheehan et al. 2001)

Among the different classes of GSTs, 3 different binding modes are observed. Although the γ-glutamyl side chain of GSH interacts with the enzyme in a very similar manner in well known GST structures (Ji et al. 1995), the interactions between the cysteinyl and glycyl residues of the tripeptide show significant differences depending on the class (Ji et al. 1995). GST classes alpha, pi and sigma share the same binding mode while GST class mu and GST from *S. japonicum* share another. Theta class GSTs shows the third mode of binding. The glutathionyl portion of the tripeptide binds to the enzyme in an extended conformation with the involvement of a network of electrostatic interactions. The similarities and the differences of the interactions among the three binding modes are indicated in the table below. Most highly conserved and crucial residues in recognition of the γ–glutamyl moiety of GSH, a glutamine residue along with the subsequent serine or threonine residue could not be found in Ralbp1 (Ji et al.

1997; Ji et al. 1995; Ji et al. 1992; Lim et al. 1994; Reinemer et al. 1991; Sinning et al. 1993).

Table 5.1 Electrostatic interactions between 1-(*S*-glutathionyl)-2,4-dinitrobenzene (GSDNB) and GSTs (Ji et al. 1993; Ji et al. 1995)

GSDNB	GST mu, *S. Japonicum*	GST sigma, alpha, pi
γ-Glu-N	Q71	Q62
γ-Glu-N	D105	D96 (3.90 Å)[1]
γ-Glu-N	D105	D96 (3.68 Å)
γ-Glu-O	S72	S63
γ-Glu-O	S72	S63
γ-Glu-O	Q71	Q62
γ-Glu-O	S72	S63
Cys-N	N58	
Cys-N	L59	M50
Cys-O	W7	
Cys-O		M50
Gly-N	N58	
Gly-O		K42
Gly-O		N48
Gly-O	R42	W38
Gly-O	W45	
Gly-O		K42
Gly-O	K49	

[1]Distance criterion for hydrogen bonds and salt bridges is 3.5 Å. Distances exceeding this criterion are given in parentheses.

GSTs carry out the activation of glutathione by lowering the pKa of the cysteinyl thiol group which in its unbound form is ~9, to a value of ~ 6-7 (Chen et al. 1988). Therefore, enzyme bound GSH is largely in deprotonated form under the physiological pH. The negative charge on the enzyme bound thiolate is stabilized by hydrogen bonding with the hydroxyl group of a tyrosine closer to the N terminal, in

alpha, mu, sigma and pi classes (Parsons et al. 1996), but with a serine in GST class theta (Board et al. 1995). In GST alpha, it is further stabilized by a secondary interaction with the nitrogen of arginine (Bjornestedt et al. 1995; Rushmore et al. 1993) while in GST class theta, arginine (107) may play the same role (Caccuri et al. 2001b).

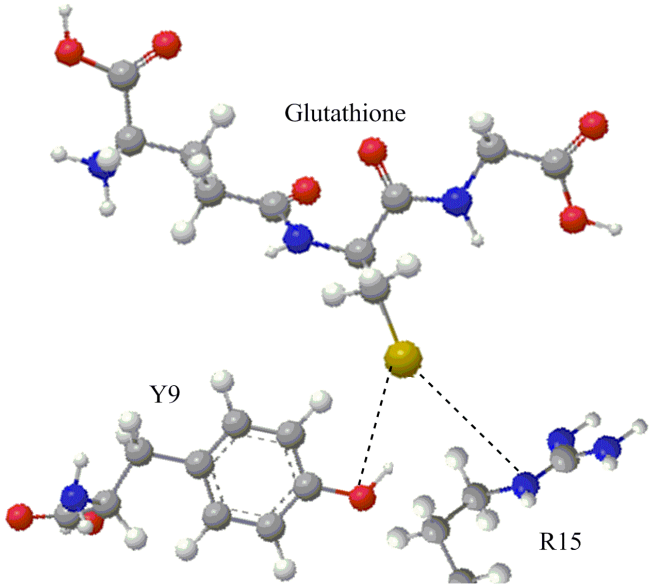

Figure 5.2 Catalytic activity of GST

In contrast to the GSH binding site which consists of some conserved amino acids, substrate binding sites (H site) among GST families are highly variable due to the wide range of substrate specificity. The H site utilizes structural elements from both N and C terminal domains. Evolutionally older enzymes such as theta has a much rigid H site while much evolved GSTs, alpha, mu and pi are more flexible, optimizing the substrate binding (Caccuri et al. 2001a; Caccuri et al. 2001b; Holm et al. 2002; Schmidt-Krey et al. 2000; Svensson et al. 2004). Unlike the G site, detailed structural

information about the H site in different classes of enzymes is not available due to the lack of crystal structures.

In search of additional proteins with the ability to bind with glutathione conjugates we came across SMC1, a member of structural maintenance of chromosomes family which is conserved from bacteria to humans and implicated in chromatid cohesion, chromosomal organization during recombination, repair as well as in activation of cell cycle check points. Sequence comparison of SMC1 with Ralbp1 revealed similarity with respect to key residues important for GSH binding. It is being observed that SMC1 could be purified by DNP-SG affinity chromatography as well as carryout substrate stimulated ATPase activity as well as transport in the presence of glutathione conjugates. Hence SMC1 is another candidate protein used for sequence homology analysis in identification of potential amino acids that play a key role in binding of glutathione conjugates (Sanjay Awasthi unpublished data).

Cephalopod lens *S*-crystallin is another protein, which binds with glutathione conjugates of CDNB (2,4-dinitrophenyl *S*-glutathione, DNP-SG), although with less affinity. It is categorized as a natural mutant of proteins that bind with DNP-SG (Chuang et al. 1999; Shoichet et al. 1995). Although squid major soluble lens crystallin, possess substantial GST activity it could not be purified by *S*-hexylglutathione affinity column. Sequence alignment of crystallin with the GSTs indicate all but 3 of the conserved 16 residues to be present in squid S11 crystallin. Furthermore GST sigma bears more similarity (42–44 %) to crystallins as compared to (19–34 %) to GSTs alpha, mu and pi (Tomarev et al. 1995; Tomarev et al. 1993). Although crystallin S11

has substantial activity towards DNP-SG, other crystallins are devoid of activity toward CDNB (Harris et al. 1991; Tomarev et al. 1995; Tomarev et al. 1993). In the absence of x-ray crystallographic structure, a model has being designed for S11 crystallin by using coordinates of GSTσ, which provides an explanation for the observed diminished activity towards conjugation of GSH and CDNB.

The residues in crystallin, which are important in binding of the substrate include asparagine 64 (asparagine 62 in GST-sigma), serine 65 (serine 63 in GST sigma), methionine 51 (methionine 50 in GST sigma), tryptophan 39 (tryptophan 38 in GST sigma) and from other subunit aspartate 98B (aspartate 96B in GST sigma). Catalytically active tyrosine 7 in GST sigma which acts as a general base to abstract the hydrogen from the thiol group lowering the pKa of the enzyme is present in crystallin (tyrosine 8) as well. Arginine 15 which stabilizes the negatively charged thiol group in GST alpha is also conserved in crystallin as arginine 14.

Discrepancy between crystallin and GST sigma include a 11 residue linker between 4 and 5 alpha helices of crystallin, which shields part of the active site causing steric hindrance. Also asparagine in GST sigma is being replaced by aspartate 101 in crystallin. Due to its location in close vicinity to arginine 14, charge to charge interactions occur between the two amino acids. This diminishes the stabilization provided by arginine to the negatively charged meisenheimer complex. It is believed that steric hindrance as well as decrease in the positively charged environment at the active site results in weakening the activity towards binding of glutathione conjugates (Chuang et al. 1999).

In an attempt to identify the amino acids important for binding of glutathione conjugates with Ralbp1, we aligned the sequences of GSTs, SMC1 and squid crystallin that are known to interact with GS-E. Several amino acids with high sequence homology to amino acids known to play a key role in interacting with GS-E in other proteins were selected as potential candidates that could be important for binding with GS-E in Ralbp1.

```
Squid Crystallin  (42)MRNQMPCSMMPMLEIDN—RHQIPQSMAIA(69)
Squid GST(s)        (42)LKATMYSNAMPVLDIDGT-KMS—QSMCIA(68)
Ralbp1          (222)KYGMKCEGIYRVSGIKSKVDELKAA--YDRE(250)
SMC1            (374)KYHRLKEEASK----------RAA--TLAQE(392)
```

Wild type Ralbp1	**Y(231)RVS(234)GIK(237)SKVDELK(244)AAY(247)DRE**
Y231A Mutant Ralbp1	**A(231)RVS(234)GIK(237)SKVDELK(244)AAY(247)DRE**
S234A Mutant Ralbp1	**Y(231)RVA(234)GIK(237)SKVDELK(244)AAY(247)DRE**
K237A Mutant Ralbp1	**Y(231)RVS(234)GIA(237)SKVDELK(244)AAY(247)DRE**
S234A K237A Ralbp1	**Y(231)RVA(234)GIA(237)SKVDELK(244)AAY(247)DRE**
K244A Mutant Ralbp1	**Y(231)RVS(234)GIA(237)SKVDELA(244)AAY(247)DRE**
Y247A Mutant Ralbp1	**Y(231)RVS(234)GIK(237)SKVDELK(244)AAA(247)DRE**

Figure 5.3 Sequence alignment of Ralbp1 with other glutathione conjugate binding proteins

Possible correlation between the transport properties and endocytosis function of Ralbp1 was studied by clathrin coated pit mediated endocytosis of EGF in Ralbp1 gene knockout mouse embryonic fibroblast (Ralbp1$^{-/-}$ MEFs) cells transfected with full length or transport deficient mutant Ralbp1. A detailed outcome of the study is included here.

5.3 Results and Discussion

5.3.1 Construction of substitution mutants of potential glutathione conjugate site

Potential candidate amino acids selected through sequence alignment using IBM bioinformatics group multiple sequence alignment algorithm, were substituted with alanine using QuickChange II site directed mutagenesis kit from Stratagene, CA. Full length Ralbp1 cloned to eukaryotic expression vector pcDNA 3.1 was used as the template during PCR. Plasmid DNA was purified from randomly picked *E. coli* colonies transformed with the PCR mixtures followed by Dpn I digestion and tested for the presence of the Ralbp1 gene (~ 2 kb) by digesting with restriction endonucleases BamH I and Xho I.

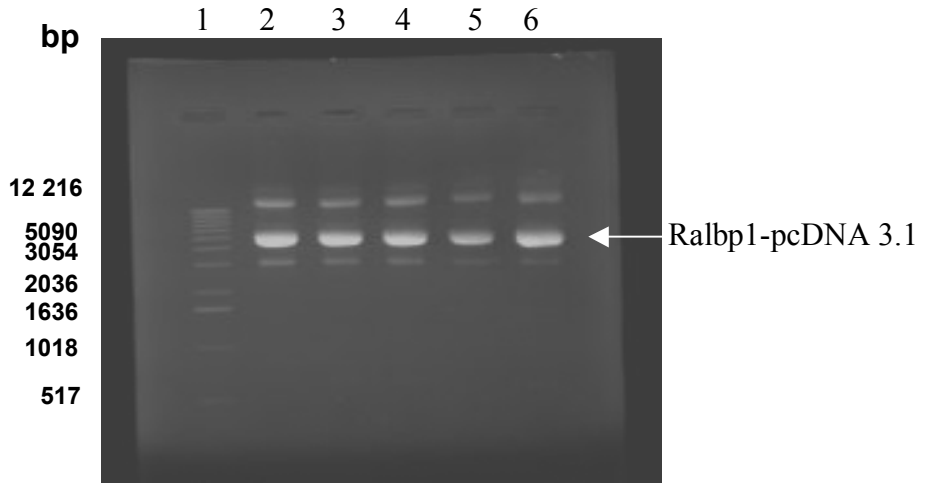

Figure 5.4 pcDNA 3.1 cloned with substitution mutants of Ralbp1 (undigested)

Samples loaded in the gel were as follows; 1 kB plus DNA ladder (lane 1), pcDNA 3.1 cloned with Y231A substitution mutant of Ralbp1 (lane 2), pcDNA 3.1 cloned with S234A substitution mutant of Ralbp1 (lane 3), pcDNA 3.1 cloned with K237A substitution mutant of Ralbp1 (lane 4), pcDNA 3.1 cloned with K244A substitution mutant of Ralbp1 (lane 5), pcDNA 3.1 cloned with Y247A substitution mutant of Ralbp1 (lane 6)

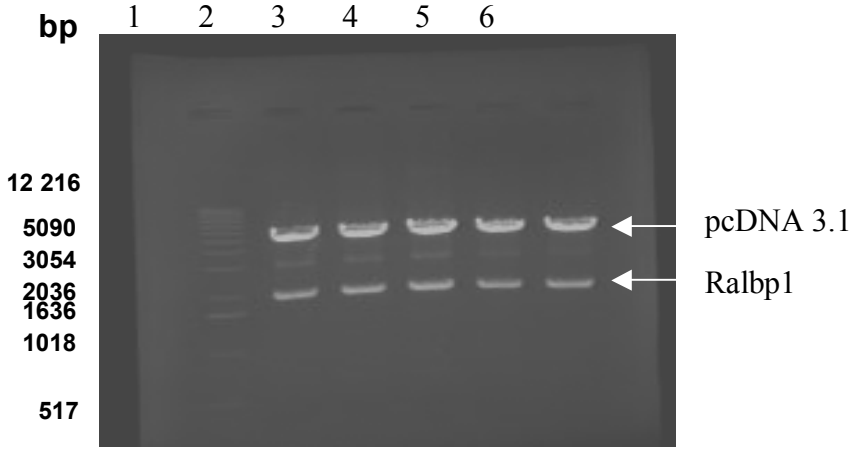

Figure 5.5 pcDNA 3.1 cloned with substitution mutants of Ralbp1, digested with restriction endonucleases BamH I and Xho I

Samples loaded in the gel were as follows; 1 kB plus DNA ladder (lane1), pcDNA 3.1 cloned with Y231A substitution mutant of Ralbp1 (lane 2), pcDNA 3.1 cloned with S234A substitution mutant of Ralbp1 (lane 3), pcDNA 3.1 cloned with K237A substitution mutant of Ralbp1 (lane 4), pcDNA 3.1 cloned with K244A substitution mutant of Ralbp1 (lane 5), pcDNA 3.1 cloned with Y247A substitution mutant of Ralbp1 (lane 6)

Successfully ligated colonies were screened for the mutation by DNA sequencing. The genes with the confirmed mutations through DNA sequencing, was separated by digesting with restriction endonuclease BamH I and Xho I and cloned into prokaryotic expression vector pET30a(+).

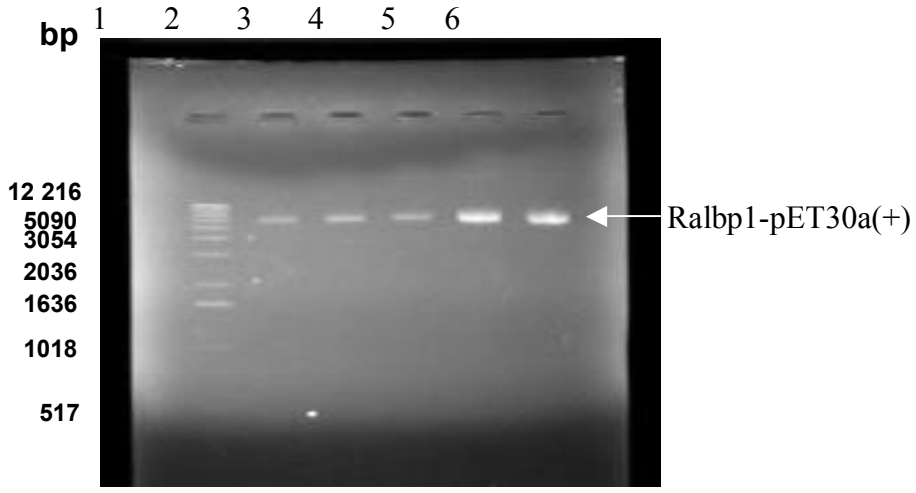

Figure 5.6 pET30a(+) cloned with substitution mutants of Ralbbp1 (undigested)

Samples loaded in the gel were as follows; 1 kb plus DNA ladder (lane 1), pET30a(+) cloned with Y231A substitution mutant of Ralbp1 (lane 2), pET30a(+) cloned with S234A substitution mutant of Ralbp1 (lane 3), pET30a(+) cloned with K237A substitution mutant of Ralbp1 (lane 4), pET30a(+) cloned with K244A substitution mutant of Ralbp1 (lane 5), pET30a(+) cloned with Y247A substitution mutant of Ralbp1 (lane 6)

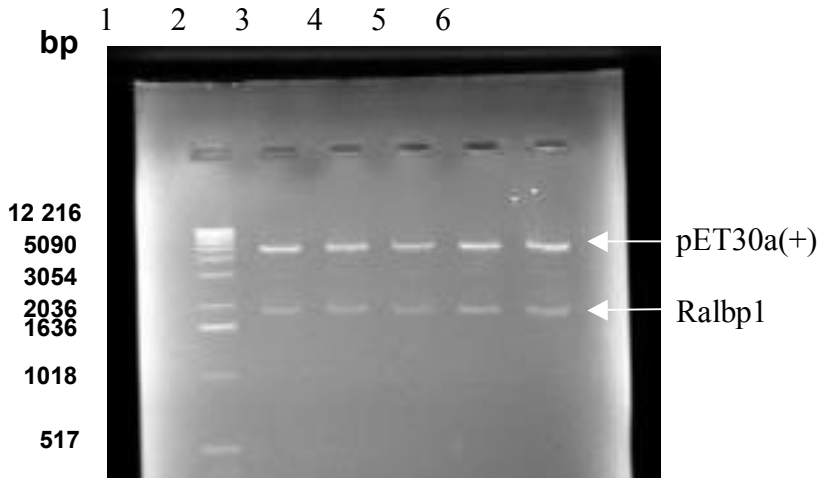

Figure 5.7 pET30a(+) cloned with substitution mutants of Ralbp1, digested with restriction endonucleases BamH I and Xho I

Samples loaded in the gel were as follows; 1 kb plus DNA ladder (lane 1), pET30a(+) cloned with Y231A substitution mutant of Ralbp1 (lane 2), pET30a(+) cloned with S234A substitution mutant of Ralbp1 (lane 3), pET30a(+) cloned with K237A substitution mutant of Ralbp1 (lane 4), pET30a(+) cloned with K244A substitution mutant of Ralbp1 (lane 5), pET30a(+) cloned with Y247A substitution mutant of Ralbp1 (lane 6)

5.3.2 Expression of substitution mutants of potential glutathione conjugate binding site in E. coli

The possible effects of substitution mutations on expression of the protein were assessed by conducting western blot analysis with equal amount of protein (100 μg) from *E. coli* (transfected with full length or mutant Ralbp1) crude cell lysate. Expression of the protein was induced with isopropyl thio-β-galactoside (IPTG). Polyclonal rabbit anti-human rec-Ralbp1 IgG was used as the primary antibody. The protein was visualized by development of purple color product, 4-chloro-1–napthone by enzymatic reaction with horseradish peroxidase conjugated goat anti-rabbit secondary antibodies.

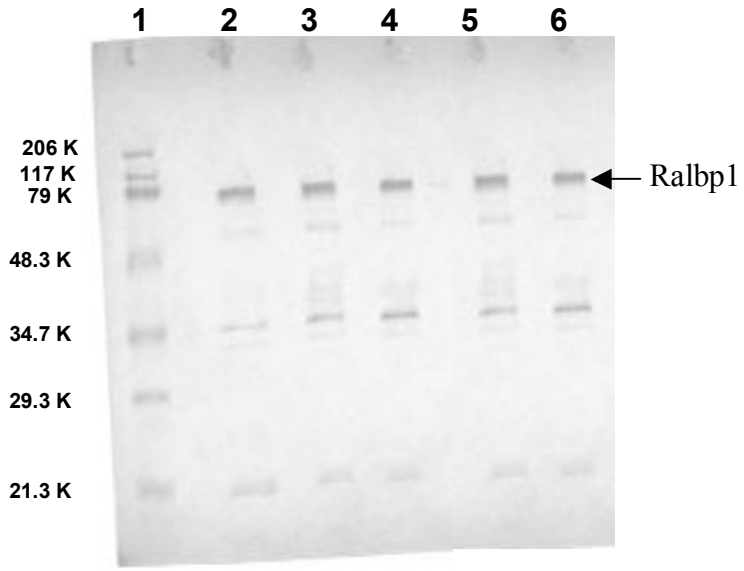

Figure 5.8 Expression of Ralbp1 and the substitution mutants in *E. coli* crude cell lysate

Samples loaded in the gel were as follows; Broad range protein marker (lane 1), full length rec-Ralbp1 (lane 2), Y231A substitution mutant of Ralbp1 (lane 3), S234A substitution mutant of Ralbp1 (lane 4), K237A substitution mutant of Ralbp1 (lane 5), K244A substitution mutant of Ralbp1 (lane 6)

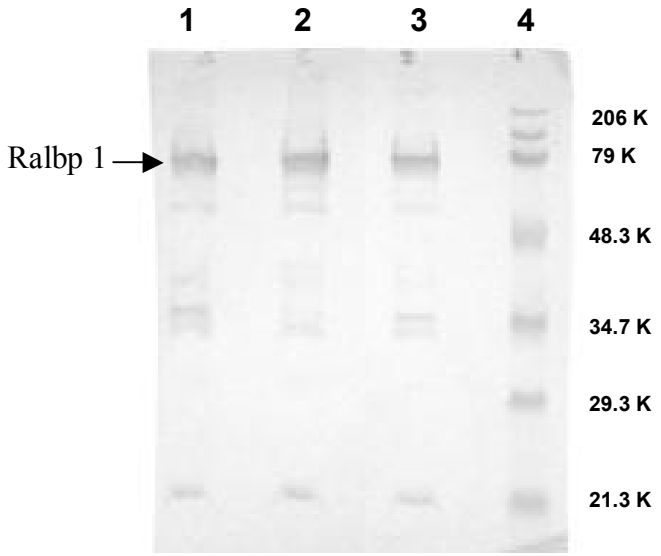

Figure 5.9 Expression of Ralbp1 and the substitution mutants in *E. coli* crude cell lysate

Samples loaded in the gel were a follows; S234A K237A substitution mutant of Ralbp1 (lane 1), Y247A substitution mutant of Ralbp1 (lane 2), Full length rec-Ralbp1 (lane 3), Broad range protein marker (lane 4)

Presence of multiple bands with two prominent fragments at 76 kDa referring to full length Ralbp1 and 38 kDa, C-terminal domain of Ralbp1 has being reported from previous studies as well, due to proteolytic degradation of Ralbp1. From the intensity of the fragments seen in the western blot it is evident that regardless of the substitution mutations, all proteins are expressed to the same extent as the full length Ralbp1.

5.3.3 Effect of potential glutathione conjugate site mutations on in vitro Melphalan transport

It has been observed that over expression of Ralbp1 increases the cell survival during treatment of chemotherapeutic drugs most likely due to enhanced drug efflux. This difference in efficacy is also evident through cytotoxicity assays on cultured cell lines. The efficiency of drug efflux is dependent on the ability of the particular compound or the glutathione conjugate of the compound to interact with the transporter protein. Hence the IC_{50} value of a certain drug determined through cytotoxicity assays can be used to evaluate the binding affinity of the particular drug with the protein.

During this study we used IC_{50} value of melphalan as an indication of its efficiency to interact with the transporter proteins and get removed from cells. It is known from literature that melphalan forms glutathione conjugates within the cells by binding with cellular glutathione (Barnouin et al. 1998; Paumi et al. 2001). In order to evaluate the effect of substitution mutations on binding affinity of Ralbp1 with the glutathione conjugates, the IC_{50} values of Ralbp1 gene knockout mouse embryonic fibroblast cells ($Ralbp1^{-/-}$ MEF) transiently transfected with full length Ralbp1 or mutated Ralbp1 was compared.

Over expression of Ralbp1 through transient transfection increases the efflux of chemotherapeutic agents as well as their glutathione conjugates causing a decrease in the IC_{50} value of melphalan in $Ralbp1^{-/-}$ MEF cells. In the event the substitution mutations may affect the binding affinity of Ralbp1 with glutathione conjugates, the efficiency of the transport would be affected, thereby increasing sensitivity to Melphalan. Untransfected $Ralbp1^{-/-}$ MEF cells, which lack the expression of Ralbp1,

were used as the negative control and indicate contribution of other proteins to drug efflux.

Table 5.2 Melphalan IC_{50} values of Ralbp1$^{-/-}$ MEFs transfected with full length or transport deficient mutants of Ralbp1

	IC50 (μM)	SD
Ralbp1$^{+/+}$ MEF	9.2	1.4
Ralbp1$^{-/-}$ MEF	2.1	0.33
Ralbp1$^{-/-}$ MEF transfected with Ralbp1	8.5	1.1
Ralbp1$^{-/-}$ MEF transfected with Y231A Ralbp1	6.1	0.42
Ralbp1$^{-/-}$ MEF transfected with S234A Ralbp1	4.4	0.62
Ralbp1$^{-/-}$ MEF transfected with K237A Ralbp1	5.6	0.48
Ralbp1$^{-/-}$ MEF transfected with K244A Ralbp1	4.2	0.27
Ralbp1$^{-/-}$ MEF transfected with S234A + K237A Ralbp1	3.2	0.24
Ralbp1$^{-/-}$ MEF transfected with Y247A Ralbp1	6.5	0.38
Ralbp1$^{-/-}$ MEF transfected with RLIP Δ65-80	3.8	0.3
Ralbp1$^{-/-}$ MEF transfected with RLIP Δ415-448	3.7	0.23

Of the transport deficient mutants of Ralbp1, S234A, K237A and K244A of potential glutathione conjugate binding site mutants showed the highest effect towards the binding with the glutathione conjugate and thus the IC_{50} value. In all 3 mutants, melphalan IC_{50} value has decreased by 50 % from that of the wild type full length protein while double mutant S234AK237A indicated a 60 % decrease as expected. Hence amino acids S234, K237 and K244 must play a key role in binding of glutathione conjugates with Ralbp1. Two other potential glutathione conjugate binding site mutants Y231A and Y247A indicated a ~30 % reduction in the IC_{50} value possibly due to effects on conformational changes on binding. N and C terminal ATP binding site deletion mutants also indicated ~50 % reduction in the IC_{50} value due to lack of energy supplement for the active transport.

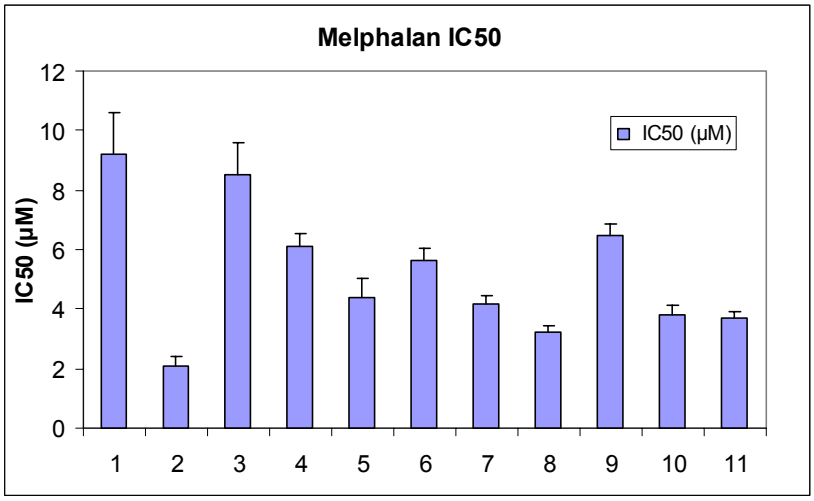

Figure 5.10 Melphalan IC_{50} values of Ralbp1$^{-/-}$ MEFs transfected with full length Ralbp1 and transport deficient mutants of Ralbp1

The samples in the graph were as follows; mouse embryonic fibroblast cells with Ralbp1 (Ralbp1$^{+/+}$ MEFs) (1), Ralbp1 gene knockout mouse embryonic fibroblast cells (Ralbp1$^{-/-}$ MEFs) (2), Ralbp1$^{-/-}$ MEFs transfected with full length Ralbp1 (3), Ralbp1$^{-/-}$ MEFs transfected with Y231A mutant of Ralbp1 (4), Ralbp1$^{-/-}$ MEFs transfected with S234A mutant of Ralbp1 (5), Ralbp1$^{-/-}$ MEFs transfected with K237A mutant of Ralbp1 (6), Ralbp1$^{-/-}$ MEFs transfected with K244A mutant of Ralbp1 (7), Ralbp1$^{-/-}$ MEFs transfected with S234A, K237A double mutant Ralbp1 (8), Ralbp1$^{-/-}$ MEFs transfected with Y247A mutant of Ralbp1 (9), Ralbp1$^{-/-}$ MEFs transfected with N terminal ATP binding site deletion mutant (10), Ralbp1$^{-/-}$ MEFs transfected with C terminal ATP binding site deletion mutant (11)

5.3.4 Effects of potential glutathione-conjugate site mutations on cellular Melphalan uptake

Cellular melphalan uptake studies follow a similar concept as IC_{50} determinations. Incubation of cells with the radiolabeled melphalan causes the cells to gain radioactivity by incorporation of the drug through diffusion. The transport proteins in the cell efflux the chemotherapeutic agents through active transport. This minimizes the cellular accumulation of radioactivity. The efficiency of the efflux is dependent on the ability of the protein to interact with the chemotherapeutic agent. Less efficient binding of the protein with the drug or its conjugates results in decrease in efflux and increase retention of the radiolabeled drug.

For the study ^{14}C-labeled melphalan was specially chosen since it is known to form glutathione conjugates in the cell (Barnouin et al. 1998; Paumi et al. 2001). Hence the effect of substitution mutations on the binding affinity of Ralbp1 with glutathione conjugates could be assessed by comparing the radioactivity retained in the $Ralbp1^{-/-}$ MEFs transfected with full length or the mutated Ralbp1. The retention of radioactivity in untransfected $Ralbp1^{-/-}$ MEFs which do not express Ralbp1 was used to evaluate the contribution of all other transporters towards the efflux of glutathione conjugates.

Table 5.3 Melphalan uptake of Ralbp1$^{-/-}$ MEFs transfected with full length or transport deficient mutants of Ralbp1

	^{14}C-MEL uptake (pmol / 5 x 10^6 cells)	SD	Fold retention
Ralbp1$^{+/+}$ MEF	56.00	5	1.0
Ralbp1$^{-/-}$ MEF	129.36	11	2.2
Ralbp1$^{-/-}$ MEF transfected with Ralbp1	58.84	4	1.0
Ralbp1$^{-/-}$ MEF transfected with Y231A Ralbp1	76.09	7	1.3
Ralbp1$^{-/-}$ MEF transfected with S234A Ralbp1	93.43	7	1.6
Ralbp1$^{-/-}$ MEF transfected with K237A Ralbp1	85.02	6	1.4
Ralbp1$^{-/-}$ MEF transfected with K244A Ralbp1	96.89	6	1.6
Ralbp1$^{-/-}$ MEF transfected with S234A + K237A Ralbp1	102.84	3	1.7
Ralbp1$^{-/-}$ MEF transfected with Y247A Ralbp1	69.41	6	1.2
Ralbp1$^{-/-}$ MEF transfected with Δ65-80 Ralbp1	98.10	4	1.7
Ralbp1$^{-/-}$ MEF transfected with Δ415-448 Ralbp1	99.51	6	1.7

The results of the ^{14}C-Melphalan uptake studies followed a similar pattern as seen with IC_{50} studies. Fold retention of melphalan in the absence of Ralbp1 (Ralbp1$^{-/-}$ MEFs) was as twice as that in the presence of Ralbp1 (Ralbp1$^{+/+}$ MEF and RAlbp1$^{-/-}$ MEF transfected with Ralbp1). Transfections with S234A and K244A mutant Ralbp1 indicated a 1.6 fold increase as compared to the wild type protein while the K237A mutant Ralbp1 had a 1.4 fold increase in retention. The double mutant S234A K237A had 1.7 fold retention of Melphalan as compared to wild type protein. This suggests that amino acids S234, K237 and K244 must play a key role in binding of the glutathione conjugates with Ralbp1. Mutants, Y231A (1.3 fold) and Y247A (1.2 fold) had a slight increase in the retention of Melphalan. These might be caused by minor conformational changes. Deletion mutants of the two ATP binding sites in N and C terminal domains

both indicated a 1.7 fold increase in the retention due to the lack of energy supplement for the active transport.

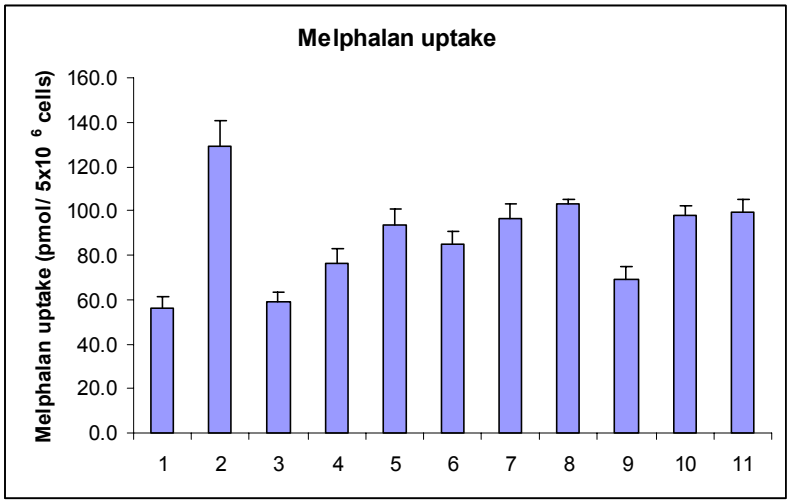

Figure 5.11 Melphalan uptake of Ralbp1$^{-/-}$ MEFs transfected with full length Ralbp1 and transport deficient mutants of Ralbp1

Samples included in the graph were as follows; mouse embryonic fibroblast cells with Ralbp1 (Ralbp1$^{+/+}$ MEFs) (1), Ralbp1 gene knockout mouse embryonic fibroblast cells (Ralbp1$^{-/-}$ MEFs) (2), Ralbp1$^{-/-}$ MEFs transfected with full length Ralbp1 (3), Ralbp1$^{-/-}$ MEFs transfected with Y231A mutant of Ralbp1 (4), Ralbp1$^{-/-}$ MEFs transfected with S234A mutant of Ralbp1 (5), Ralbp1$^{-/-}$ MEFs transfected with K237A mutant of Ralbp1 (6), Ralbp1$^{-/-}$ MEFs transfected with K244A mutant of Ralbp1 (7), Ralbp1$^{-/-}$ MEFs transfected with S234A, K237A double mutant of Ralbp1 (8), Ralbp1$^{-/-}$ MEFs transfected with Y247A mutant of Ralbp1 (9), Ralbp1$^{-/-}$ MEFs transfected with N terminal ATP binding site deletion mutant (10), Ralbp1$^{-/-}$ MEFs transfected with C terminal ATP binding site deletion mutant (11)

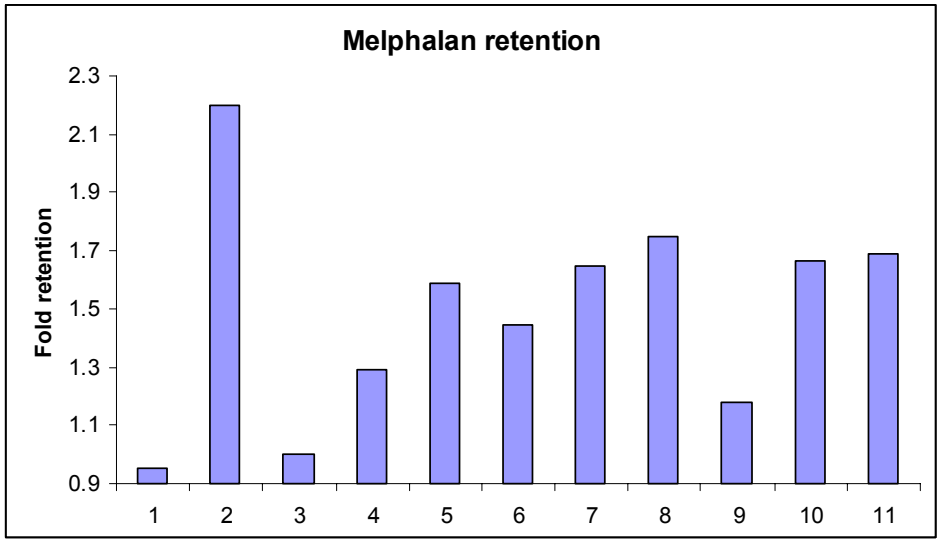

Figure 5.12 Fold retention of Melphalan in Ralbp1$^{-/-}$ MEFs transfected with full length Ralbp1 and transport deficient mutants of Ralbp1

Samples included in the graph were as follows; mouse embryonic fibroblast cells with Ralbp1 (Ralbp1$^{+/+}$ MEFs) (1), Ralbp1 gene knockout mouse embryonic fibroblast cells (Ralbp1$^{-/-}$ MEFs) (2), Ralbp1$^{-/-}$ MEFs transfected with full length Ralbp1 (3), Ralbp1$^{-/-}$ MEFs transfected with Y231A mutant of Ralbp1 (4), Ralbp1$^{-/-}$ MEFs transfected with S234A mutant of Ralbp1 (5), Ralbp1$^{-/-}$ MEFs transfected with K237A mutant of Ralbp1 (6), Ralbp1$^{-/-}$ MEFs transfected with K244A mutant of Ralbp1 (7), Ralbp1$^{-/-}$ MEFs transfected with S234A, K237A double mutant of Ralbp1 (8), Ralbp1$^{-/-}$ MEFs transfected with Y247A mutant of Ralbp1 (9), Ralbp1$^{-/-}$ MEFs transfected with N terminal ATP binding site deletion mutant (10), Ralbp1$^{-/-}$ MEFs transfected with C terminal ATP binding site deletion mutant (11)

5.3.5 Cellular localization of full length wild type and the transport deficient mutants of Ralbp1

In order to confirm that the difference in IC_{50} values and uptake studies are caused by the differential affects on binding of Ralbp1 with the melphalan glutathione conjugate and not by the translocation of the protein, we carried out immunohistochemistry on mouse embryonic fibroblast cells transfected with full length wild type and transport deficient mutants of Ralbp1. The protein was localized by using polyclonal anti-Ralbp1 IgG developed in rabbit as the primary antibody followed by fluoroscene isothiocyante (FITC) conjugated goat anti-rabbit IgG as secondary antibodies. The nucleus was localized by nuclear stain DAPI. The confocal laser microscopic images were obtained with 40X magnification. Each sample was carried out in duplicate.

The substitution mutants of potential glutathione conjugate binding site as well as the deletion mutants of the two ATP binding sites have a similar distribution in the cell as that of full length wild type Ralbp1. This indicates that the effect towards the IC_{50} values and uptake of Melphalan are not caused through translocation of the protein but by an alteration of interactions between the protein and allocrite.

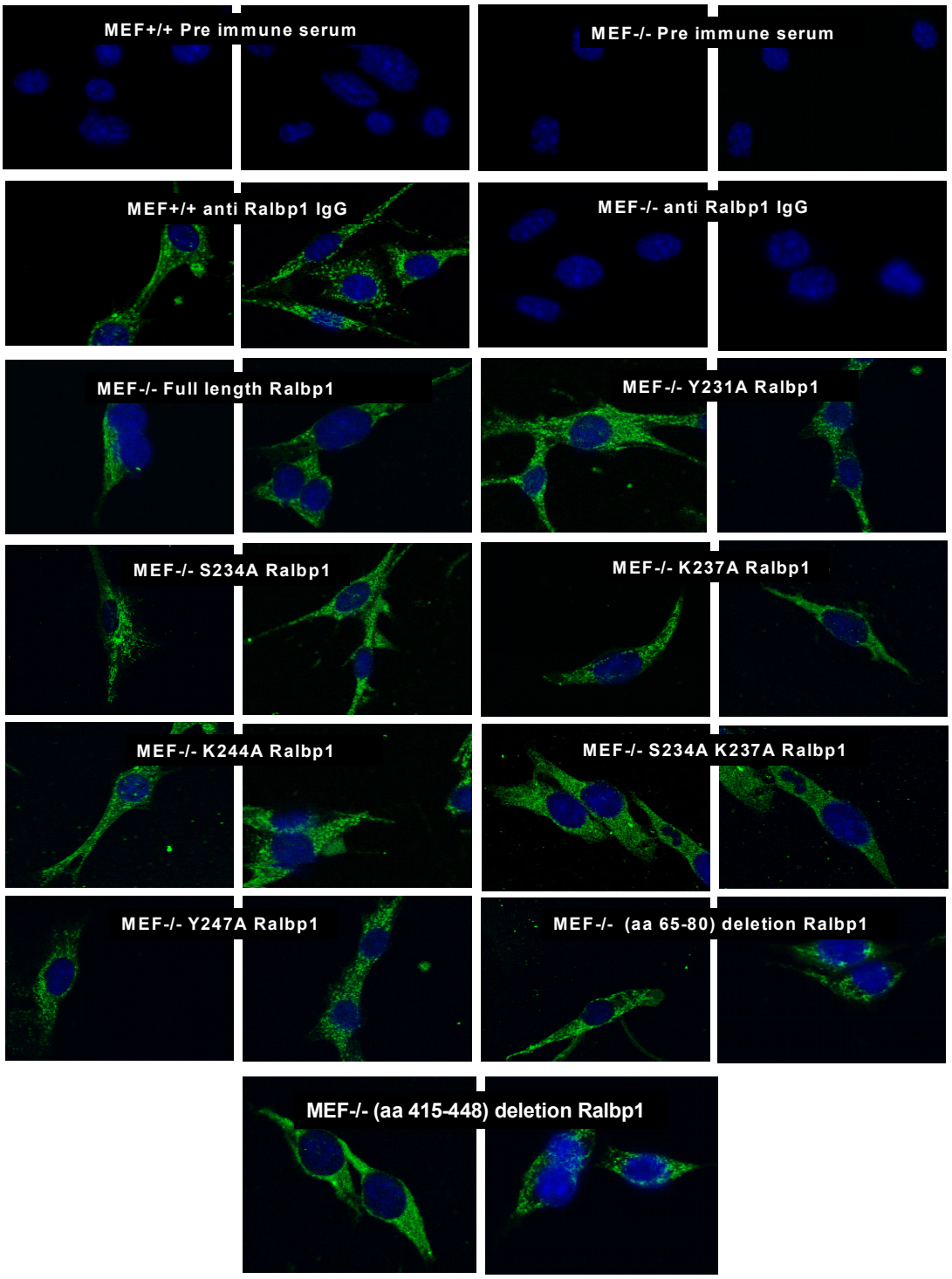

Figure 5.13 Immunohistochemical localization of full length wild type and transport deficient mutants of Ralbp1

5.3.6 Endocytosis studies

Ralbp1 and POB1 are downstream molecules of small GTP binding protein Ral, which are involved in receptor mediated endocytosis together with Epsin and EPS15. In the course of endocytosis Ralbp1, POB1, Epsin, EPS15 form a complex with alpha-adaptin of AP2, causing clathrin coated pit mediated endocytosis.

In order to test the hypothesis whether endocytosis and xenobiotic transport function of Ralbp1 are linked together or two independent processes of the same protein, the endocytosis of the epidermal growth factor (EGF) was studied by wild type full length Ralbp1 as well as transport deficient mutants of Ralbp1. The efficiency of the transport is dependent on the binding of the substrate as well as binding and hydrolysis of ATP. Therefore deletion mutants of the two ATP binding sites in N and C terminal of Ralbp1, amino acids 65-80 and 415-448 respectively, as well as the substitution mutants of potential glutathione conjugate binding site were used as transport deficient forms of Ralbp1.

The endocytosis of the rhodamine red-x labeled EGF receptor was studied in Ralbp1 gene knock out mouse embryonic fibroblast cells ($Ralbp1^{-/-}$ MEFs) transfected with wild-type full length Ralbp1 or transport-deficient mutants of Ralbp1. Untransfected $Ralbp1^{-/-}$ MEFs which do not express Ralbp1 were used as negative control to assess the endocytosis in the absence of Ralbp1. The study was performed according to the published procedure by (Oosterhoff et al. 2003).

$Ralbp1^{-/-}$ MEFs untransfected (control) or transfected with full length or mutant Ralbp1 (0.2×10^6 cells) were grown on sterilized cover slips in a 12 well plate, over

night at 37 ^{o}C with 5 % CO_2. Afterwards the cells were washed several times with PBS followed by incubation with EGF in DMEM (50 ng/ mL) for 1 h at 4 ^{o}C. The endocytosis was carried out by incubation of the plate at 37 ^{o}C for 10 min. The cells were then fixed with 4 % para formaldehyde in PBS. The confocal laser microscopic images of the cells were obtained at 40X magnification using excitation at 505 nm and 533 nm as the emission wave length. Each sample was tested in duplicate.

Although none of the mutants indicated complete abrogation of endocytosis, several of the potential glutathione conjugate binding site mutant Ralbp1 transfected cells showed diminished endocytosis as compared to wild type full length Ralbp1 transfected cells. Particularly S234A and K244A substitution mutants of Ralbp1 indicated almost 50 % decrease in the endocytosis. Substitution mutant K237A indicated approximately 40 % reduction of endocytosis while the double substitution mutant S234A K237A indicated greater than 50 % reduction. From the N and C terminal ATP binding site deletion mutants, N terminal ATP binding site (amino acids 65-80) deletion mutant indicated approximately 40 % reduction of endocytosis, while the effects of deletion of C terminal ATP binding site (amino acids 415-448) on endocytosis were less significant.

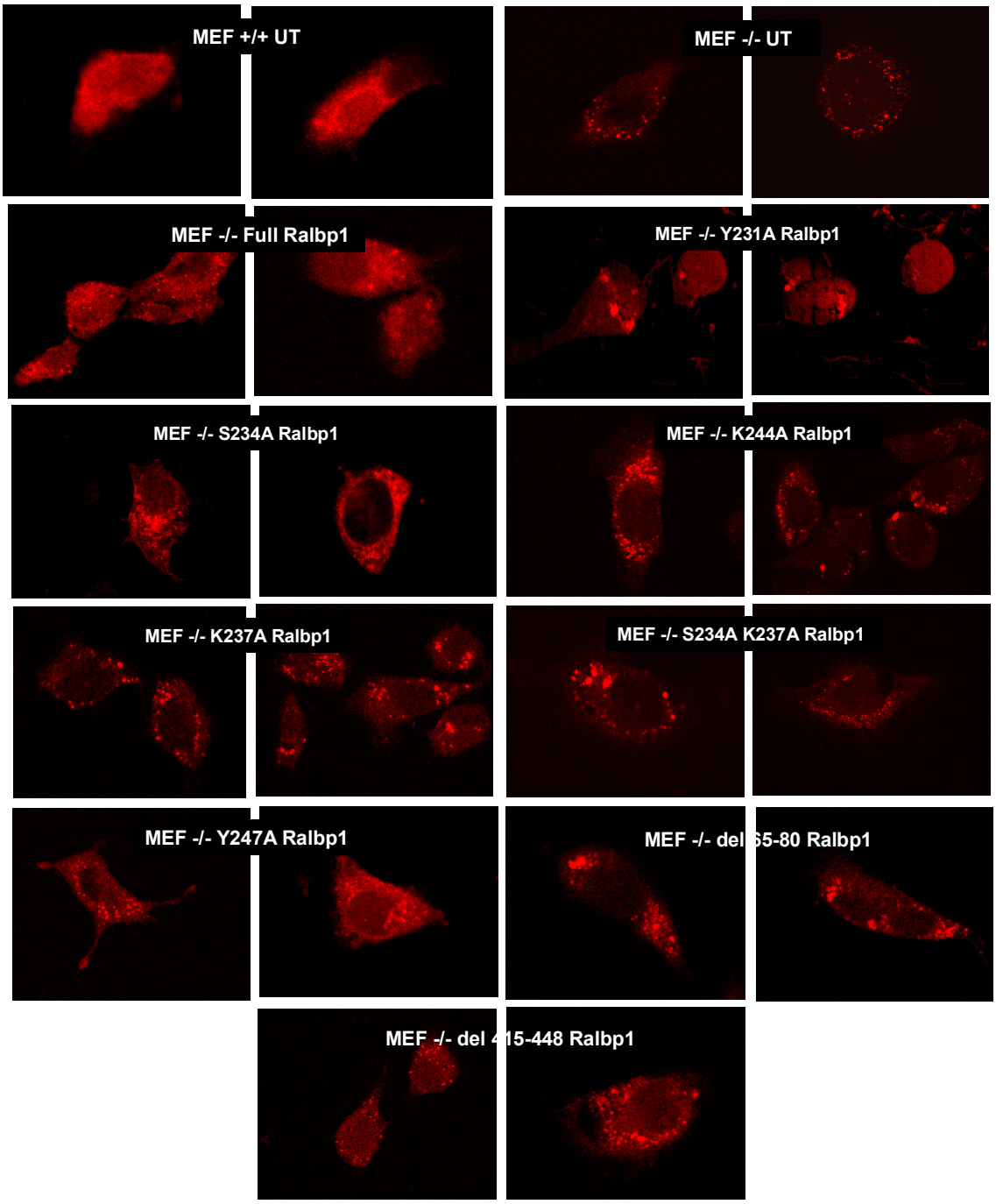

Figure 5.14 Endocytosis of epidermal growth factor (EGF) by wild type full length and transport deficient mutants of Ralbp1

Table 5.4 Fluorescent intensity from endocytosis of EGF by Ralbp1$^{-/-}$ MEFs transfected with Ralbp1 and its transport deficient mutants

	Average fluorescent intensity per unit area	SD
(1) MEF $^{+/+}$	104.2	11.4
(2) MEF $^{-/-}$	14.8	5.4
(3) MEF $^{-/-}$ transfected wild type Ralbp1	88.9	12.7
(4) MEF $^{-/-}$ transfected with Y231A Ralbp1	85.8	33.8
(5) MEF $^{-/-}$ transfected with S234A Ralbp1	46.4	3.4
(6) MEF $^{-/-}$ transfected with K237A Ralbp1	60.2	11.2
(7) MEF $^{-/-}$ transfected with K244A Ralbp1	41.6	12.2
(8) MEF $^{-/-}$ transfected with S234A K237A Ralbp1	34.4	2.7
(9) MEF $^{-/-}$ transfected with Y247A Ralbp1	50.2	0.0
(10) MEF $^{-/-}$ transfected with del 65-80 Ralbp1	61.9	10.6
(11) MEF $^{-/-}$ transfected with del 415-448 Ralbp1	82.5	7.8

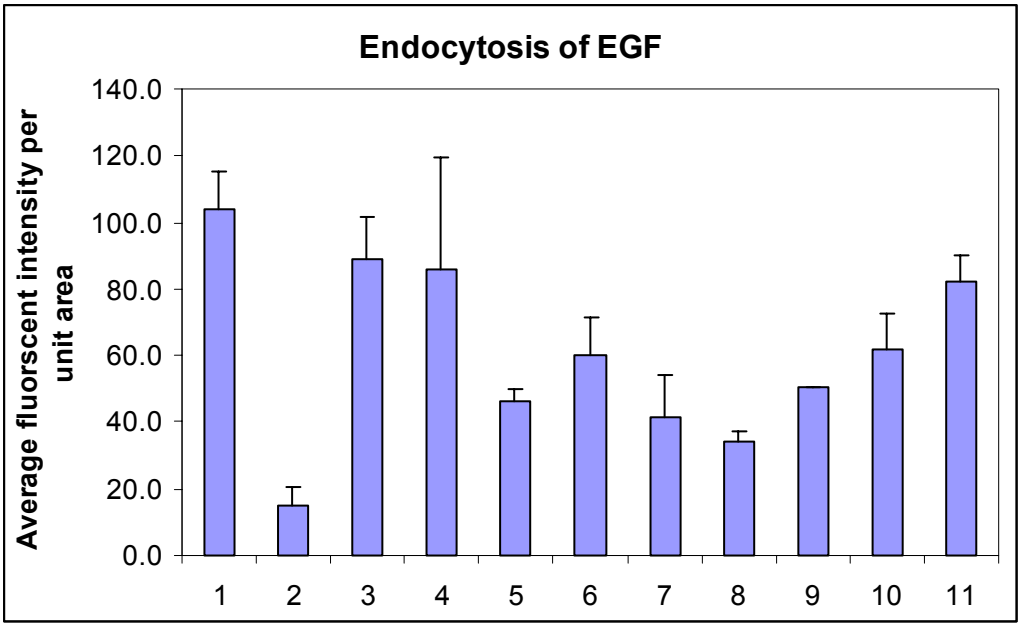

Figure 5.15 Fluorescence intensity from endocytosis of EGF by Ralbp1$^{-/-}$ MEFs transfected with Ralbp1 and its transport deficient mutants

The different quantitative measures of function of Ralbp1 were compared graphically (figure 5.16) and correlated statistically using Pearson product moment correlation (table 5.5). An inverse correlation was found between IC_{50} and uptake that is total drug-retention by the cell was inversely correlated with the cytotoxicity. There was also good, but imperfect correlation of drug-uptake with endocytosis, but IC_{50} and endocytosis were better correlated. Diagrammatic representation of these results (figure 5.16) indicated that the Y247A mutant differed from the others in that endocytosis was preferentially affected without affecting IC_{50} or drug-uptake as significantly. These results provide direct experimental evidence to reveal an intricate link between transport function and endocytosis function of Ralbp1 while an alteration in GTPase activity could not be ruled out since all these mutations fall in the Rho Gap domain.

Table 5.5 Correlation of Melphalan IC_{50}, uptake, and endocytosis activities of different Ralbp1 mutants

Pearson Correlations (values in parenthesis exclude the Y247A mutant)

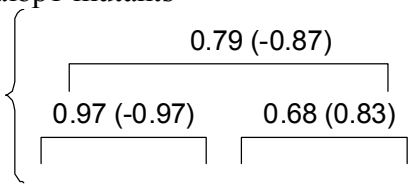

	uptake	IC_{50}	endocytosis
Ralbp1 MEF+/+	0.43	4.38	7.04
Ralbp1 MEF-/-	1.00	1.00	1.00
Ralbp1 MEF-/- transfected with Ralbp1	0.45	4.05	6.01
Ralbp1 MEF-/- transfected with Y231A Ralbp1	0.59	2.90	5.80
Ralbp1 MEF-/- transfected with S234A Ralbp1	0.72	2.10	3.14
Ralbp1 MEF-/- transfected with K237A Ralbp1	0.66	2.67	4.07
Ralbp1 MEF-/- transfected with K244A Ralbp1	0.75	2.00	2.81
Ralbp1 MEF-/- transfected with S234A + K237A Ralbp1	0.79	1.52	2.32
Ralbp1 MEF-/- transfected with Y247A Ralbp1	0.54	3.10	3.39

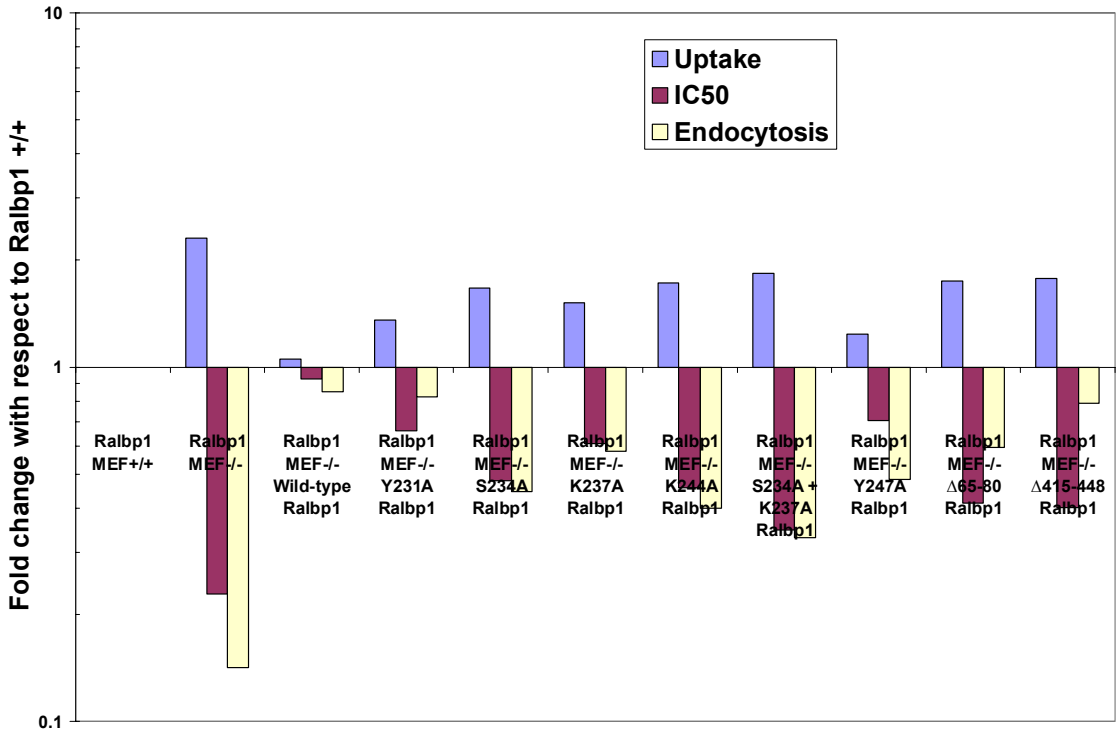

Figure 5.16 The relative effect of Ralbp1 mutants on melphalan uptake, IC_{50} and endocytosis of EGF

5.4 Conclusions

In search for the potential glutathione, conjugate binding site of Ralbp1 by sequence homology with well-known glutathione conjugate binding proteins using the IBM Bioinformatics Group Multiple Sequence Alignment algorithm, several amino acids have been found to be the potential candidates. Both IC_{50} and uptake studies using [^{3}H]-Melphalan indicated that substitution of S234, K237 and K244 with alanine markedly affect the transport and thus the binding of the melphalan glutathione conjugate with the mutants of Ralbp1 as compared to the wild type full length protein. Other candidate amino acids indicated a minor affect toward binding possibly due to minor conformational changes.

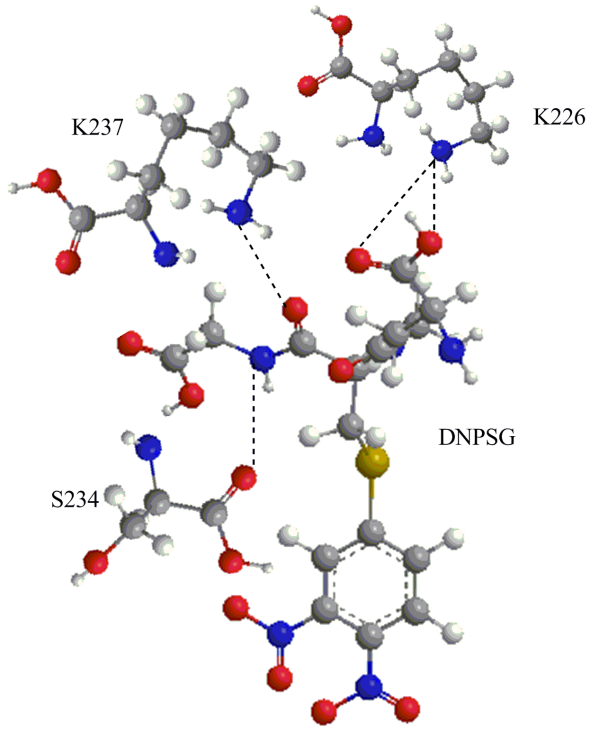

Figure 5.17 Interactions of Ralbp1 with glutathione conjugates

With the aid of crystal structures of proteins (crystallin and glutathione *S*-transferases) that bind with glutathione conjugates, we designed a model for the possible interactions of these amino acids of Rallbp1 (which may be associated in the binding of glutathione conjugates) with a glutathione conjugate (DNPSG was taken as an example).

Analysis of the hypothesis whether the xeno/ endobiotic transport and endocytosis regulated by Ralbp1 are linked with each other or to be two independent functions of the same protein revealed through structure function studies indicated that there is an intricate link between the two functions. Several mutants lacking the glutathione conjugate binding site had deficient transport properties, showed a notable decrease in endocytosis as well. These studies demonstrated that the transport and endocytic functions of Ralbp1 are very closely linked. We did not find a mutant that had reduced transport activity without a concomitant decrease in its ability to reconstitute endocytosis. The K244A mutant had a greater effect on endocytosis than on drug-resistance, indicating that it may have additional functions related to endocytosis.

REFERENCES

1. Ahmad, S.; Safa, A. R.; Glazer, R. I. Biochemistry 1994, 33, 10313-8.
2. Ahmad, S.; Trepel, J. B.; Ohno, S.; Suzuki, K.; Tsuruo, T.; Glazer, R. I. Mol Pharmacol 1992, 42, 1004-9.
3. Allen, J. D.; Brinkhuis, R. F.; Wijnholds, J.; Schinkel, A. H. Cancer Res 1999, 59, 4237-41.
4. Allikmets, R.; Gerrard, B.; Hutchinson, A.; Dean, M. Hum Mol Genet 1996, 5, 1649-55.
5. Allikmets, R.; Schriml, L. M.; Hutchinson, A.; Romano-Spica, V.; Dean, M. Cancer Res 1998, 58, 5337-9.
6. Ambudkar, S. V.; Dey, S.; Hrycyna, C. A.; Ramachandra, M.; Pastan, I.; Gottesman, M. M. Annu Rev Pharmacol Toxicol 1999, 39, 361-98.
7. Andersson, S.; Davis, D. L.; Dahlback, H.; Jornvall, H.; Russell, D. W. J Biol Chem 1989, 264, 8222-9.
8. Apel, K.; Hirt, H. Annu Rev Plant Biol 2004, 55, 373-99.
9. Armstrong, R. N. Chem Res Toxicol 1997, 10, 2-18.
10. Awasthi, S.; Cheng, J.; Singhal, S. S.; Saini, M. K.; Pandya, U.; Pikula, S.; Bandorowicz-Pikula, J.; Singh, S. V.; Zimniak, P.; Awasthi, Y. C. Biochemistry 2000, 39, 9327-34.

11. Awasthi, S.; Cheng, J. Z.; Singhal, S. S.; Pandya, U.; Sharma, R.; Singh, S. V.; Zimniak, P.; Awasthi, Y. C. Biochemistry 2001, 40, 4159-68.
12. Awasthi, S.; Sharma, R.; Singhal, S. S.; Zimniak, P.; Awasthi, Y. C. Drug Metab Dispos 2002, 30, 1300-10.
13. Awasthi, S.; Sharma, R.; Yang, Y.; Singhal, S. S.; Pikula, S.; Bandorowicz-Pikula, J.; Singh, S. V.; Zimniak, P.; Awasthi, Y. C. Acta Biochim Pol 2002, 49, 855-67.
14. Awasthi, S.; Singhal, S. S.; Pandya, U.; Gopal, S.; Zimniak, P.; Singh, S. V.; Awasthi, Y. C. Toxicol Appl Pharmacol 1999, 155, 215-26.
15. Awasthi, S.; Singhal, S. S.; Pikula, S.; Piper, J. T.; Srivastava, S. K.; Torman, R. T.; Bandorowicz-Pikula, J.; Lin, J. T.; Singh, S. V.; Zimniak, P.; Awasthi, Y. C. Biochemistry 1998, 37, 5239-48.
16. Awasthi, S.; Singhal, S. S.; Sharma, R.; Zimniak, P.; Awasthi, Y. C. Int J Cancer 2003, 106, 635-46.
17. Awasthi, S.; Singhal, S. S.; Singhal, J.; Yang, Y.; Zimniak, P.; Awasthi, Y. C. Int J Oncol 2003, 22, 721-32.
18. Awasthi, S.; Singhal, S. S.; Srivastava, S. K.; Torman, R. T.; Zimniak, P.; Bandorowicz-Pikula, J.; Singh, S. V.; Piper, J. T.; Awasthi, Y. C.; Pikula, S. Biochemistry 1998, 37, 5231-8.
19. Awasthi, S.; Singhal, S. S.; Srivastava, S. K.; Zimniak, P.; Bajpai, K. K.; Saxena, M.; Sharma, R.; Ziller, S. A., 3rd; Frenkel, E. P.; Singh, S. V.; et al. J Clin Invest 1994, 93, 958-65.

20. Awasthi, S.; Singhal, S. S.; Yadav, S.; Singhal, J.; Drake, K.; Nadkar, A.; Zajac, E.; Wickramarachchi, D.; Rowe, N.; Yacoub, A.; Boor, P.; Dwivedi, S.; Dent, P.; Jarman, W. E.; John, B.; Awasthi, Y. C. Cancer Res 2005, 65, 6022-8.
21. Toxicology of glutathione transferases; Awasthi, Y. C., Ed.; Taylor and Francis: Florida, 2006.
22. Awasthi, Y. C.; Garg, H. S.; Dao, D. D.; Partridge, C. A.; Srivastava, S. K. Blood 1981, 58, 733-8.
23. Awasthi, Y. C.; Sharma, R.; Yadav, S.; Dwivedi, S.; Sharma, A.; Awasthi, S. Curr Drug Metab 2007, 8, 315-23.
24. Awasthi, Y. C.; Singh, S. V.; Ahmad, H.; Wronski, L. W.; Srivastava, S. K.; LaBelle, E. F. Mol Cell Biochem 1989, 91, 131-6.
25. Awasthi, Y. C.; Singhal, S. S.; Gupta, S.; Ahmad, H.; Zimniak, P.; Radominska, A.; Lester, R.; Sharma, R. Biochem Biophys Res Commun 1991, 175, 1090-6.
26. Awasthi, Y. C.; Yang, Y.; Tiwari, N. K.; Patrick, B.; Sharma, A.; Li, J.; Awasthi, S. Free Radic Biol Med 2004, 37, 607-19.
27. Baas, F.; Jongsma, A. P.; Broxterman, H. J.; Arceci, R. J.; Housman, D.; Scheffer, G. L.; Riethorst, A.; van Groenigen, M.; Nieuwint, A. W.; Joenje, H. Cancer Res 1990, 50, 5392-8.
28. Bailey-Dell, K. J.; Hassel, B.; Doyle, L. A.; Ross, D. D. Biochim Biophys Acta 2001, 1520, 234-41.

29. Bakos, E.; Evers, R.; Szakacs, G.; Tusnady, G. E.; Welker, E.; Szabo, K.; de Haas, M.; van Deemter, L.; Borst, P.; Varadi, A.; Sarkadi, B. J Biol Chem 1998, 273, 32167-75.

30. Barnouin, K.; Leier, I.; Jedlitschky, G.; Pourtier-Manzanedo, A.; Konig, J.; Lehmann, W. D.; Keppler, D. Br J Cancer 1998, 77, 201-9.

31. Belinsky, M. G.; Bain, L. J.; Balsara, B. B.; Testa, J. R.; Kruh, G. D. J Natl Cancer Inst 1998, 90, 1735-41.

32. Belinsky, M. G.; Kruh, G. D. Br J Cancer 1999, 80, 1342-9.

33. Bellamy, W. T. Annu Rev Pharmacol Toxicol 1996, 36, 161-83.

34. Bernat, B. A.; Laughlin, L. T.; Armstrong, R. N. Biochemistry 1997, 36, 3050-5.

35. Biedler, J. L. Cancer 1992, 70, 1799-809.

36. Bjornestedt, R.; Stenberg, G.; Widersten, M.; Board, P. G.; Sinning, I.; Jones, T. A.; Mannervik, B. J Mol Biol 1995, 247, 765-73.

37. Blanco, P.; Palucka, A. K.; Gill, M.; Pascual, V.; Banchereau, J. Science 2001, 294, 1540-3.

38. Board, P. G. FEBS Lett 1981, 124, 163-5.

39. Board, P. G.; Coggan, M.; Wilce, M. C.; Parker, M. W. Biochem J 1995, 311 (Pt 1), 247-50.

40. Borst, P.; Elferink, R. O. Annu Rev Biochem 2002, 71, 537-92.

41. Bos, J. L. EMBO J 1998, 17, 6776-82.

42. Bradford, M. M. Anal Biochem 1976, 72, 248-54.

43. Caccuri, A. M.; Antonini, G.; Allocati, N.; Di Ilio, C.; De Maria, F.; Innocenti, F.; Parker, M. W.; Masulli, M.; Lo Bello, M.; Turella, P.; Federici, G.; Ricci, G. J Biol Chem 2002, 277, 18777-84.

44. Caccuri, A. M.; Antonini, G.; Allocati, N.; Di Ilio, C.; Innocenti, F.; De Maria, F.; Parker, M. W.; Masulli, M.; Polizio, F.; Federici, G.; Ricci, G. Biochemistry 2002, 41, 4686-93.

45. Caccuri, A. M.; Antonini, G.; Board, P. G.; Flanagan, J.; Parker, M. W.; Paolesse, R.; Turella, P.; Chelvanayagam, G.; Ricci, G. J Biol Chem 2001, 276, 5432-7.

46. Caccuri, A. M.; Antonini, G.; Board, P. G.; Flanagan, J.; Parker, M. W.; Paolesse, R.; Turella, P.; Federici, G.; Lo Bello, M.; Ricci, G. J Biol Chem 2001, 276, 5427-31.

47. Callen, D. F.; Baker, E.; Simmers, R. N.; Seshadri, R.; Roninson, I. B. Hum Genet 1987, 77, 142-4.

48. Cantor, S. B.; Urano, T.; Feig, L. A. Mol Cell Biol 1995, 15, 4578-84.

49. Carter, L. L.; Redelmeier, T. E.; Woollenweber, L. A.; Schmid, S. L. J Cell Biol 1993, 120, 37-45.

50. Chen, C. J.; Chin, J. E.; Ueda, K.; Clark, D. P.; Pastan, I.; Gottesman, M. M.; Roninson, I. B. Cell 1986, 47, 381-9.

51. Chen, W. J.; Graminski, G. F.; Armstrong, R. N. Biochemistry 1988, 27, 647-54.

52. Cheng, J. Z.; Sharma, R.; Yang, Y.; Singhal, S. S.; Sharma, A.; Saini, M. K.; Singh, S. V.; Zimniak, P.; Awasthi, S.; Awasthi, Y. C. J Biol Chem 2001, 276, 41213-23.

53. Cheng, J. Z.; Singhal, S. S.; Saini, M.; Singhal, J.; Piper, J. T.; Van Kuijk, F. J.; Zimniak, P.; Awasthi, Y. C.; Awasthi, S. Arch Biochem Biophys 1999, 372, 29-36.

54. Cheng, J. Z.; Singhal, S. S.; Sharma, A.; Saini, M.; Yang, Y.; Awasthi, S.; Zimniak, P.; Awasthi, Y. C. Arch Biochem Biophys 2001, 392, 197-207.

55. Chin, J. E.; Soffir, R.; Noonan, K. E.; Choi, K.; Roninson, I. B. Mol Cell Biol 1989, 9, 3808-20.

56. Chuang, C. C.; Wu, S. H.; Chiou, S. H.; Chang, G. G. Biophys J 1999, 76, 679-90.

57. Cisternino, S.; Mercier, C.; Bourasset, F.; Roux, F.; Scherrmann, J. M. Cancer Res 2004, 64, 3296-301.

58. Clark, A. S.; West, K. A.; Blumberg, P. M.; Dennis, P. A. Cancer Res 2003, 63, 780-6.

59. Cole, S. P.; Bhardwaj, G.; Gerlach, J. H.; Mackie, J. E.; Grant, C. E.; Almquist, K. C.; Stewart, A. J.; Kurz, E. U.; Duncan, A. M.; Deeley, R. G. Science 1992, 258, 1650-4.

60. Coley, H. M.; Workman, P.; Twentyman, P. R. Br J Cancer 1991, 63, 351-7.

61. Cooray, H. C.; Blackmore, C. G.; Maskell, L.; Barrand, M. A. Neuroreport 2002, 13, 2059-63.

62. Cordon-Cardo, C.; O'Brien, J. P.; Casals, D.; Rittman-Grauer, L.; Biedler, J. L.; Melamed, M. R.; Bertino, J. R. Proc Natl Acad Sci U S A 1989, 86, 695-8.

63. Delaunay, A.; Isnard, A. D.; Toledano, M. B. Embo J 2000, 19, 5157-66.

64. Delaunay, A.; Pflieger, D.; Barrault, M. B.; Vinh, J.; Toledano, M. B. Cell 2002, 111, 471-81.

65. Dietrich, C. G.; de Waart, D. R.; Ottenhoff, R.; Bootsma, A. H.; van Gennip, A. H.; Elferink, R. P. Carcinogenesis 2001, 22, 805-11.

66. Dietrich, C. G.; de Waart, D. R.; Ottenhoff, R.; Schoots, I. G.; Elferink, R. P. Mol Pharmacol 2001, 59, 974-80.

67. Ding, L.; Wang, H.; Lang, W.; Xiao, L. J Biol Chem 2002, 277, 35305-13.

68. Doyle, L. A.; Ross, D. D. Oncogene 2003, 22, 7340-58.

69. Doyle, L. A.; Yang, W.; Abruzzo, L. V.; Krogmann, T.; Gao, Y.; Rishi, A. K.; Ross, D. D. Proc Natl Acad Sci U S A 1998, 95, 15665-70.

70. Drake, K. J.; Singhal, J.; Yadav, S.; Nadkar, A.; Pungaliya, C.; Singhal, S. S.; Awasthi, S. Int J Oncol 2007, 30, 139-44.

71. Drin, G.; Cottin, S.; Blanc, E.; Rees, A. R.; Temsamani, J. J Biol Chem 2003, 278, 31192-201.

72. Echtay, K. S. Free Radic Biol Med 2007, 43, 1351-71.

73. Eisenblatter, T.; Huwel, S.; Galla, H. J. Brain Res 2003, 971, 221-31.

74. Elbashir, S. M.; Harborth, J.; Lendeckel, W.; Yalcin, A.; Weber, K.; Tuschl, T. Nature 2001, 411, 494-8.

75. Ellman, G. L.; Courtney, K. D.; Andres, V., Jr.; Feather-Stone, R. M. Biochem Pharmacol 1961, 7, 88-95.

76. Erdbruegger U, D. M. A., Falk R.J Drug Discovery Today: Disease Mechanisms 2004, 1, 73-81.

77. Evers, R.; de Haas, M.; Sparidans, R.; Beijnen, J.; Wielinga, P. R.; Lankelma, J.; Borst, P. Br J Cancer 2000, 83, 375-83.

78. Feig, L. A.; Urano, T.; Cantor, S. Trends Biochem Sci 1996, 21, 438-41.

79. Fromm, M. F.; Kauffmann, H. M.; Fritz, P.; Burk, O.; Kroemer, H. K.; Warzok, R. W.; Eichelbaum, M.; Siegmund, W.; Schrenk, D. Am J Pathol 2000, 157, 1575-80.

80. Giese, B. Curr Opin Chem Biol 2002, 6, 612-8.

81. Gill, M. A.; Blanco, P.; Arce, E.; Pascual, V.; Banchereau, J.; Palucka, A. K. Hum Immunol 2002, 63, 1172-80.

82. Goldfinger, L. E.; Ptak, C.; Jeffery, E. D.; Shabanowitz, J.; Hunt, D. F.; Ginsberg, M. H. J Cell Biol 2006, 174, 877-88.

83. Gonzalez, F. J.; Nebert, D. W. Trends Genet 1990, 6, 182-6.

84. Gotoh, Y.; Suzuki, H.; Kinoshita, S.; Hirohashi, T.; Kato, Y.; Sugiyama, Y. J Pharmacol Exp Ther 2000, 292, 433-9.

85. Gottesman, M. M.; Pastan, I. Annu Rev Biochem 1993, 62, 385-427.

86. Gromer, S.; Urig, S.; Becker, K. Med Res Rev 2004, 24, 40-89.

87. Gros, P.; Ben Neriah, Y. B.; Croop, J. M.; Housman, D. E. Nature 1986, 323, 728-31.

88. Harris, J.; Coles, B.; Meyer, D. J.; Ketterer, B. Comp Biochem Physiol B 1991, 98, 511-5.

89. Hattori, Y.; Hattori, S.; Kasai, K. Arterioscler Thromb Vasc Biol 2001, 21, 1179-83.

90. Higgins, C. F. Annu Rev Cell Biol 1992, 8, 67-113.

91. Hirohashi, T.; Suzuki, H.; Sugiyama, Y. J Biol Chem 1999, 274, 15181-5.

92. Hirohashi, T.; Suzuki, H.; Takikawa, H.; Sugiyama, Y. J Biol Chem 2000, 275, 2905-10.

93. Hitchens, T. K.; Mannervik, B.; Rule, G. S. Biochemistry 2001, 40, 11660-9.

94. Holm, P. J.; Morgenstern, R.; Hebert, H. Biochim Biophys Acta 2002, 1594, 276-85.

95. Hopper, E.; Belinsky, M. G.; Zeng, H.; Tosolini, A.; Testa, J. R.; Kruh, G. D. Cancer Lett 2001, 162, 181-91.

96. Horio, M.; Gottesman, M. M.; Pastan, I. Proc Natl Acad Sci U S A 1988, 85, 3580-4.

97. Hu, Y.; Mivechi, N. F. J Biol Chem 2003, 278, 17299-306.

98. Imlay, J. A. Annu Rev Microbiol 2003, 57, 395-418.

99. Ishikawa, T.; Kobayashi, K.; Sogame, Y.; Hayashi, K. FEBS Lett 1989, 259, 95-8.

100. Ishikawa, T.; Muller, M.; Klunemann, C.; Schaub, T.; Keppler, D. J Biol Chem 1990, 265, 19279-86.

101. Ito, K.; Olsen, S. L.; Qiu, W.; Deeley, R. G.; Cole, S. P. J Biol Chem 2001, 276, 15616-24.

102. Jaganathan, L.; Boopathy, R. Indian J Biochem Biophys 1998, 35, 142-7.

103. Jedlitschky, G.; Leier, I.; Buchholz, U.; Center, M.; Keppler, D. Cancer Res 1994, 54, 4833-6.

104. Ji, X.; Armstrong, R. N.; Gilliland, G. L. Biochemistry 1993, 32, 12949-54.

105. Ji, X.; Johnson, W. W.; Sesay, M. A.; Dickert, L.; Prasad, S. M.; Ammon, H. L.; Armstrong, R. N.; Gilliland, G. L. Biochemistry 1994, 33, 1043-52.

106. Ji, X.; Tordova, M.; O'Donnell, R.; Parsons, J. F.; Hayden, J. B.; Gilliland, G. L.; Zimniak, P. Biochemistry 1997, 36, 9690-702.

107. Ji, X.; von Rosenvinge, E. C.; Johnson, W. W.; Tomarev, S. I.; Piatigorsky, J.; Armstrong, R. N.; Gilliland, G. L. Biochemistry 1995, 34, 5317-28.

108. Ji, X.; Zhang, P.; Armstrong, R. N.; Gilliland, G. L. Biochemistry 1992, 31, 10169-84.

109. Jones, P. M.; George, A. M. Cell Mol Life Sci 2004, 61, 682-99.

110. Jowsey, I. R.; Thomson, R. E.; Orton, T. C.; Elcombe, C. R.; Hayes, J. D. Biochem J 2003, 373, 559-69.

111. Juliano, R. L.; Ling, V. Biochim Biophys Acta 1976, 455, 152-62.

112. Jullien-Flores, V.; Dorseuil, O.; Romero, F.; Letourneur, F.; Saragosti, S.; Berger, R.; Tavitian, A.; Gacon, G.; Camonis, J. H. J Biol Chem 1995, 270, 22473-7.

113. Jullien-Flores, V.; Mahe, Y.; Mirey, G.; Leprince, C.; Meunier-Bisceuil, B.; Sorkin, A.; Camonis, J. H. J Cell Sci 2000, 113 (Pt 16), 2837-44.

114. Kamal, A.; Thao, L.; Sensintaffar, J.; Zhang, L.; Boehm, M. F.; Fritz, L. C.; Burrows, F. J. Nature 2003, 425, 407-10.

115. Kampinga, H. H. Handb Exp Pharmacol 2006, 1-42.

116. Kant, J. A.; Steck, T. L. J Biol Chem 1973, 248, 8457-64.

117. Kariya, K.; Koyama, S.; Nakashima, S.; Oshiro, T.; Morinaka, K.; Kikuchi, A. J Biol Chem 2000, 275, 18399-406.

118. Klaunig, J. E.; Kamendulis, L. M. Annu Rev Pharmacol Toxicol 2004, 44, 239-67.

119. Knutsen, T.; Rao, V. K.; Ried, T.; Mickley, L.; Schneider, E.; Miyake, K.; Ghadimi, B. M.; Padilla-Nash, H.; Pack, S.; Greenberger, L.; Cowan, K.; Dean, M.; Fojo, T.; Bates, S. Genes Chromosomes Cancer 2000, 27, 110-6.

120. Koike, K.; Oleschuk, C. J.; Haimeur, A.; Olsen, S. L.; Deeley, R. G.; Cole, S. P. J Biol Chem 2002, 277, 49495-503.

121. Kondo, T.; Kawakami, Y.; Taniguchi, N.; Beutler, E. Proc Natl Acad Sci U S A 1987, 84, 7373-7.

122. Kondo, T.; Miyamoto, K.; Gasa, S.; Taniguchi, N.; Kawakami, Y. Biochem Biophys Res Commun 1989, 162, 1-8.

123. Kondo, T.; Murao, M.; Taniguchi, N. Eur J Biochem 1982, 125, 551-4.

124. Kondo, T.; Yoshida, K.; Urata, Y.; Goto, S.; Gasa, S.; Taniguchi, N. J Biol Chem 1993, 268, 20366-72.

125. Konig, J.; Nies, A. T.; Cui, Y.; Leier, I.; Keppler, D. Biochim Biophys Acta 1999, 1461, 377-94.

126. Konig, P.; Giraldo, R.; Chapman, L.; Rhodes, D. Cell 1996, 85, 125-36.

127. Kool, M.; de Haas, M.; Scheffer, G. L.; Scheper, R. J.; van Eijk, M. J.; Juijn, J. A.; Baas, F.; Borst, P. Cancer Res 1997, 57, 3537-47.

128. Kool, M.; van der Linden, M.; de Haas, M.; Baas, F.; Borst, P. Cancer Res 1999, 59, 175-82.

129. Kowal-Bielecka, O.; Kowal, K.; Distler, O.; Gay, S. Nat Clin Pract Rheumatol 2007, 3, 43-51.

130. Kozak, M. Nucleic Acids Res 1987, 15, 8125-48.

131. Krishnamurthy, P.; Schuetz, J. D. Annu Rev Pharmacol Toxicol 2006, 46, 381-410.

132. Kwon, K. J.; Jung, Y. S.; Lee, S. H.; Moon, C. H.; Baik, E. J. J Neurosci Res 2005, 81, 73-84.

133. LaBelle, E. F.; Singh, S. V.; Ahmad, H.; Wronski, L.; Srivastava, S. K.; Awasthi, Y. C. FEBS Lett 1988, 228, 53-6.

134. LaBelle, E. F.; Singh, S. V.; Srivastava, S. K.; Awasthi, Y. C. Biochem J 1986, 238, 443-9.

135. LaBelle, E. F.; Singh, S. V.; Srivastava, S. K.; Awasthi, Y. C. Biochem Biophys Res Commun 1986, 139, 538-44.

136. Ladner, J. E.; Parsons, J. F.; Rife, C. L.; Gilliland, G. L.; Armstrong, R. N. Biochemistry 2004, 43, 352-61.

137. Laemmli, U. K. Nature 1970, 227, 680-5.

138. Leier, I.; Jedlitschky, G.; Buchholz, U.; Cole, S. P.; Deeley, R. G.; Keppler, D. J Biol Chem 1994, 269, 27807-10.

139. Letoha, T.; Gaal, S.; Somlai, C.; Czajlik, A.; Perczel, A.; Penke, B. J Mol Recognit 2003, 16, 272-9.

140. Lim, K.; Ho, J. X.; Keeling, K.; Gilliland, G. L.; Ji, X.; Ruker, F.; Carter, D. C. Protein Sci 1994, 3, 2233-44.

141. Litman, T.; Brangi, M.; Hudson, E.; Fetsch, P.; Abati, A.; Ross, D. D.; Miyake, K.; Resau, J. H.; Bates, S. E. J Cell Sci 2000, 113 (Pt 11), 2011-21.

142. Loe, D. W.; Almquist, K. C.; Deeley, R. G.; Cole, S. P. J Biol Chem 1996, 271, 9675-82.

143. Matsuzaki, T.; Hanai, S.; Kishi, H.; Liu, Z.; Bao, Y.; Kikuchi, A.; Tsuchida, K.; Sugino, H. J Biol Chem 2002, 277, 19008-18.

144. McAleer, M. A.; Breen, M. A.; White, N. L.; Matthews, N. J Biol Chem 1999, 274, 23541-8.

145. Minamide, L. S.; Bamburg, J. R. Anal Biochem 1990, 190, 66-70.

146. Miyake, K.; Mickley, L.; Litman, T.; Zhan, Z.; Robey, R.; Cristensen, B.; Brangi, M.; Greenberger, L.; Dean, M.; Fojo, T.; Bates, S. E. Cancer Res 1999, 59, 8-13.

147. Mohrmann, K.; van Eijndhoven, M. A.; Schinkel, A. H.; Schellens, J. H. Cancer Chemother Pharmacol 2005, 56, 344-50.

148. Morgenstern, R.; Guthenberg, C.; Depierre, J. W. Eur J Biochem 1982, 128, 243-8.

149. Morinaka, K.; Koyama, S.; Nakashima, S.; Hinoi, T.; Okawa, K.; Iwamatsu, A.; Kikuchi, A. Oncogene 1999, 18, 5915-22.

150. Mosmann, T. J Immunol Methods 1983, 65, 55-63.

151. Mottino, A. D.; Hoffman, T.; Jennes, L.; Vore, M. J Pharmacol Exp Ther 2000, 293, 717-23.

152. Nadkar, A.; Pungaliya, C.; Drake, K.; Zajac, E.; Singhal, S. S.; Awasthi, S. Expert Opin Drug Metab Toxicol 2006, 2, 753-77.

153. Nakashima, S.; Morinaka, K.; Koyama, S.; Ikeda, M.; Kishida, M.; Okawa, K.; Iwamatsu, A.; Kishida, S.; Kikuchi, A. Embo J 1999, 18, 3629-42.

154. Nguyen, T.; Gupta, S. J Immunol 1997, 158, 4916-20.

155. Nielsen, D.; Skovsgaard, T. Biochim Biophys Acta 1992, 1139, 169-83.

156. Oosterhoff, J. K.; Penninkhof, F.; Brinkmann, A. O.; Anton Grootegoed, J.; Blok, L. J. Oncogene 2003, 22, 2920-5.

157. Park, S. H.; Weinberg, R. A. Oncogene 1995, 11, 2349-55.

158. Paul, E. C.; Quaroni, A. J Cell Sci 1993, 106 (Pt 3), 967-81.

159. Paulusma, C. C.; Bosma, P. J.; Zaman, G. J.; Bakker, C. T.; Otter, M.; Scheffer, G. L.; Scheper, R. J.; Borst, P.; Oude Elferink, R. P. Science 1996, 271, 1126-8.

160. Paumi, C. M.; Ledford, B. G.; Smitherman, P. K.; Townsend, A. J.; Morrow, C. S. J Biol Chem 2001, 276, 7952-6.

161. Pikula, S.; Hayden, J. B.; Awasthi, S.; Awasthi, Y. C.; Zimniak, P. J Biol Chem 1994, 269, 27566-73.

162. Pikula, S.; Hayden, J. B.; Awasthi, S.; Awasthi, Y. C.; Zimniak, P. J Biol Chem 1994, 269, 27574-9.

163. Quaroni, A.; Paul, E. C. J Cell Sci 1999, 112 (Pt 5), 707-18.

164. Rabindran, S. K.; He, H.; Singh, M.; Brown, E.; Collins, K. I.; Annable, T.; Greenberger, L. M. Cancer Res 1998, 58, 5850-8.

165. Ramana, K. V.; Bhatnagar, A.; Srivastava, S.; Yadav, U. C.; Awasthi, S.; Awasthi, Y. C.; Srivastava, S. K. J Biol Chem 2006, 281, 17652-60.

166. Reinemer, P.; Dirr, H. W.; Ladenstein, R.; Schaffer, J.; Gallay, O.; Huber, R. Embo J 1991, 10, 1997-2005.

167. Renes, J.; de Vries, E. G.; Jansen, P. L.; Muller, M. Drug Resist Updat 2000, 3, 289-302.

168. Renes, J.; de Vries, E. G.; Nienhuis, E. F.; Jansen, P. L.; Muller, M. Br J Pharmacol 1999, 126, 681-8.

169. Ridley, A. J.; Paterson, H. F.; Johnston, C. L.; Diekmann, D.; Hall, A. Cell 1992, 70, 401-10.

170. Roepe, P. D. Biochemistry 1992, 31, 12555-64.

171. Molecular and Cellular Biology of Multidrug Resistance in Tumor Cells; Roninson, I. B., Ed.; Plenum: New York, 1991.

172. Roninson, I. B.; Chin, J. E.; Choi, K. G.; Gros, P.; Housman, D. E.; Fojo, A.; Shen, D. W.; Gottesman, M. M.; Pastan, I. Proc Natl Acad Sci U S A 1986, 83, 4538-42.

173. Rosse, C.; L'Hoste, S.; Offner, N.; Picard, A.; Camonis, J. J Biol Chem 2003, 278, 30597-604.

174. Rossjohn, J.; Polekhina, G.; Feil, S. C.; Allocati, N.; Masulli, M.; De Illio, C.; Parker, M. W. Structure 1998, 6, 721-34.

175. Roth, M. G. Nat Rev Mol Cell Biol 2006, 7, 63-8.

176. Rushmore, T. H.; Pickett, C. B. J Biol Chem 1993, 268, 11475-8.

177. Molecular Cloning: A Laboratory Manual 2nd ed.; Sambrook J, F. E., Miniatis T, Ed.; Cold Spring Harbor Laboratory Press: New York, 1989.

178. Samuelsson, B.; Dahlen, S. E.; Lindgren, J. A.; Rouzer, C. A.; Serhan, C. N. Science 1987, 237, 1171-6.

179. Saraste, M.; Sibbald, P. R.; Wittinghofer, A. Trends Biochem Sci 1990, 15, 430-4.

180. Saxena, M.; Singhal, S. S.; Awasthi, S.; Singh, S. V.; Labelle, E. F.; Zimniak, P.; Awasthi, Y. C. Arch Biochem Biophys 1992, 298, 231-7.

181. Schaub, T.; Ishikawa, T.; Keppler, D. FEBS Lett 1991, 279, 83-6.

182. Schaub, T. P.; Kartenbeck, J.; Konig, J.; Vogel, O.; Witzgall, R.; Kriz, W.; Keppler, D. J Am Soc Nephrol 1997, 8, 1213-21.

183. Scheffer, G. L.; Kool, M.; de Haas, M.; de Vree, J. M.; Pijnenborg, A. C.; Bosman, D. K.; Elferink, R. P.; van der Valk, P.; Borst, P.; Scheper, R. J. Lab Invest 2002, 82, 193-201.

184. Schmidt-Krey, I.; Mitsuoka, K.; Hirai, T.; Murata, K.; Cheng, Y.; Fujiyoshi, Y.; Morgenstern, R.; Hebert, H. Embo J 2000, 19, 6311-6.

185. Schwab, M.; Eichelbaum, M.; Fromm, M. F. Annu Rev Pharmacol Toxicol 2003, 43, 285-307.

186. Sharma, R.; Awasthi, S.; Zimniak, P.; Awasthi, Y. C. Acta Biochim Pol 2000, 47, 751-62.

187. Sharma, R.; Brown, D.; Awasthi, S.; Yang, Y.; Sharma, A.; Patrick, B.; Saini, M. K.; Singh, S. P.; Zimniak, P.; Singh, S. V.; Awasthi, Y. C. Eur J Biochem 2004, 271, 1690-701.

188. Sharma, R.; Gupta, S.; Singh, S. V.; Medh, R. D.; Ahmad, H.; LaBelle, E. F.; Awasthi, Y. C. Biochem Biophys Res Commun 1990, 171, 155-61.

189. Sharma, R.; Singhal, S. S.; Cheng, J.; Yang, Y.; Sharma, A.; Zimniak, P.; Awasthi, S.; Awasthi, Y. C. Arch Biochem Biophys 2001, 391, 171-9.

190. Sharma, R.; Singhal, S. S.; Wickramarachchi, D.; Awasthi, Y. C.; Awasthi, S. Int J Cancer 2004, 112, 934-42.

191. Sheehan, D.; Meade, G.; Foley, V. M.; Dowd, C. A. Biochem J 2001, 360, 1-16.

192. Shoichet, B. K.; Baase, W. A.; Kuroki, R.; Matthews, B. W. Proc Natl Acad Sci U S A 1995, 92, 452-6.

193. Singhal, S. S.; Awasthi, Y. C.; Awasthi, S. Cancer Res 2006, 66, 2354-60.

194. Singhal, S. S.; Saxena, M.; Ahmad, H.; Awasthi, Y. C. Biochim Biophys Acta 1992, 1117, 105.

195. Singhal, S. S.; Saxena, M.; Ahmad, H.; Awasthi, Y. C. Biochim Biophys Acta 1992, 1116, 137-46.

196. Singhal, S. S.; Saxena, M.; Awasthi, S.; Ahmad, H.; Sharma, R.; Awasthi, Y. C. Biochim Biophys Acta 1992, 1171, 19-26.

197. Singhal, S. S.; Sharma, R.; Gupta, S.; Ahmad, H.; Zimniak, P.; Radominska, A.; Lester, R.; Awasthi, Y. C. FEBS Lett 1991, 281, 255-7.

198. Singhal, S. S.; Singhal, J.; Cheng, J.; Pikula, S.; Sharma, R.; Zimniak, P.; Awasthi, Y. C.; Awasthi, S. Acta Biochim Pol 2001, 48, 551-62.

199. Singhal, S. S.; Singhal, J.; Nair, M. P.; Lacko, A. G.; Awasthi, Y. C.; Awasthi, S. Int J Oncol 2007, 30, 717-25.

200. Singhal, S. S.; Singhal, J.; Sharma, R.; Singh, S. V.; Zimniak, P.; Awasthi, Y. C.; Awasthi, S. Int J Oncol 2003, 22, 365-75.

201. Singhal, S. S.; Wickramarachchi, D.; Singhal, J.; Yadav, S.; Awasthi, Y. C.; Awasthi, S. FEBS Lett 2006, 580, 2258-64.

202. Singhal, S. S.; Yadav, S.; Singhal, J.; Awasthi, Y. C.; Awasthi, S. Biochem Biophys Res Commun 2006, 348, 722-7.

203. Singhal, S. S.; Yadav, S.; Singhal, J.; Drake, K.; Awasthi, Y. C.; Awasthi, S. FEBS Lett 2005, 579, 4635-41.

204. Singhal, S. S.; Yadav, S.; Singhal, J.; Zajac, E.; Awasthi, Y. C.; Awasthi, S. Biochem Pharmacol 2005, 70, 481-8.

205. Sinning, I.; Kleywegt, G. J.; Cowan, S. W.; Reinemer, P.; Dirr, H. W.; Huber, R.; Gilliland, G. L.; Armstrong, R. N.; Ji, X.; Board, P. G.; et al. J Mol Biol 1993, 232, 192-212.

206. Slupphaug, G.; Kavli, B.; Krokan, H. E. Mutat Res 2003, 531, 231-51.

207. Spitaler, M.; Utz, I.; Hilbe, W.; Hofmann, J.; Grunicke, H. H. Biochem Pharmacol 1998, 56, 861-9.

208. Spoelstra, E. C.; Westerhoff, H. V.; Dekker, H.; Lankelma, J. Eur J Biochem 1992, 207, 567-79.

209. Stadtman, E. R.; Levine, R. L. Amino Acids 2003, 25, 207-18.

210. Steck, T. L.; Kant, J. A. Methods Enzymol 1974, 31, 172-80.

211. Stuckler, D.; Singhal, J.; Singhal, S. S.; Yadav, S.; Awasthi, Y. C.; Awasthi, S. Cancer Res 2005, 65, 991-8.

212. Sugawara, I.; Kataoka, I.; Morishita, Y.; Hamada, H.; Tsuruo, T.; Itoyama, S.; Mori, S. Cancer Res 1988, 48, 1926-9.

213. Svensson, R.; Alander, J.; Armstrong, R. N.; Morgenstern, R. Biochemistry 2004, 43, 8869-77.

214. Experimental Biochemistry; Third ed.; Switzer RL, G. L., Ed.; Michelle Russel Julet: New York, 2001.

215. Tammur, J.; Prades, C.; Arnould, I.; Rzhetsky, A.; Hutchinson, A.; Adachi, M.; Schuetz, J. D.; Swoboda, K. J.; Ptacek, L. J.; Rosier, M.; Dean, M.; Allikmets, R. Gene 2001, 273, 89-96.

216. Thiebaut, F.; Tsuruo, T.; Hamada, H.; Gottesman, M. M.; Pastan, I.; Willingham, M. C. Proc Natl Acad Sci U S A 1987, 84, 7735-8.

217. Thiebaut, F.; Tsuruo, T.; Hamada, H.; Gottesman, M. M.; Pastan, I.; Willingham, M. C. J Histochem Cytochem 1989, 37, 159-64.

218. Tomarev, S. I.; Chung, S.; Piatigorsky, J. J Mol Evol 1995, 41, 1048-56.

219. Tomarev, S. I.; Zinovieva, R. D.; Guo, K.; Piatigorsky, J. J Biol Chem 1993, 268, 4534-42.

220. Towbin, H.; Staehelin, T.; Gordon, J. Proc Natl Acad Sci U S A 1979, 76, 4350-4.

221. Versantvoort, C. H.; Broxterman, H. J.; Pinedo, H. M.; de Vries, E. G.; Feller, N.; Kuiper, C. M.; Lankelma, J. Cancer Res 1992, 52, 17-23.

222. Volm, M.; Koomagi, R.; Rittgen, W. Methods Mol Med 2003, 75, 39-51.

223. Walker, J. E.; Saraste, M.; Runswick, M. J.; Gay, N. J. Embo J 1982, 1, 945-51.

224. Watson, W. H.; Yang, X.; Choi, Y. E.; Jones, D. P.; Kehrer, J. P. Toxicol Sci 2004, 78, 3-14.

225. Willingham, M. C.; Richert, N. D.; Cornwell, M. M.; Tsuruo, T.; Hamada, H.; Gottesman, M. M.; Pastan, I. H. J Histochem Cytochem 1987, 35, 1451-6.

226. Cytotoxicity and viability assays in animal cell culture: A practical approach; third ed.; Wilson, A. P., Ed.; Oxford university press, 2000; Vol. 1.

227. Wink, D. A.; Hanbauer, I.; Laval, F.; Cook, J. A.; Krishna, M. C.; Mitchell, J. B. Ann N Y Acad Sci 1994, 738, 265-78.

228. Yadav, S.; Singhal, S. S.; Singhal, J.; Wickramarachchi, D.; Knutson, E.; Albrecht, T. B.; Awasthi, Y. C.; Awasthi, S. Biochemistry 2004, 43, 16243-53.

229. Yadav, S.; Zajac, E.; Singhal, S. S.; Awasthi, S. Cancer Metastasis Rev 2007, 26, 59-69.

230. Yang, Y.; Sharma, A.; Sharma, R.; Patrick, B.; Singhal, S. S.; Zimniak, P.; Awasthi, S.; Awasthi, Y. C. J Biol Chem 2003, 278, 41380-8.

231. Zeng, H.; Liu, G.; Rea, P. A.; Kruh, G. D. Cancer Res 2000, 60, 4779-84.

232. Zhang, D. W.; Gu, H. M.; Vasa, M.; Muredda, M.; Cole, S. P.; Deeley, R. G. Biochemistry 2003, 42, 9989-10000.

233. Zhang, D. W.; Nunoya, K.; Vasa, M.; Gu, H. M.; Theis, A.; Cole, S. P.; Deeley, R. G. Biochemistry 2004, 43, 9413-25.

234. Zhang, Y.; Han, H.; Elmquist, W. F.; Miller, D. W. Brain Res 2000, 876, 148-53.

235. Zimniak, P.; Ziller, S. A., 3rd; Panfil, I.; Radominska, A.; Wolters, H.; Kuipers, F.; Sharma, R.; Saxena, M.; Moslen, M. T.; Vore, M.; et al. Arch Biochem Biophys 1992, 292, 534-8.

BIOGRAPHICAL INFORMATION

Dilki Wickramarachchi was born on 17th of November 1973, obtained her bachelors degree in Biochemistry and Molecular Biology from University of Colombo, Sri Lanka, in 2000. Upon graduation she moved on to quality assurance of pharmaceuticals as an analyst in State Pharmaceutical Corporation, Sri Lanka. As a graduate student she worked under the guidance of Sanjay Awasthi (M.D.) on biochemical and molecular biological analysis of Ralbp1 in stress protection which led to her Ph.D. at University of Texas at Arlington (UTA). She was fortunate to work under the guidance of Dwight Kono (M.D.) on a research project leading to the creation of a transgenic mouse model for systemic lupus erythamotosus during the research internship which is a mandatory part of the PhD program at UTA. She graduated with her Ph.D. in spring 2008. She hopes to purse a carrier in biomedical sciences and contribute to novel findings in biomedical research